Heat and Mass Transfer Analysis of Liquid Desiccant-Air Contact System in a Gauze-Type Structured Packing Tower

by

Musaad Ali Al-Mutairi

A Thesis Presented to the

FACULTY OF THE COLLEGE OF GRADUATE STUDIES

KING FAHD UNIVERSITY OF PETROLEUM & MINERALS

DHAHRAN, SAUDI ARABIA

In Partial Fulfillment of the
Requirements for the Degree of

MASTER OF SCIENCE

In

MECHANICAL ENGINEERING

December, 2000

INFORMATION TO USERS

This manuscript has been reproduced from the microfilm master. UMI films the text directly from the original or copy submitted. Thus, some thesis and dissertation copies are in typewriter face, while others may be from any type of computer printer.

The quality of this reproduction is dependent upon the quality of the copy submitted. Broken or indistinct print, colored or poor quality illustrations and photographs, print bleedthrough, substandard margins, and improper alignment can adversely affect reproduction.

In the unlikely event that the author did not send UMI a complete manuscript and there are missing pages, these will be noted. Also, if unauthorized copyright material had to be removed, a note will indicate the deletion.

Oversize materials (e.g., maps, drawings, charts) are reproduced by sectioning the original, beginning at the upper left-hand corner and continuing from left to right in equal sections with small overlaps.

Photographs included in the original manuscript have been reproduced xerographically in this copy. Higher quality 6" x 9" black and white photographic prints are available for any photographs or illustrations appearing in this copy for an additional charge. Contact UMI directly to order.

Bell & Howell Information and Learning
300 North Zeeb Road, Ann Arbor, MI 48106-1346 USA
800-521-0600

HEAT AND MASS TRANSFER ANALYSIS OF LIQUID DESICCANT-AIR CONTACT SYSTEM IN A GAUZE-TYPE STRUCTURED PACKING TOWER

BY

MUSAAD ALI AL-MUTAIRI

A Thesis Presented to the
DEANSHIP OF GRADUATE STUDIES

KING FAHD UNIVERSITY OF PETROLEUM & MINERALS
DHAHRAN, SAUDI ARABIA

In Partial Fulfillment of the
Requirements for the Degree of

MASTER OF SCIENCE

In

Mechanical Engineering

Ramadan, 1421H
December, 2000

UMI Number: 1402841

UMI Microform 1402841

Bell & Howell Information and Learning Company
300 North Zeeb Road
P.O. Box 1346
Ann Arbor, MI 48106-1346

KING FAHD UNIVERSITY OF PETROLEUM AND MINERALS
DHAHRAN, SAUDI ARABIA

DEANSHIP OF GRADUATE STUDIES

This thesis, written by

Musaad Ali Al-Mutairi

under the direction of Thesis Advisor and approved by his Thesis Committee, has been presented to and approved by the Dean of the Graduate Studies, in partial fulfillment of the requirements of the degree of

MASTER OF SCINCE IN MECHANICAL ENGINEERING.

Thesis Committee

22/1/2001
Dr. P. Gandhidasan (Chairman)

Dr. A. A. Al-Farayedhi (Member)

22/1/01
Dr. Mohamed A. Antar (Member)

27/10/1421
Department Chairman (Mechanical Engineering)

Dean of Graduate Studies

عمادة الدراسات العليا
DEANSHIP OF GRADUATE STUDIES

Date :

This thesis is dedicated to my

PARENTS,

WIFE,

and

DAUGHTERS

whose patience and perseverance led me to this accomplishment.

ACKNOWLEDGMENTS

First of all I thank Almighty **ALLAH** (**SWT**), the only **LORD** and **CREATOR,** For His Eternal Blessing and Guidance.

Acknowledgment is due to the King Fahd University of Petroleum & Minerals for supporting this study.

I wish to express my appreciation to Dr. P. Gandhidasan who served as my major advisor. I also wish to thank the other members of my thesis committee Dr. A. A. Al-Farayedhi and Dr. Mohamed A. Antar.

Finally I thank all my Brothers for their constant advice and prayers.

TABLE OF CONTENTS

Page #

LIST OF TABLES viii

LIST OF FIGURES ix

ABSTRACT xiii

CHAPTER 1: INTRODUCTION AND LITERATURE REVIEW 1

1.1 General 1
1.2 Objective 4
1.3 Literature Review 5
1.3.1 Desiccants 5
1.3.1.1 Solid Desiccants 6
1.3.1.2 Liquid Desiccants 7
1.3.2 Liquid Desiccant Dehumidification/Regeneration Process 9
1.3.3 Liquid Desiccant-Air Contact Devices 9
1.3.3.1 Random Packings 14
1.3.3.2 Regular packings 17

CHAPTER 2: CALCULATION OF HEAT AND MASS TRANSFER COEFFICIENTS 19

2.1 Introduction 19
2.2 Gauze-Type Structured Packings 22
2.3 System Analysis 27
2.4 Results and Discussion 35

CHAPTER 3: HEAT AND MASS TRANSFER ANALYSIS OF THE STRUCTURED PACKING DEHUMIDIFIER 49

3.1 Introduction 49
3.2 Modeling Considerations 51
3.3 Finite Difference Model 52
3.4 Vapor-Liquid Equilibrium Data 56
3.5 Computational Procedure 57
3.6 Results and Discussion 58
3.6.1 Comparison between Random and Structured Packing 58
3.6.2 Parametric Investigation of the Structured Packing Dehumidifier .. 64

Page #

CHAPTER 4: REGENERATION PROCESS IN STRUCTURED PACKING TOWER 80

4.1 Regeneration of Weak Desiccants..... 80
4.1.1 Solar Regeneration of Weak Desiccants..... 81
4.1.2 Regeneration in a Packed Column Using Solar Heated Air..... 82
4.1.3 Regeneration of Weak Desiccants by Mechanical Energy..... 83
4.1.4 Regeneration of Weak Desiccants in a Structured Packing Tower. 84
4.2 Simultaneous Heat and Mass Transfer Analysis of the Regeneration Process..... 85
4.3 Results and Discussion..... 90

CHAPTER 5: EFFECTIVENESS FOR AN ADIABATIC COUNTERFLOW STRUCTURED PACKING REGENERATOR 103

5.1 Introduction..... 103
5.2 Effectiveness for a Humidification/Dehumidification Process..... 104
5.3 Need for the Definition of Packing bed Regenerator Effectiveness..... 105
5.3.1 Definition of Regenerator Effectiveness for a System Using Heated Air..... 106
5.3.2 Definition of Regenerator Effectiveness for a System Using Heated Desiccant..... 108
5.4 Results and Discussion..... 114

CHAPTER 6: PRESSURE DROP IN THE STRUCTURED PACKING DEHUMIDIFIER/REGENERATOR 123

6.1 Introduction..... 123
6.2 Models for Predicting Pressure Drop in A Liquid-Gas Contact System..... 126
6.2.1 Channel Model..... 127
6.2.2 Particle Model..... 129
6.3 System Analysis for Desiccant-Air System..... 132
6.3 Results and Discussion..... 134

Page #

CHAPTER 7: CONCLUSIONS AND RECOMMENDATIONS 142

7.1 Conclusions..... 142
7.2 Recommendations..... 144

APPENDICES..... 145

NOMENCLATURE..... 159

REFERENCES..... 164

VITA

LIST OF TABLES

Table #		Page #
2.1	Summary of correlations.....	21
2.2	Geometric information of the gauze-type structured packing.....	26
3.1	Packed bed dehumidifier performance.....	50
3.2	Dehumidifier parameters for the comparison of packings.....	60
3.3	Geometric information of the random and structured packings.....	61
3.4	Dehumidifier parameters for the parametric investigation.....	65
4.1	Packed bed regenerator performance.....	86
4.2	Regenerator parameters used for the parametric investigation in the regenerator sizing program.....	92
4.3	Geometric information of the regenerator packing.....	93
5.1	The geometry coefficients.....	115
6.1	The physical characteristics of packing materials extracting from [62].....	141

LIST OF FIGURES

Fig. #		Page #
1.1	Desiccant cooling system.....	2
1.2	Finned-tube surface type dehumidifier.....	11
1.3	Spray chamber dehumidifier.....	12
1.4	Packed bed dehumidifier.....	13
1.5	Packed tower with random packing.....	15
1.6	Examples of random packings.....	16
1.7	Packed tower with structured packing.....	18
2.1	Gauze-type structured packing.....	23
2.2	Definition of structured packing dimensions and geometric orientation.....	25
2.3	Comparison of predicted volumetric heat transfer coefficient for air with those obtained using Chung et al. data.....	38
2.4	Comparison of predicted volumetric mass transfer coefficient for air with those obtained using Chung et al. data.....	39
2.5	Effect of desiccant velocity on liquid-phase mass transfer coefficient.....	41
2.6	Effect of desiccant concentration on liquid-phase mass transfer coefficient.....	43

Fig. #		Page #
2.7	Effect of desiccant inlet temperature on liquid-phase mass transfer coefficient.....	44
2.8	Effect of desiccant inlet temperature on liquid-phase heat transfer coefficient.....	45
2.9	Effect of desiccant velocity on liquid-phase heat transfer coefficient.....	47
2.10	Effect of desiccant concentration on liquid-phase heat transfer coefficient.....	48
3.1	Differential section of a structured packing tower.....	53
3.2	Comparison of packing materials – Effect of desiccant inlet temperature.....	62
3.3	Comparison of packing materials – Effect of desiccant inlet concentration.....	63
3.4	Humidity ratio profile for the desiccant inlet temperature of 25 °C.....	66
3.5	Humidity ratio profile for the desiccant inlet temperature of 30 °C.....	67
3.6	Variation of humidity ratio on the packing height for three different desiccants.....	69
3.7	Effect of desiccant inlet temperature on the packing height.....	71
3.8	Effect of desiccant inlet concentration on the packing height.....	72

Fig. #		Page #
3.9	Effect of air inlet temperature on the packing height.....	74
3.10	Desiccant temperature profile for two different air inlet humidity ratios.....	75
3.11	Air temperature profile for two different air inlet humidity ratios.....	76
3.12	Effect of desiccant inlet flow rate on the packing height.....	78
3.13	Effect of air inlet flow rate on the packing height.....	79
4.1	Differential section of a structured packing regenerator.....	87
4.2	Effect of air inlet temperature on the regenerator packing height.....	94
4.3	Effect of desiccant inlet temperature on the regenerator packing height.....	96
4.4	Effect of inlet humidity ratio on the regenerator packing height.....	97
4.5	Effect of desiccant inlet concentration on the regenerator packing height.....	99
4.6	Effect of air flow rate on the regenerator packing height.....	100
4.7	Effect of desiccant flow rate on the regenerator packing height.....	101
5.1	Variation of regeneration factor with inlet temperature ratio for different concentrations.....	113

Fig. #		Page #
5.2	Effect of regeneration air inlet temperature on effectiveness....	116
5.3	Effect of desiccant inlet concentration on effectiveness.....	118
5.4	Effect of regeneration air humidity ratio (vapor pressure) on effectiveness.....	119
5.5	Variation of regeneration factor with inlet temperature ratio for several $P_{G,in}$.....	120
5.6	Effect of packing height on effectiveness.....	121
6.1	Variation of pressure drop per height with volumetric flow rate of air for structured packing.....	125
6.2	Comparison of calculated values of pressure drop for this work with those obtained using Rocha et al. and Stichlmair et al.	135
6.3	Effect of superficial liquid velocity on flooding superficial gas velocity for different desiccants.....	136
6.4	Effect of superficial liquid velocity on flooding pressure drop for different desiccants.....	138
6.5	Effect of superficial gas velocity on pressure drop for different desiccants.....	139
6.6	Pressure drop for different packing materials.....	140

THESIS ABSTRACT

FULL NAME OF STUDENT: MUSAAD ALI AL-MUTAIRI.

TITAL OF STUDY: HEAT AND MASS TRANSFER ANALYSIS OF LIQUID DESICCANT-AIR CONTACT SYSTEM IN A GAUZ-TYPE STRUCTURED PACKING TOWER.

MAJOR FIELD: MECHANICAL ENGINEERING.

DATE OF DEGREE: RAMADAN, 1421H (DECEMBER, 2000).

In this research, high performance packing namely, structured packing that combines good heat and mass transfer characteristics with low pressure drop, is proposed for dehumidification of air using liquid desiccants and for regeneration of weak liquid desiccants. This study is concerned with the interface transfer of heat and mass when air is brought into contact with the liquid desiccant solution. A theoretical study of heat and mass transfer analysis in an air-desiccant contact system employing three different liquid desiccants, namely lithium chloride, calcium chloride and a mixture of 50% lithium chloride and 50% calcium chloride (called as Cost Effective Liquid Desiccant, CELD) is investigated. The heat and mass transfer coefficients are evaluated for lithium chloride-air, calcium chloride-air and CELD-air contact systems using gauze-type structured packing as the packing material. The derived transfer coefficients are used to analyze the performance of the dehumidifier and the regenerator. The heat and mass transfer analysis are extended to study the effect of various parameters such as liquid inlet temperature, liquid inlet concentration and its flow rate, air inlet temperature and its flow rate, air outlet humidity, etc. on the performance of the dehumidifier and the regenerator. The performance of structured and random packings are compared and discussed. Moreover, effectiveness of the regenerator and the system pressure drop are calculated and discussed.

Master of Science Degree
Department of Mechanical Engineering
KING FAHD UNIVERSITY OF PETROLUM AND MINERALS
Dhahran, Saudi Arabia

Ramadan, 1421H (December, 2000)

ملخص الرسالة

الاســـــــــم: مساعد علي المطيري.

عنوان الرسالة: تحليل انتقال الحرارة والكتلة عند تلامس سائل التجفيف مع الهواء باستخدام أبراج معبأة إنشائيا من نوع (gauze).

التخصـــــص: الهندسة الميكانيكية.

تاريخ الدرجـة: رمضان ١٤٢١هـ (ديسمبر، ٢٠٠٠).

في هذا البحث، رزم تعبئة إنشائية ذات أداء عالي من حيث انتقال الحرارة والكتلة والتقليل من انخفاض الضغط اقترحت في برج لتجفيف الهواء باستخدام سوائل التجفيف وكذلك في برج لاسترجاع السوائل الضعيفة. هذه الدراسة اهتمت بانتقال الحرارة والكتلة عندما يوضع الهواء في تلامس مع سائل التجفيف. التحليل النظري لانتقال الحرارة والكتلة بين الهواء و والليثيوم كلورايد، كالسيوم كلورايد و مخلوط من الليثيوم كلورايد والكالسيوم كلورايد بنسبة متساوية بحثت في هذه الدراسة. معاملات انتقال الحرارة والكتلة لهذه السوائل الثلاثة قيمت باستخدام رزم إنشائية من نوع (gauze). هذه المعاملات استخدمت لتقييم أداء برج التجفيف وكذلك برج الاسترجاع. هذا البحث توسع لدراسة تأثير عدة كميات مثل درجة حرارة سائل التجفيف الداخل، تركيز سائل التجفيف الداخل ومعدل تدفقه وكذلك درجة حرارة الهواء الداخل ومعدل تدفقه ورطوبته عند الخروج الخ. على أداء برج التجفيف والاسترجاع. كذلك فقد تم مقارنة ومناقشة أداء الرزم الإنشائية مع أداء الرزم العشوائية. علاوة على ذلك فقد تم حساب ومناقشة فعالية المسترجع وانخفاض الضغط في هذا النظام.

درجـة الماجـستير فـي العلـــوم
قسم الهندسة الميكانيكية
جامعـــة المـــلك فـــهد للبتـــرول والمعـــــــادن
الظهران، المملكة العربية السعودية
رمضان، ١٤٢١هـ (ديسمبر، ٢٠٠٠)

CHAPTER 1

INTRODUCTION AND LITERATURE REVIEW

1.1 General

Desiccants are materials that can attract and hold moisture. Recently desiccants are used for dehumidification of air. In humid climates, cooling can be accomplished by non-conventional methods where the air to be conditioned is first dehumidified by means of a suitable desiccant followed by adiabatic evaporative cooling [1]. Desiccant technology has the potential to make major contributions to energy conservation, improve indoor air quality through reduced microbial growth and by removing air pollutant [2]. With desiccant cooling system, air humidity and temperature are controlled separately, as shown in Fig. 1.1, enabling better humidity control.

Two types of desiccants, namely solids and liquids, are widely used to dehumidify the air. The use of liquid desiccants may be advantageous compared to solid desiccants. The regeneration temperature required for liquid desiccants is lower than solid desiccants. The pressure drop through a liquid desiccant system is smaller than the pressure drop through a solid desiccant wheel. Also, the ability to pump the liquid makes it possible to connect several small dehumidifiers to one large unit of regenerator that may be advantageous in large buildings. Another advantage of using

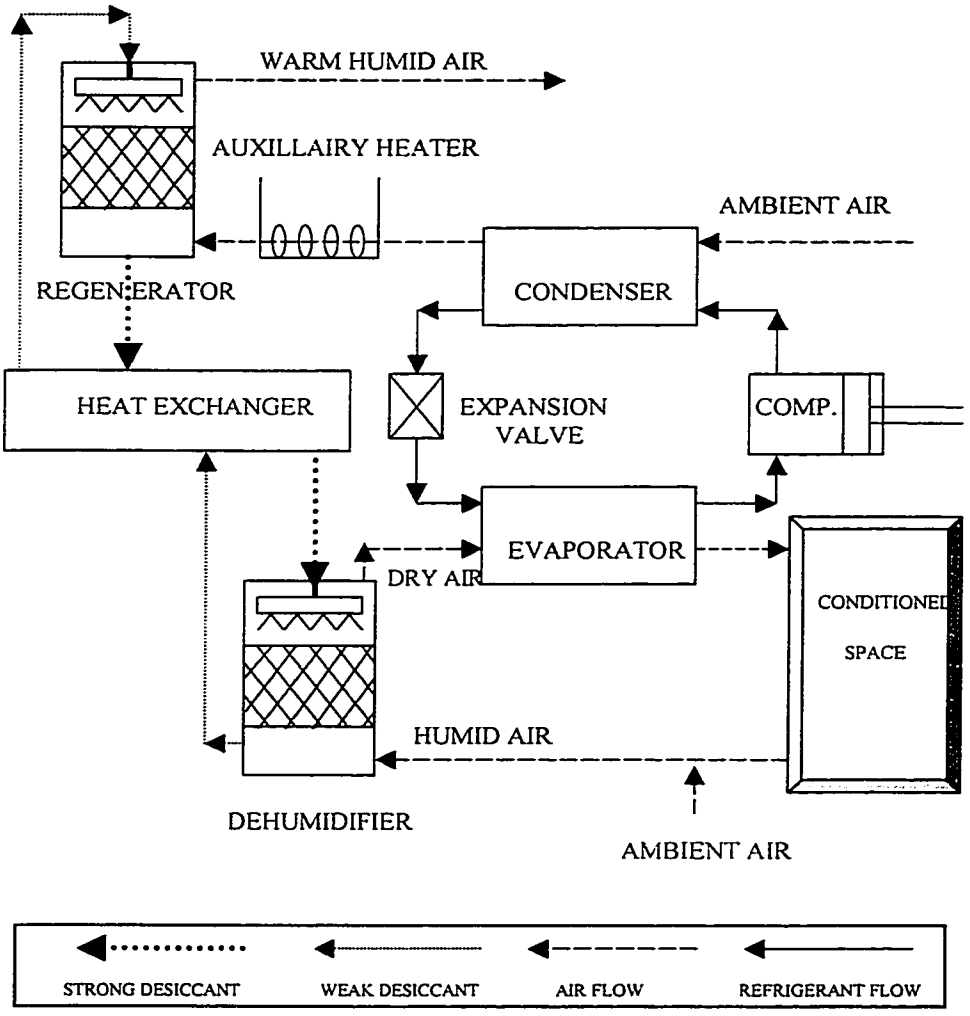

Fig. 1.1 Desiccant cooling system.

liquid desiccants is that they can be used as a heat transfer medium in a heat exchanger. Hence the desiccant can be pre-cooled or pre-heated when required. Also, dehumidifying with a liquid desiccant usually scrubs the air stream, not only conditioning but also cleaning and disinfecting the air. Finally, the energy is stored as chemical energy rather than thermal energy. These reasons make liquid desiccant dehumidification system more attractive [3]. However, one should consider that some liquid desiccants might be expensive, corrosive, unsafe, or unstable.

Different types of liquid desiccants are available in the market. In most applications the general properties requirements are low vapor pressure, the capability of maintaining dehydrating ability over a considerable range of concentration, non-corrosive, low viscosity, high density, low crystallization point, low regeneration temperature, low cost and safe. These requirements are not fully answered by any single desiccant, but after making some compromises, the aqueous solution of mixtures of lithium chloride and calcium chloride are considered to be the best neutral salts for use today. In the present study, a liquid desiccant is proposed, which is called CELD (Cost Effective Liquid Desiccant). It is a mixture of 50% lithium chloride and 50% calcium chloride by weight.

Out of three configurations for a liquid desiccant dehumidifier/regenerator, namely spray chamber, packed tower, and sprayed coil arrangement, packed tower configuration has received more attention [4] because of a large rate of heat and mass transfer per unit volume, thus lending themselves to compact design. In a packed tower dehumidifier strong, cool desiccant is distributed uniformly from the top and allowed to trickle down through the tower in a thin film covering the packing material surface.

Different kinds of packing material made of various materials in different sizes are available in the market. Among these packing materials, Raschig rings, flexi rings and Berl saddles are widely used for dehumidification of air in a packed tower. Although these random packed towers facilitate more mass transfer by providing a large area in a relatively small volume, the air pressure drop through the packing is generally high. This study deals with a new kind of packing materials called as "structured packing" used for liquid desiccant systems. The regenerator is used to reconcentrate the weak desiccant during the process. A solar regenerator or an auxiliary heater can supply the heat required for regeneration.

1.2 Objective

In this research, high performance packing namely, structured packing that combines good heat and mass transfer characteristics with low pressure drop, will be proposed for dehumidification of air using liquid desiccants and for regeneration of weak liquid desiccants. In order to design a structured packing tower for liquid desiccant-air contact operation, heat and mass transfer coefficients for each phase are required. This study is concerned with the interface transfer of heat and mass when air is brought into contact with the liquid desiccant solution. A theoretical study of heat and mass transfer analysis in an air-desiccant contact system employing three different liquid desiccants, namely lithium chloride, calcium chloride and a mixture of 50% lithium chloride and 50% calcium chloride (called as Cost Effective Liquid Desiccant, CELD) will be investigated. The heat and mass transfer coefficients will be evaluated

for lithium chloride-air, calcium chloride-air and CELD-air contact systems using gauze-type structured packing as the packing material. The derived transfer coefficients will be used to analyze the performance of the dehumidifier and the regenerator. The heat and mass transfer analysis will be extended to study the effect of various parameters such as liquid inlet temperature, liquid inlet concentration and its flow rate, air inlet temperature and its flow rate, air outlet humidity, etc. on the performance of the dehumidifier and the regenerator. The performance of structured and random packings will be compared and discussed. Moreover, effectiveness of the regenerator and the system pressure drop will be calculated and discussed.

1.3 Literature Review

1.3.1 Desiccants

Desiccant systems and components are a useful addition to the HVAC engineer's tool kit. They allow independent control of humidity, as well as potential energy savings and increased comfort level. Nearly any material is a desiccant-even glass can collect a small amount of moisture. But desiccants used in commercial equipment are selected for their ability to hold large amounts of moisture. For example, the silica gel packets often sealed into vitamin bottles can hold moisture equal to about 20% of their dry weight. Liquid desiccant materials can hold even more moisture. But all desiccants used in commercial systems work the same way. Desiccants remove water vapor by chemical attraction caused by difference in vapor pressure. When air is humid, it has a high water vapor pressure. In contrast, there are very few water

molecules on a dry desiccant surface, so the water vapor pressure at the desiccant surface is very low. Water molecules move from the humid air to the dry desiccant in order to equalize this pressure differential. With desiccants, moisture removal occurs in the vapor phase. There is no liquid condensate. Consequently, desiccant dehumidification can continue even when the dew point of the air is below freezing. This is different from cooling-based dehumidification, in which the moisture freezes and halts the process if part of the coil surface is below 0°C. Desiccants can be either liquid or solid, and there are many different materials of both types.

1.3.1.1 Solid Desiccants

Solid desiccants such as silica gel, activated alumina, activated bauxite, micro sieves, etc., which have great affinity for water are used for producing dehumidified air. Different types of dehumidifiers and regenerators are available for solid desiccant. Solid packed tower, rotating horizontal bed, multiple vertical bed and rotating Honeycombe® are examples. The air to be dehumidified is passed through the desiccant bed, the moisture in the air is condensed out in the pores of the desiccant and the latent heat of vaporization of the moisture condensed is converted to sensible heat, thereby raising the temperature of the air. In conventional units gas, steam, or electrical energy are used to regenerate the adsorbent beds. Several different investigators have studied the behavior of solid desiccant dryers, the objective being the prediction of its performance. Solid desiccant have been used for drying operation where solar energy is used for regeneration [5]. The regeneration temperature required for such systems is about 70°- 80°C.

Solid desiccant systems can operate at lower regeneration temperature, but require large volumes of desiccant and also entail significant operating costs for the parasitic systems of blowers required to circulate both the air to be conditioned and the hot air for regeneration. Further as time progresses, efficiency of the desiccant bed can be reduced due to dust and foreign matter deposited in the pores. To avoid this, additional air filtering can be added but only at the cost of additional air pressure drop through the system. These drawbacks make the solid desiccant system less attractive, hence a liquid desiccant system is chosen for the present study.

1.3.1.2 Liquid Desiccants

Air may be dehumidified when it is brought to contact with a suitable liquid desiccant. Different types of liquid desiccants are available in the market and the application of the proper desiccant in hot, humid climates would improve the dehumidification effectiveness. The driving potential for a dehumidification process is the difference in the vapor pressure of water in the air and the vapor pressure of water above the desiccant. The vapor pressure of a liquid desiccant is a function of its temperature and concentration. Among the various desiccants available, lithium chloride, lithium bromide, calcium chloride, and triethylene glycol have received much attention. The cost of the desiccants varies from SR 2/kg (for calcium chloride) to SR 60/kg (for lithium bromide). Health and Minger [6] have shown that by combining salts such as calcium chloride and lithium chloride, improved solubility characteristics can be expected as well as a possible reduction in viscosity, while achieving a considerable cost reduction relative to pure lithium chloride. Isshiki [7] studied the

possibility of power generation by absorption system using liquid desiccants. For selecting the suitable desiccant for the proposed system, various desiccants were investigated and finally that mixture of LiCl and $CaCl_2$ was selected as the best desiccant because this mixture is fairly efficient, non-corrosive, inexpensive, generates less alkali cracking, and safe. Ertas et al. [8] conducted experiments to measure the physical properties of three combinations of calcium chloride and lithium chloride mixtures. On the basis of cost and performance, it is reported that 50% LiCl and 50% $CaCl_2$ mixture would be the best combination. Ameel et al. [9] reported that a mixture of the chlorides of zinc, calcium, and lithium might exhibit more of the desirable characteristics for liquid desiccant than the single salts from which they are comprised. They concluded that the most promising mixture would be one part of the zinc chloride and two part of lithium chloride. Different combinations of various desiccants are also found in the literature [10]. However, it is interesting to note that the properties of various desiccant mixtures can be found using the classical Thermodynamics approach [11].

The liquid desiccants have many potential areas of application. Liquid desiccants can be used for: drying of grains and crops, controlling the ripening of fruits, in storage compartments to prevent corrosion, mildew and fermentation, drying of gases before storage, in energy storage systems, concentration of fruit juices, and power generation.

1.3.2 Liquid Desiccant Dehumidification/Regeneration Process

Liquid desiccant cooling systems require two desiccant-air contact devices: a dehumidifier and a regenerator. Dehumidifier is a device that removes moisture from air. Dehumidifiers are commonly used in order to make homes more comfortable. Lowering the moisture level of the air also helps to prevent the growth of mold and milden in the home. Dehumidification is also important in many industrial and food processes. As cool and concentrated desiccant is brought in contact with air, the desiccant absorbs water vapor in the air because the desiccant has a low vapor pressure than water. The desiccant falls down through the dehumidifier because of gravity while the air moves upwards due to the pressure difference created by the blower. There is a considerable pressure drop in the air phase, whereas for liquid phase the only power requirement is for pumping the liquid to the top of the dehumidifier.

A regenerator is used to reconcentrate the weak desiccant during the process. In the regenerator, water will be transferred from the desiccant to the air because the desiccant has a high vapor pressure than water. This can be achieved by two methods. The first method is to heat the air to decrease its relative humidity. The second method is to heat the liquid desiccant in order to raise its vapor pressure above the ambient air vapor pressure.

1.3.3 Liquid Desiccant-Air Contact Devices

Simple boilers and trickle solar collectors are used to regenerate the desiccant. Finned-tube surfaces in a column, spray tower and packed tower have been commonly

used as liquid-air contact devices. Some of the less common desiccant-air contact devices proposed in the literature include a mesh covered rotating cylindrical frame dehumidifier [12] and a passively controlled simultaneous dehumidifier and regenerator [13].

The finned-tube surface tower, as shown in Fig. 1.2, was first proposed by Turner [14]. This unit is essentially a finned-tube heat exchanger having a number of vertical, laterally elongated spaced parallel metallic fins. The solution passing from the header onto the fins of the unit would normally flow downward by gravity, along the surface of the fins. The air flows through the slots of the finned tube arrangement and exerts a force on the solution in such a way that the solution flows laterally across the fin surface. However, such equipment requires unreasonably high air velocity for certain cases. It is also difficult to control the liquid film on the fin. The cooling water is also circulated through the tubes. This arrangement is highly suitable for isothermal dehumidification/regeneration process.

In the spray tower, as shown in Fig. 1.3, the solution is atomized into the air stream by mean of high-pressure nozzles. The large surface area of the dispersed solution serves to enhance the mass transfer rate. The advantage of a spray chamber is the low air pressure drop, but this is offset by a relative high pumping cost for the solution. Also the tendency of entertainment of liquid by the air leaving is considerable [15].

Packed bed absorption towers, as shown in Fig. 1.4, have been commonly used as air dehumidifiers and desiccant regenerators. Packed towers, used for continuous contact of liquid and air in both countercurrent and cocurrent flow, are vertical

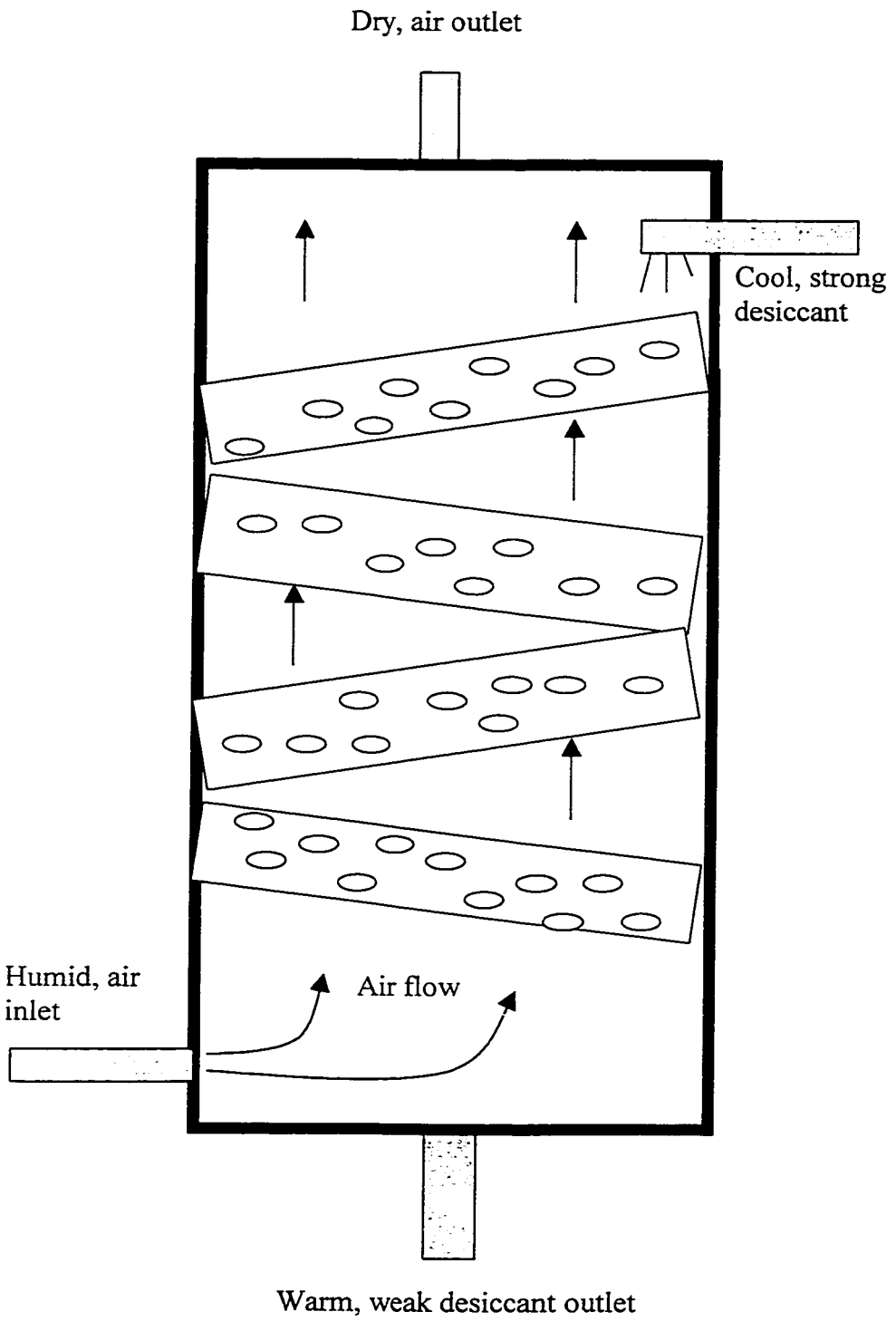

Fig. 1.2 Finned-tube surface type dehumidifier.

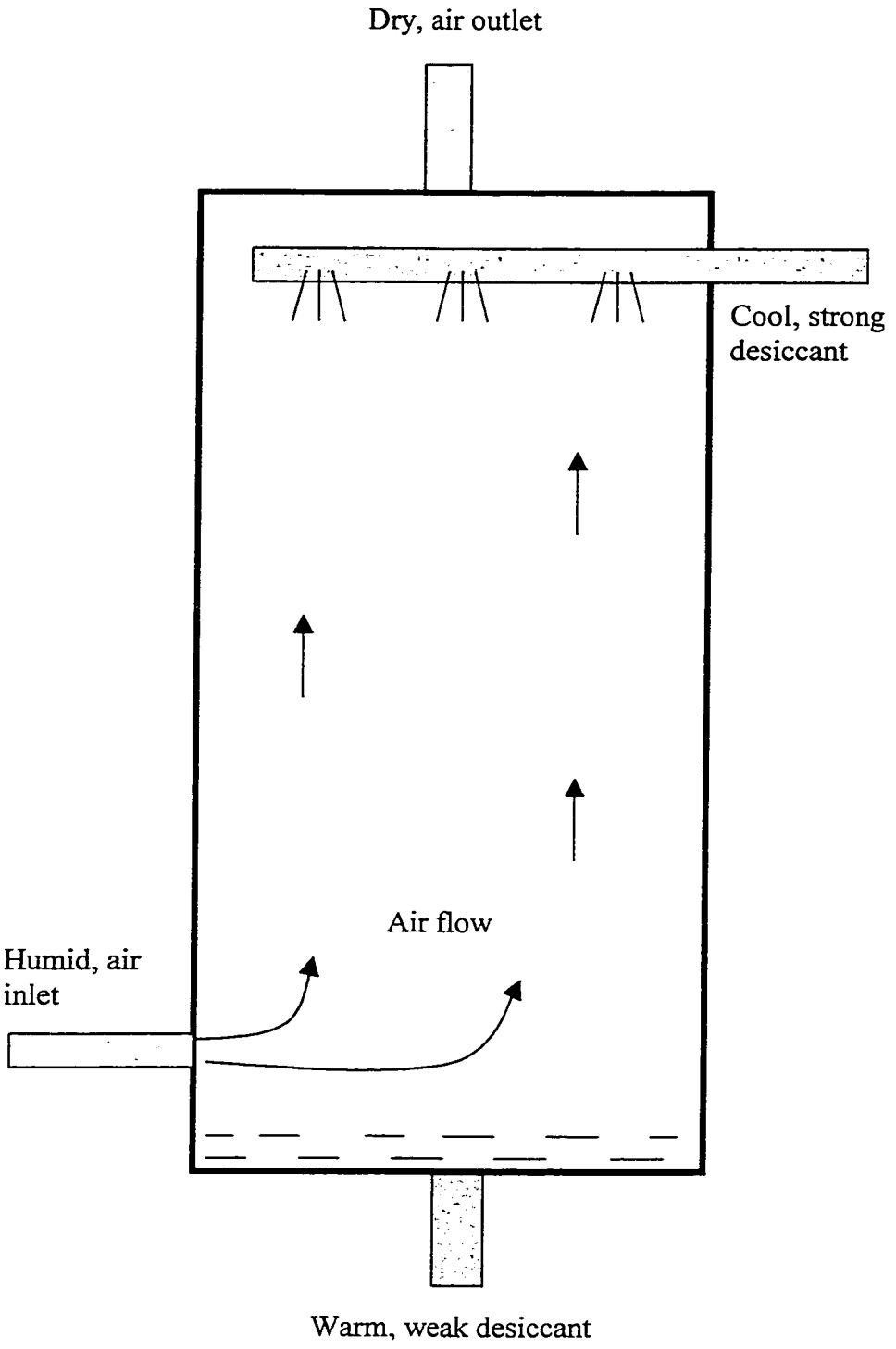

Fig. 1.3 Spray chamber dehumidifier.

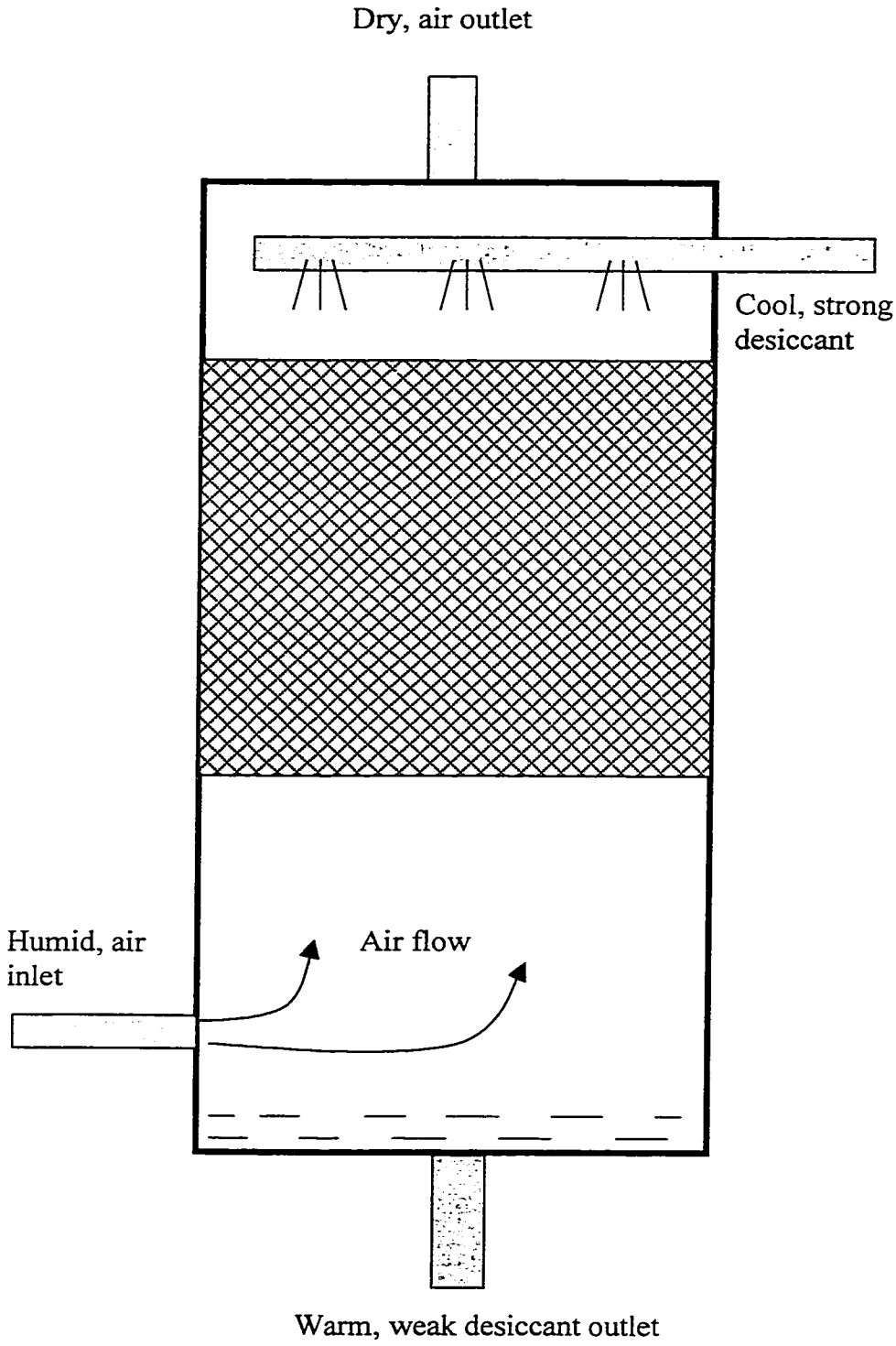

Fig 1.4 Packed bed dehumidifier.

columns which have been filled with packing or devices of large surface. The liquid is distributed over the packing, and trickles down through the packed bed, exposing a large surface area to contact with the air. The desirable properties of the tower packings are:

1. Large void volume to decrease pressure drop.
2. Chemically inert to the fluids being processed.
3. Large surface area per unit volume of packing.
4. Lightweight but strong.
5. Good distribution of liquid.
6. Good wettability.
7. Represent low cost.

Packings are of two types, namely random and regular.

1.3.3.1 Random Packings

Figure 1.5 illustrates a packed tower with random packings. Random packings are simply dumped into the tower during installation and allowed to fall at random. In the past such readily available materials as broken stone, gravel, or lumps of coke were used, but although inexpensive, they are not desirable for reasons of small surface and poor fluid-flow characteristics. Random packings most frequently used at present are manufactured, and the common types are Raschig rings and Berl saddles, see Fg. 1.6. They are widely used for dehumidification of air in a packed tower. A mathematical model is presented by Radhwan et al. [16] to predict the performance of a packed bed

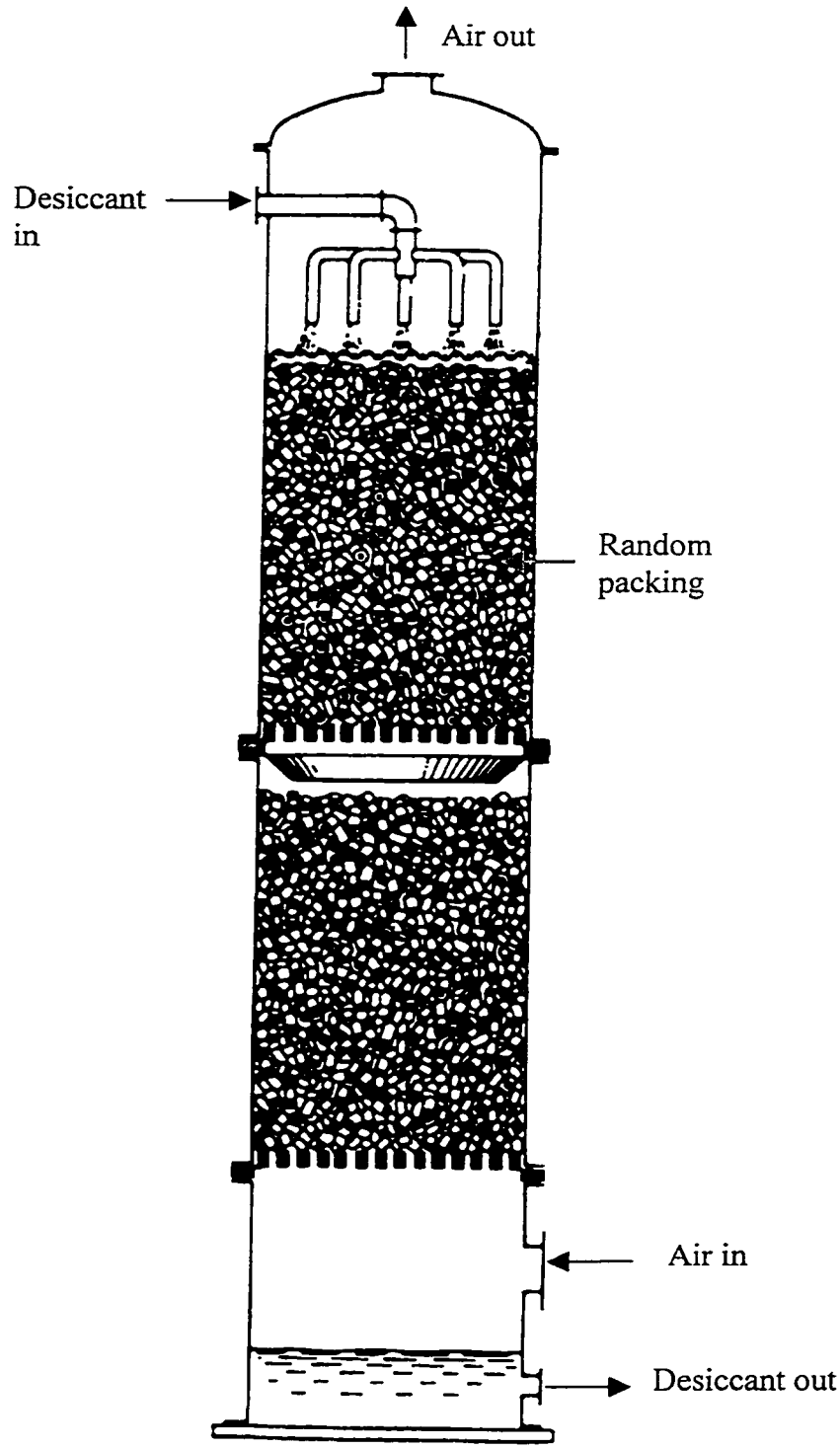

Fig. 1.5 Packed tower with random packing.

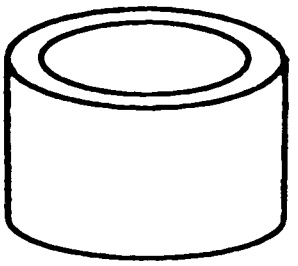

Raschig Ring
(ceramic)

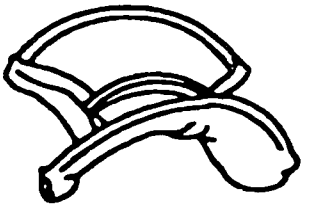

Intalox Saddle
(ceramic)

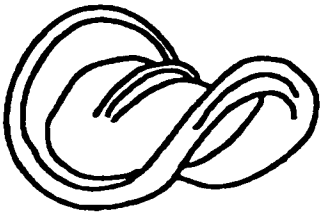

Berl Saddle
(ceramic)

Fig. 1.6 Examples of random packings.

made up of 25 mm ceramic Raschig rings operating with counter-flow of air and calcium chloride as the liquid desiccant. Charts have also been developed by Elsayed et al. [17] using a finite difference model to predict the effectiveness of heat and mass transfer in packed beds operated for air dehumidification using a liquid desiccant or for the regeneration of the weak liquid desiccant. Although the random packed tower facilitates high mass transfer by providing a large surface area in a relatively small volume, the air pressure drop through the packing is generally high. However, new types of regular packings have been introduced recently in contrast to the traditional, randomly placed packing materials [18].

1.2.3.2 Regular Packings

The new packing materials are fitted in an ordered and structured manner in the column to carefully match its size and operations. These packing materials are called as "structured packing" and have shown the excellent performance characteristics with a relatively low-pressure drop, in addition to easy installation. Illustration of a packed tower with structured packing is shown in Fig. 1.7. These packings are widely used in different industrial application such as crude oil distillation, cryogenic air separation plants, natural gas dehydration plants, acid gas removal in ammonia plants, OTEC research, etc. Recently attempts have been made to use structured packing for dehumidification/regeneration processes. In this study a method is developed to predict the performance of gauze-type structured packing column using liquid desiccant and air stream.

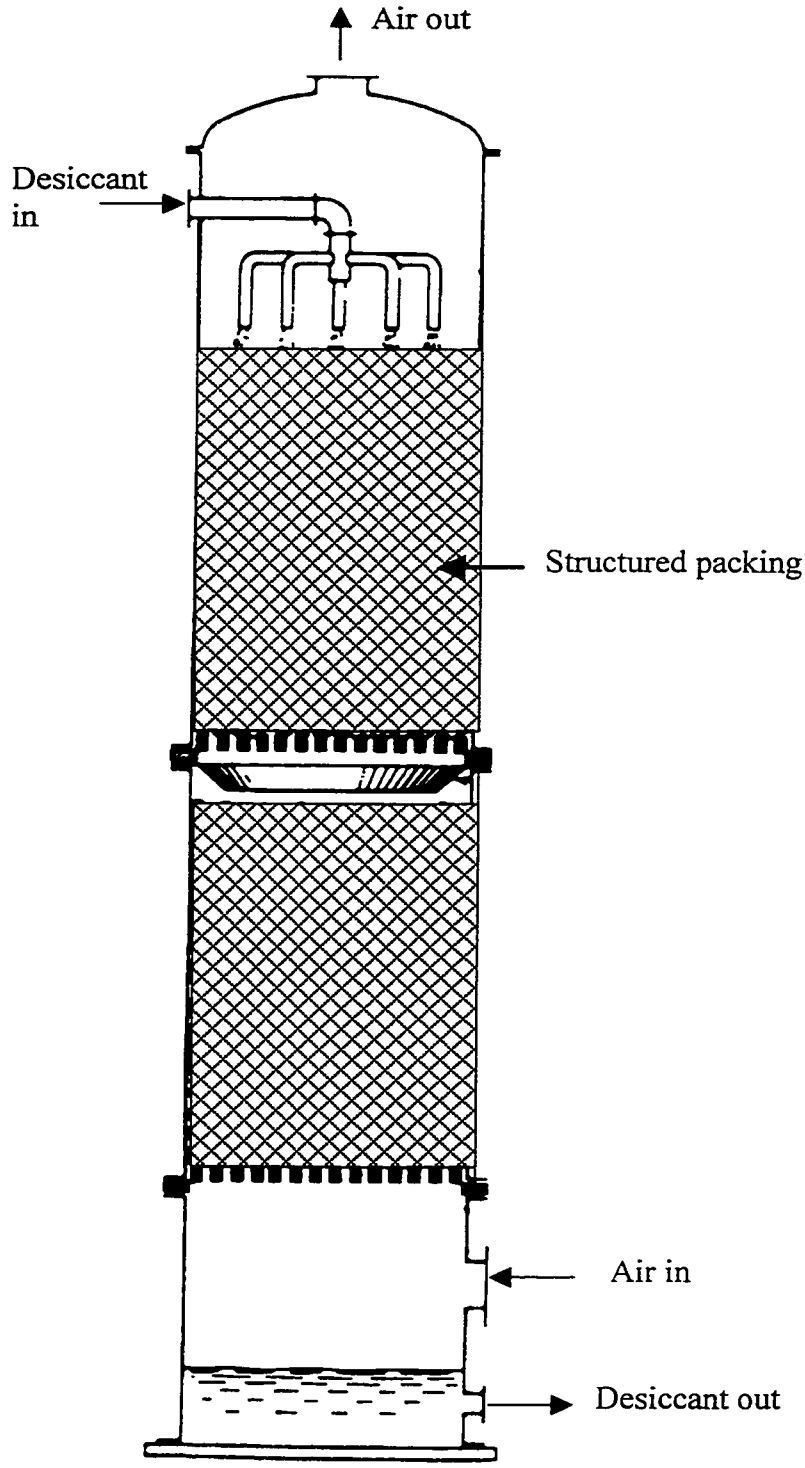

Fig. 1.7 Packed tower with structured packing.

CHAPTER 2

CALCULATION OF HEAT AND MASS TRANSFER COEFFICIENTS

2.1 Introduction

The dehumidifier and regenerator columns can be packed either with structured packing or random packing. The correlations for heat and mass transfer coefficients are required to design the dehumidifier/regenerator. A few reliable correlations for heat and mass transfer coefficients are available for random packing column [19, 20,21]; however, the data for structured packing towers are limited in the open literature. Potnis and Lenz [22] conducted experiments with random (polypropylene Tripack) and structured (Munters CELDEK) packings in the dehumidifier/regenerator of a solar assisted liquid desiccant (lithium bromide solution) system. The local overall liquid phase mass transfer coefficients in terms of the solution flow rate per unit cross sectional area for the packed bed alone were obtained by separating the contributions of the regions of small droplets created by the spray nozzles and the film flowing down the wall of the contactor. These mass transfer coefficients and the experimentally determined diffusivity values were then utilized to obtain dimensionless correlations between Sherwood number, Reynolds number and Schmidt number. Chung *et al.*[23] also conducted experiments with random (polypropylene flexi rings and Berl saddles) and structured (cross corrugated

cellulose and polyvinyl chloride) packings in the dehumidifier using lithium chloride solution. The overall gas phase heat and mass transfer correlations were developed that considered the change in driving force due to the change in lithium chloride concentration by using the Buckingham pi method. The above correlations are summarized in Table 2.1.

Bravo *et al.* [24] developed both the gas and liquid side mass transfer correlations for gauze-type structured packings when used under distillation conditions but they did not take into account the liquid phase mass transfer resistance. Further, they used HETP (Height Equivalent to a Theoretical Plate) approach. This is a simple method to design packed towers but ignores the differences between stepwise and continuous contact. In this method the number of theoretical plates required for a given change in concentration was computed and then multiplied by a quantity, the height equivalent to a theoretical plate (HETP) to give the required height of packing. The HETP must be an experimentally determined quantity characteristic for each packing. Unfortunately, HETP varies not only with the type and size of the packing but also vary strongly with flow rates of each fluid and for every system with concentration as well, so that enormous amounts of experimental data have to be accumulated. Hence this method has now largely been abandoned. From the above literature survey it is clear that only a few publications have appeared to date for using structured packing in the liquid desiccant applications. In this chapter a method is developed to predict the performance of gauze-type structured packing column using three different types of liquid desiccants namely calcium chloride solution, lithium

TABLE 2.1: Summary of Correlations

Author	Correlations
Potnis, Lenz[22] for double layer structured packing	For the dehumidifier, $K_x = 0.02(L^*)^{0.9}$ } for packing of 30 cm $Sh = 0.04\,\mathrm{Re}^{0.9}\,Sc^{0.5}$ $K_x = 0.015L^*$ } for packing of 55 cm $Sh = 0.03\,\mathrm{Re}\,Sc^{0.5}$ For the regenerator, $K_x = 0.01(L^*)^{1.1}$ } for packing of 30 cm $Sh = 0.01\,\mathrm{Re}\,Sc^{0.5}$ $K_x = 0.015L^*$ } for packing of 55 cm $Sh = 0.02\,\mathrm{Re}\,Sc^{0.5}$ where K_x = local overall liquid mass transfer coefficient, kmol/ m^2.s L^* = solution flow rate per unit cross-sectional area, kg/m^2.s
Chung, Ghosh, Hines[23] for the cross corrugated cellulose based structured packing	Mass transfer correlation, $K_{GA}a\left(\frac{M_t d_{eq}^{\ 2}}{D_G \rho_G}\right) = 2.25*10^{-4}(1-X)^{-0.75}\left(\frac{\dot{L}}{\dot{G}}\right)^{0.1}(Sc_G)^{0.333}(\mathrm{Re}_G)^{1.0}$ Heat transfer correlation, $\dot{h_{GA}}a\left(\frac{d_{eq}^{\ 2}}{k_G}\right) = 2.78*10^{-6}(1-X)^{1.8}\left(\frac{\dot{L}}{\dot{G}}\right)^{0.4}(\mathrm{Pr}_G)^{0.333}(\mathrm{Re}_G)^{1.6}$ where K_{GA} = overall gas phase mass transfer coefficient, kmol/m^2.s $\dot{h_{GA}}$ = heat transfer coefficient corrected for mass transfer, kW/m^2.K M_t = molecular weight of water, kg/kmol X = mass fraction of the salt in liquid solution, kg/kg $\dot{L}$ = liquid mass velocity, kg/m^2.s $\dot{G}$ = mass velocity of air, kg/m^2.s k_G = gas thermal conductivity, kW/m.K

chloride solution and the mixture of 50% calcium chloride and 50% lithium chloride solution (CELD) and an air stream. Heat and mass transfer coefficients of individual phases are also correlated.

2.2 Gauze-Type Structured Packings

Structured packings provide a means of continually redistributing the liquid desiccant flow, while supplying a relatively straightforward flow path for the air that reduces the pressure drop to a minimum. These packings can be either made in the form of sheet-type or gauze-type as corrugated sheets arranged such that air and liquid flowing between adjacent sheets undergo periodic redistribution within the packing. Experiments have shown that with sheet-type structured packings used for direct-contact condensation only 50% or less of the area is active but by using gauze-type structured packings the entire area can become effective [25]. Gauze-type structured packing surfaces, shown in Fig. 2.1, allow air-to-liquid contact on both sides and also provide for uniform liquid distribution due to capillary action. These packings increase the residence time of the liquid and the entire area of the packing can be effective in mass transfer.

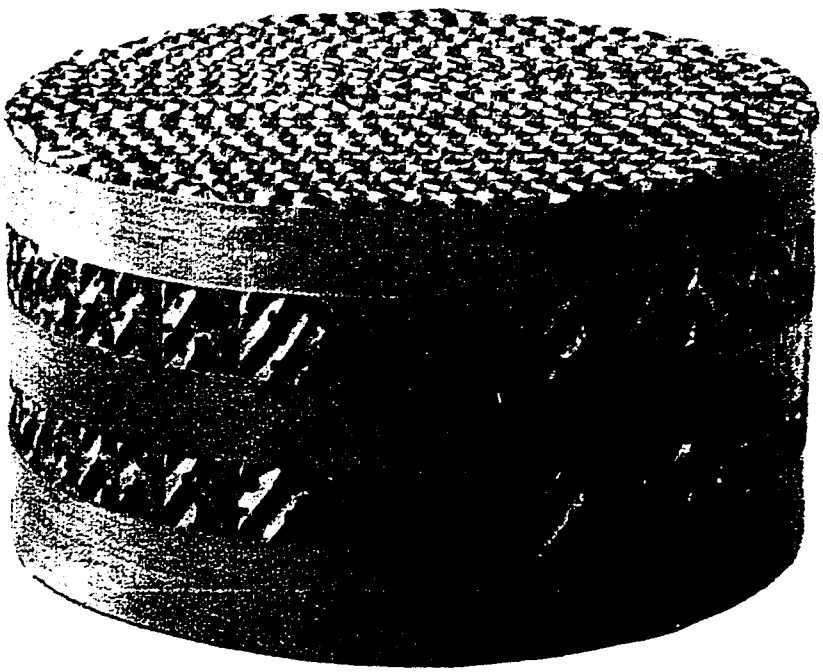

Fig. 2.1 Gauze-type structured packing.

The orientation of gauze-type structured packings as adjacent corrugated sheets are shown in Fig. 2.2a. The packing size is the variable that affects the heat and mass transfer coefficients for this type of packing. The packing size is replaced by an equivalent diameter of a flow channel in the packing, which is calculated by taking the arithmetic average of the hydraulic radius of different flow cross sections. In this geometry the cross section of the channel through which the air flows alternates between a triangle and a diamond as shown in Fig. 2.2b. To simplify the calculation, triangular and diamond-shaped geometry, as shown in Fig. 2.2c are used to estimate the hydraulic radii and equivalent diameter. To obtain a periodic redistribution of the air and the liquid flowing between adjacent sheets, the axis of the air flow channel is inclined 60° from the horizontal. The geometric information of the packing considered for the present study is given in Table 2.2.

Elements are stacked so the corrugations run at 90° orientation from the layers above and below. Liquid moves down the channel in counter-flow to the air stream. The gauze nature of the surface promotes capillary action so that very low rate of liquid flow can be spread into the liquid films covering most of the available surface. A considerable amount of surface can be placed in a given volume if the corrugation dimensions of the gauze are small.

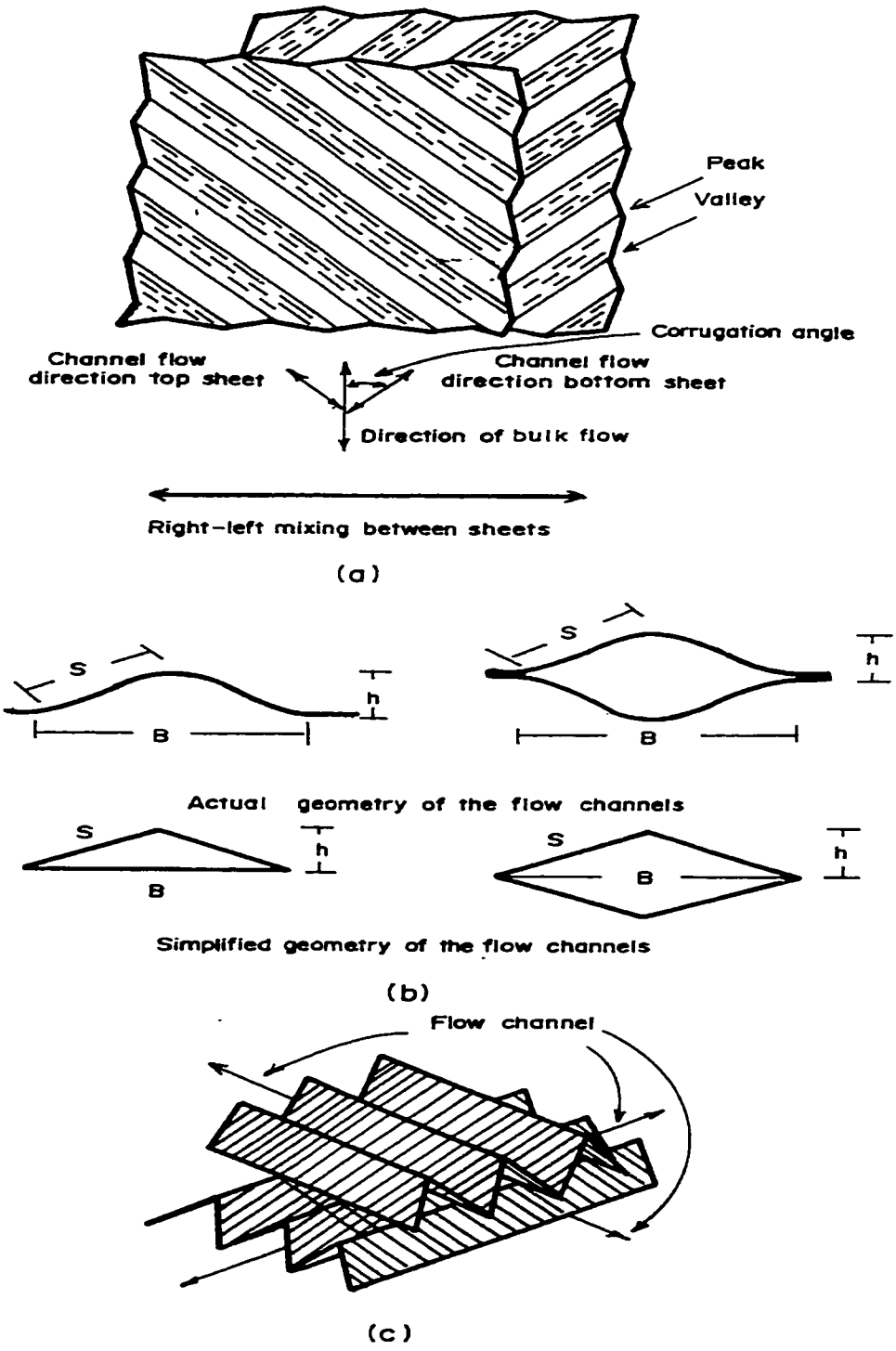

Fig. 2.2 Definition of structured packing dimensions and geometric orientation.

TABLE 2.2: Geometric Information of the Gauze-type Structured Packing

Properties	Gauze-type structured packing
Surface area, $m^2\ m^{-3}$	470
Crimp height, m	0.0067
Channel base, m	0.011
Channel side, m	0.0077
Equivalent diameter, m	0.0076
Void fraction	0.88
Crimp angle from horizontal, deg	60

2.3 System Analysis

In order to define an equivalent diameter between the triangle and the diamond cross-section for the air flow, Bravo *et al.* [24] approach is used. The hydraulic radius of triangular shaped channel is given by,

$$r_{ht} = \frac{Bh}{2(B+2S)} \tag{2-1}$$

The hydraulic radius of diamond shaped channel is given by,

$$r_{hd} = \frac{Bh}{4S} \tag{2-2}$$

The resulting equivalent diameter of a channel is given by the arithmetic average of these two hydraulic radii and is given by,

$$d = Bh\left[\frac{1}{2S} + \frac{1}{(2S+B)}\right] \tag{2-3}$$

Many investigations of heat and mass transfer in fluid-solid systems have indicated that the void fraction of packing is an important variable for the evaluation of the heat and mass transfer coefficients. The void fraction of structured packing is given by,

$$\varepsilon = 1 - \frac{4t}{d} \tag{2-4}$$

The total available packing surface area per unit volume is,

$$a_p = \frac{4\varepsilon}{d} \tag{2-5}$$

A more recent model that may be used to determine the heat and mass transfer coefficients in columns equipped with structured packings has been presented by Rocha *et al.* [26,27]. Liquid holdup as well as pressure drop is functions of liquid and air superficial velocities. The force acting on the liquid to move it downward through the packing is gravity. The three forces namely liquid buoyancy, vapor pressure drop and the drag on the liquid film by the vapor opposed gravity. The effective gravity is given by [26],

$$g_e = g\left[\left(\frac{\rho_L - \rho_G}{\rho_L}\right)\left(1 - \frac{\frac{\Delta P}{\Delta Z}}{1025}\right)\right] \tag{2-6}$$

Knowledge of liquid holdups is necessary to calculate the effective interfacial areas in the structured packing tower. The liquid physical properties and the shape and nature of the packing are important factors in determining the holdups. The total holdup refers to the total liquid in the packing under operating conditions, which comprises static and operating components. The static holdup represents the liquid that does not drain from the packing when the liquid supply to the column is discontinued. The surface tension of the liquid desiccant directly influences the static holdup. The operating holdup represents the liquid that will drain from the packing and is also a

measure of the liquid flowing through the packing when the column is in operation. The relation between the three holdups is given by,

$$H_{tot} = H_{st} + H_{op} = \frac{4}{S}\left(c_{st}\delta_{st} + c_{op}\delta_{op}\right) \tag{2-7}$$

The term c_{st} is a surface correction factor that accounts for all surfaces not being wet when only static holdup occurs. The relative static holdups and surface correction factor for various metal structured packing are given in reference [26]. c_{op} represents the corresponding correction factor when liquid flow is present. For static holdup an expression was presented [28] for film thickness on a horizontal smooth plate as a function of physical properties. Their expression has been corrected for the angle of inclination of the corrugations and for the buoyancy effect of the air density. The new expression for the thickness of the static holdup film is given by [26]

$$\delta_{st} = \left[2\sigma \frac{1-\cos\gamma}{\rho_L g\left(1-\frac{\rho_G}{\rho_L}\right)\sin\theta} \right]^{0.5} \tag{2-8}$$

where γ is the contact angle of the liquid with the solid surface, which accounts for surface material wettability.

For structured packings,

$$Cos\ \gamma = 0.9 \qquad \text{for} \qquad \sigma < 0.055\ N\,m^{-1}$$

$$Cos\,\gamma = 5.211 * 10^{-16.835\sigma} \quad \text{for} \quad \sigma \geq 0.055\ N\,m^{-1}$$

The liquid desiccants should have low surface tension so that the adequate wetting of the packing surfaces would be easily possible. Otherwise, some surfactants may be added to the desiccant solutions to lower their surface tension.

It is to be noted that the operating holdups are independent of the nature of the packing. The average film thickness during operation can be defined by a modification that incorporates the effective gravity and is given by,

$$\delta_{op} = \left[\frac{3\mu_L U_L}{\rho_L \varepsilon H_{tot} g_e Sin\theta}\right]^{0.5} \tag{2-9}$$

The contribution of static holdup to total holdup is usually very small for structured packing and it can be neglected since its calculation adds complexity to the model. Hence eqn. (2-7) can be simplified as,

$$H_{tot} = \frac{4}{S} c_{tot} \delta_{op} \tag{2-10}$$

where c_{tot} is a correction factor for total holdup in terms of available interfacial area and is given by,

$$c_{tot} = \frac{29.12(We_L Fr_L)^{0.15}(S)^{0.359}}{\mathrm{Re}_L^{0.2}\,\varepsilon^{0.6}((1-0.93Cos\gamma)(Sin\theta)^{0.3}} \tag{2-11}$$

The dimensionless numbers are based on the following:

$$We_L = \frac{U_L^{\,2}\rho_L S}{\sigma} \tag{2-12}$$

$$Fr_L = \frac{U_L^{\,2}}{Sg} \tag{2-13}$$

$$\mathrm{Re}_L = \frac{U_L S \rho_L}{\mu_L} \tag{2-14}$$

Equation (2-11) is combined with eqns. (2-9) and (2-10) to give,

$$H_{tot} = \left(4\frac{c_{tot}}{S}\right)^{\frac{2}{3}}\left[\frac{3\mu_L U_L}{\rho_L \varepsilon g_e Sin\theta}\right]^{\frac{1}{3}} \tag{2-15}$$

The effective air velocity is dependent on the superficial air velocity, the void fraction of the packing, the flow channel inclination and the total holdup. This is given by,

$$U_{Ge} = \frac{U_G}{\varepsilon(1-H_{tot})Sin\theta} \tag{2-16}$$

The gauge packing, capillary forces spread the liquid into a thin film to cover the entire available area. The effective liquid film velocity is given by,

$$U_{Le} = \frac{U_L}{\varepsilon H_{tot} Sin\theta} \tag{2-17}$$

A relative velocity of gas to liquid is defined as,

$$U_r = U_{Le} + U_{Ge} \tag{2-18}$$

The heat and mass transfer coefficients must be coupled with the effective interfacial area in order to be useful for structured packing column analysis and design. In order to evaluate the effective surface coverage, the initial liquid distribution, radial migration of liquid in the bed, surface wettability, and surface texturing must be taken into consideration. The amount of surface area available in the system is directly related to operating holdup. An expression for the interfacial area based on fluid hydraulics over an inclined plate is developed by Shi and Mersmann [28]. But structured packing interfacial areas are relatively uninfluenced by gas rate and to be much more dependent on liquid rate. Rocha *et al.* [27] evaluated the effective interfacial area for gauze surfaces and is given by,

$$a = a_p \left[1 - 1.203 \left(\frac{U_L^{\,2}}{Sg} \right)^{0.111} \right] \tag{2-19}$$

The gas-phase mass transfer coefficient based on extensive earlier investigation of wetted wall columns [29] is expressed as,

$$Sh_G = C_1 (\mathrm{Re}_G)^m (Sc_G)^n \tag{2-20}$$

where C_1 is the constant and the dimensionless groups Sh_G and Re_G are defined on the basis of packing geometry and are given by,

$$Sh_G = \frac{F_G d}{D_G} \tag{2-21}$$

$$\mathrm{Re}_G = \frac{U_r d \rho_G}{\mu_G} \tag{2-22}$$

$$Sc_G = \frac{\mu_G}{\rho_G D_G} \tag{2-23}$$

Here F_G represents the gas-side mass transfer coefficient in m/s. These F-type mass transfer coefficients can be converted to k-type coefficients as given by Treybal [30]. For the available database for structured packing, the values of $m = 0.8$ and $n = 0.333$ were found [31] but C_l to be determined experimentally. Rocha *et al.*[27] have proposed the same wetted-wall relationship for the structured packing with C_l = 0.054. By combining equations (2-20) to (2-23) the gas-side mass transfer coefficient is given by,

$$F_G = 0.054\left(\frac{D_G \rho_G}{d M_G}\right)\left(\frac{U_r d \rho_G}{\mu_G}\right)^{0..8}\left(\frac{\mu_G}{\rho_G D_G}\right)^{0.333} \tag{2-24}$$

Unlike gas-side mass transfer coefficient, little data are available in the open literature for computing the liquid side mass transfer coefficient. For the liquid-side mass transfer coefficient, a simple penetration model is used, with exposure time based on liquid flow across one corrugation face of the packing. For the present study, the

liquid resistance is significant and hence, the penetration approach can be used with a modified exposure time [27] and is given by,

$$t_e = \frac{S}{C_2 U_{Le}} \tag{2-25}$$

For many well known structured packing $C_2 \approx 0.9$ is assumed. The liquid side mass transfer coefficient is given by,

$$F_L = 2\left(\frac{D_L}{\pi t_e}\right)^{0.5}\left(\frac{\rho_L}{M_L}\right) \tag{2-26}$$

The mass transfer coefficients as given by eqns. (2-24) and (2-26) can be coupled with the effective interfacial area of eqn. (2-19) to obtain the volumetric mass transfer coefficients. The diffusion coefficient for the gas and liquid are determined as given by Treybal [30].

Through the heat-mass transfer analogy, the heat transfer coefficient for the gas phase can be calculated as follows:

$$h_G = F_G M_G C_G \left(\frac{Sc_G}{\mathrm{Pr}_G}\right)^{\frac{2}{3}} \tag{2-27}$$

Similarly the liquid phase heat transfer coefficient is given by,

$$h_L = F_L M_L C_L \left(\frac{Sc_L}{\mathrm{Pr}_L} \right)^{\frac{2}{3}} \qquad (2\text{-}28)$$

A computer program was developed to calculate the heat and mass transfer coefficients for air phase and liquid phase for gauze-type structured packing by making use of equations (2-19), (2-24), (2-26), (2-27), and (2-28) for different operating parameters.

2.4 Results and Discussion

In order to carryout the above calculation, the effect of different varying properties such as density, viscosity, specific heat and thermal conductivity of air and the liquid desiccant have been brought into account in the computer program. The property data equations for different desiccant solutions and air are given in the Appendix I. The effective gas and liquid rates take into account the flow angle, void fraction and film thickness that derives from gross flow rates and packing geometry. The effect of some of the liquid desiccant parameters such as concentration, temperature, and flow rate has been presented as correlated equations (2-31) – (2-36). To better understand the effect of these parameters, the results are also presented in the form of figures. It is observed that the correlations for $h_G a$ and $F_G a$ are independent of the properties of the desiccant used. They are dependent on the flow rates of air and liquid and the temperature of the air. Therefore, the correlations presented in this study for $h_G a$ and $F_G a$ are valid for any liquid desiccants used in the

gauze-type, structured packing and they are given as follows:

$$h_G a = 12.96(U_{Le})^{0.1}(U_{Ge})^{0.79}\exp(-0.026T_G) \tag{2-29}$$

$$F_G a = 0.55(U_{Le})^{0.1}(U_{Ge})^{0.79}\exp(-0.0293T_G) \tag{2-30}$$

It can be observed that $h_G a$ and $F_G a$ strongly depend on the flow rate of the air stream and are a weak function of the air temperature.

The computed correlations for $h_L a$ and $F_L a$ for various liquid desiccant – air contact system are given as follows:

Calcium chloride – air contact system:

$$h_L a = 15.66(U_{Le})^{0.4}(U_{Ge})^{0.07}\exp(-0.031T_L)\exp(0.0025\xi) \tag{2-31}$$

$$F_L a = 6.27(U_{Le})^{0.4}(U_{Ge})^{0.07}\exp(-0.033T_L)\exp(0.0066\xi) \tag{2-32}$$

Lithium chloride – air contact system:

$$h_L a = 15.1(U_{Le})^{0.4}(U_{Ge})^{0.07}\exp(-0.031T_L)\exp(0.003\xi) \tag{2-33}$$

$$F_L a = 8.2(U_{Le})^{0.4}(U_{Ge})^{0.07}\exp(-0.038T_L)\exp(0.009\xi) \tag{2-34}$$

Mixture of lithium chloride and calcium chloride (CELD) – air contact system:

$$h_L a = 15.28(U_{Le})^{0.4}(U_{Ge})^{0.07}\exp(-0.031T_L)\exp(0.0028\xi) \tag{2-35}$$

$$F_L a = 7.0(U_{Le})^{0.4}(U_{Ge})^{0.07}\exp(-0.0352T_L)\exp(0.0076\xi) \tag{2-36}$$

The accuracy of the above correlations is 99.8% and they are believed to be reasonably free of end effects. They are valid for the range of the following operating parameters: U_{Ge} = 8.5 to 14.5 m/s ; U_{Le} = 0.03 to 0.27 m/s ; T_G = 30 to 70°C; T_L = 30 to 60°C; for calcium chloride, ξ = 35 to 45%; for lithium chloride, ξ = 30 to 40%. The various properties for calcium chloride, lithium chloride and CELD are given in the references [32,33,11] respectively. The above ranges are selected based on the preliminary study of a 5-ton hybrid liquid desiccant-based vapor compression cooling system.

From the above correlations it can be seen that the heat and mass transfer coefficients computed for the aqueous solutions are strong functions of liquid flow rate rather than the flow rate of air and they are independent of air temperature. The effect of the temperature of the liquid desiccant is more significant than its concentration.

In order to give confidence in the correlations that have been developed in this study, the volumetric heat and mass transfer coefficients for air are compared with those predicted by correlations (based on experimental data) proposed by Chung *et al.* [23] in Figs. 2.3 and 2.4, respectively. The proposed correlation over-predicts the volumetric heat transfer coefficient for air as shown in Fig. 2.3. Discrepancies in the predicted values from Chung *et al.* may be attributed partly to experimental error and partly to the failure to maintain adiabatic conditions in the column. Further, the liquid flow rate may be small to wet the entire structured packing. It is reported that

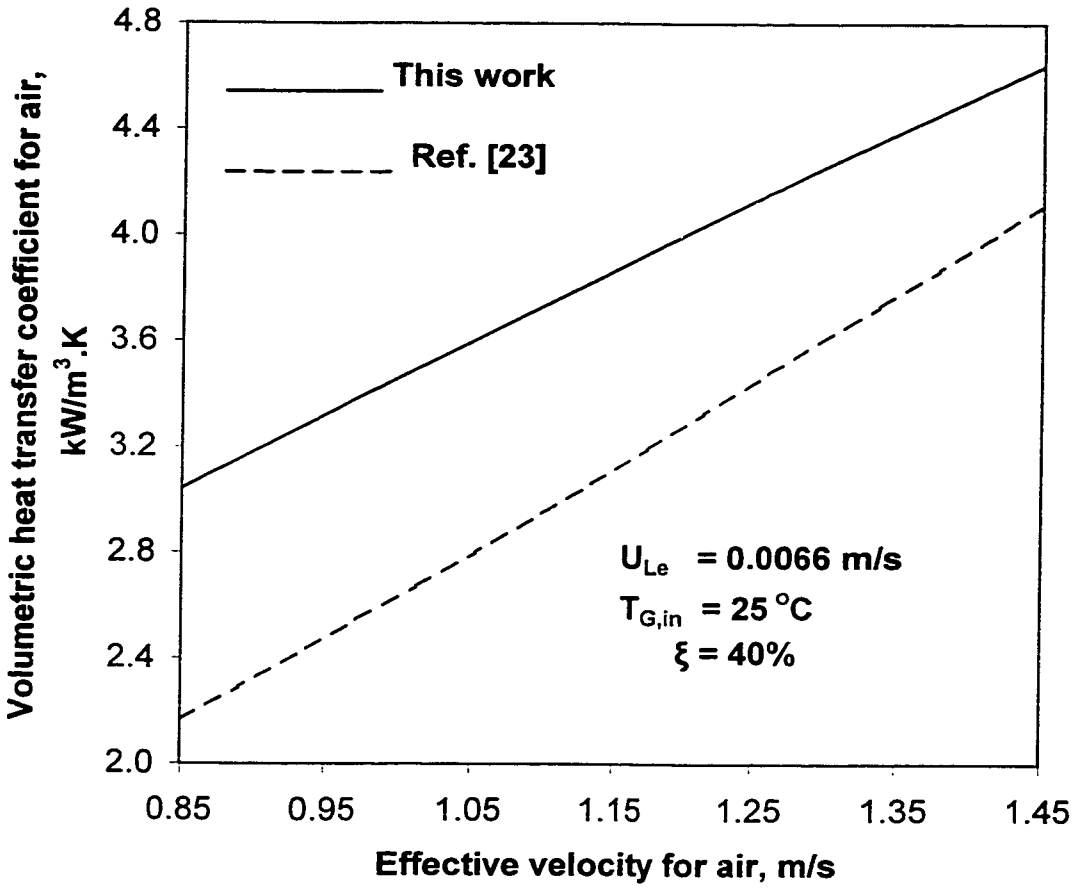

Fig. 2.3 Comparison of predicted volumetric heat transfer coefficient for air with those obtained using Chung et al. data.

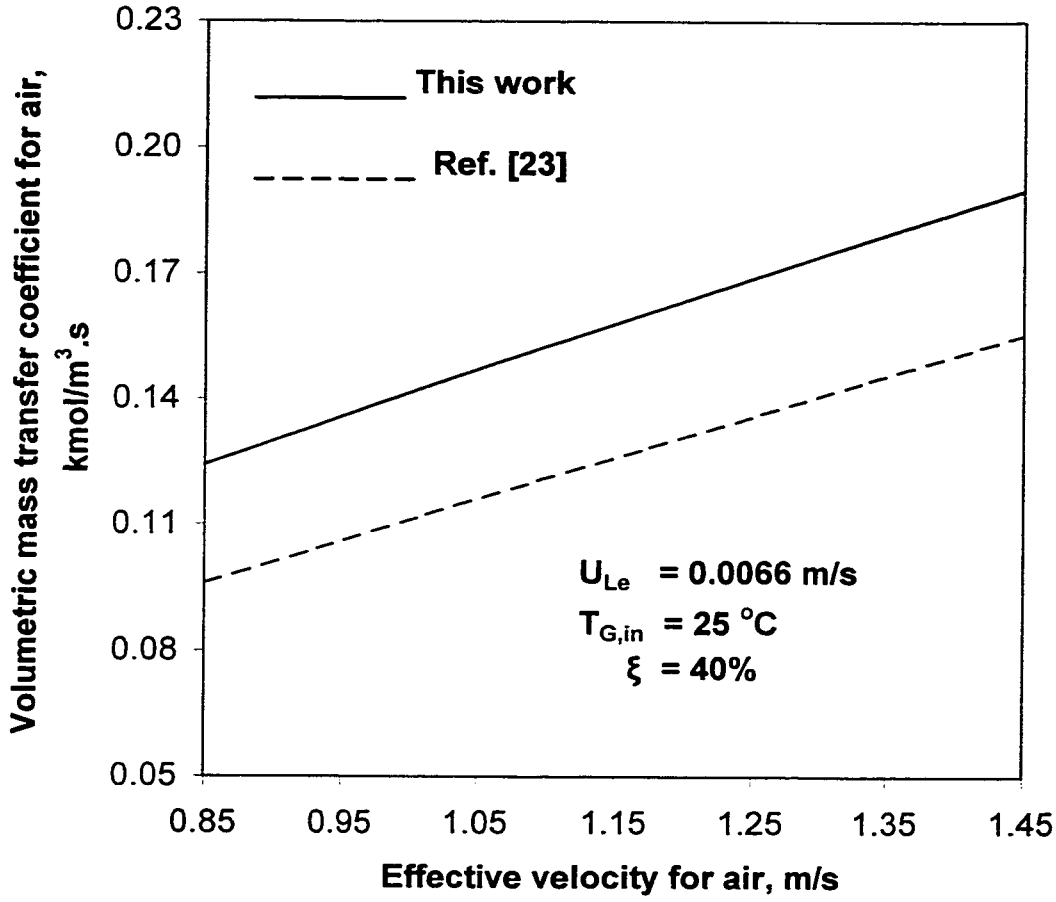

Fig. 2.4 Comparison of predicted volumetric mass transfer coefficient for air with those obtained using Chung et al. data.

[34] even though the liquid flow rates are high as compared to the air flow rate, complete wetting of the packing is difficult to maintain. Therefore, the mass transfer area is less than the packing surface area. Due to these reasons, the correlation proposed by Chung *et al.* based on experimental data under-estimates the volumetric mass transfer coefficient for air, as shown in Fig. 2.4. Further, in order to obtain the volumetric transfer coefficients for air, the effect of air temperature was not found in investigations conducted by Chung *et al.* It is to be noted that they did not develop the volumetric heat and mass transfer coefficients for liquid.

The volumetric heat and mass transfer coefficients proposed for liquid cannot be compared with the correlations developed by Potnis and Lenz [22] since they used lithium bromide solution. Further, they developed the correlations for local overall liquid phase mass transfer coefficient only in terms of solution flow rate per unit cross sectional area as given in Table 2.1 and their study showed no dependency of the air flow rate, liquid temperature, and liquid concentration on mass transfer coefficient.

The liquid-phase mass transfer coefficient as a function of effective liquid velocity is shown in Fig. 2.5. From the figure, the liquid phase mass transfer coefficient increases as the effective liquid velocity increases. The difference of volumetric mass transfer coefficient between any two desiccants increases as the effective liquid velocity increases. The lithium chloride has the highest rate of liquid-phase mass transfer coefficient when compared with the other two desiccants namely calcium chloride and the mixture of these two desiccants, due to its molecular weight as represented in eqn. (2-26). A considerable increase in

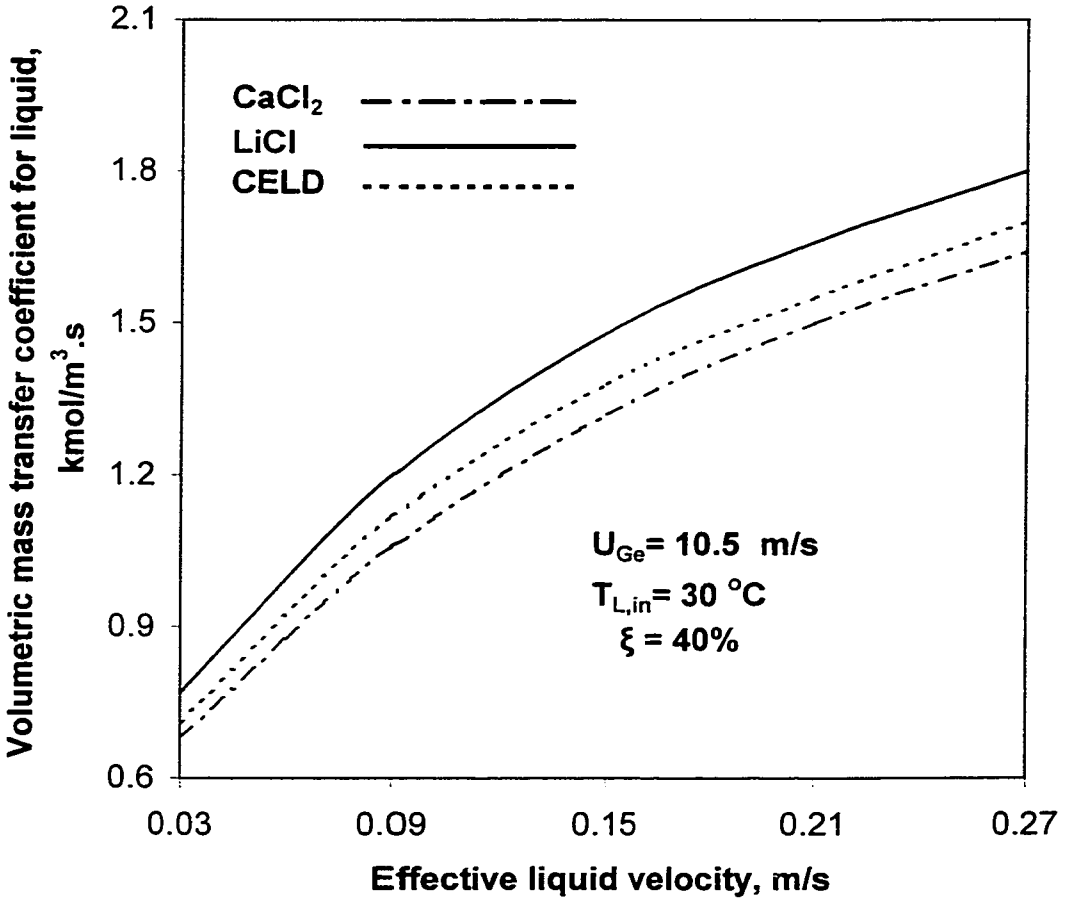

Fig. 2.5 Effect of desiccant velocity on liquid-phase mass transfer coefficient.

liquid-phase mass transfer coefficient is evident for the mixture of calcium and lithium chloride solutions compared to calcium chloride alone.

The effects of desiccant concentration on the liquid-phase mass transfer coefficient are shown in Fig. 2.6. The mass transfer coefficient increases slightly with the increase in desiccant concentration. From Figs. 2.5 and 2.6, it is clear that the mass transfer coefficient of the liquid desiccants is a stronger function of effective liquid velocity (that is, desiccant flow rate) rather than its concentration.

The liquid-phase mass transfer coefficient as a function of liquid desiccant inlet temperature is shown in Fig. 2.7. The mass transfer coefficient decreases as the desiccant inlet temperature increases. Lithium chloride has higher mass transfer coefficient compared with other desiccants. At about 55°C all the three desiccants have the same mass transfer coefficient and further increase in temperature results in reversing this trend. This is probably due to the decreasing viscosity of the desiccants with different rate with increase in temperature. A viscosity decrease may result in an increase in the effective area for mass transfer by decreasing liquid film thickness and solution holdup in the packing. From the results it is clear that for effective dehumidification process, the desiccant inlet temperature must be kept low.

The liquid-phase volumetric heat transfer coefficient as a function of desiccant inlet temperature is shown in Fig. 2.8. The heat transfer coefficient increases as the desiccant inlet temperature decreases. From Figs. 2.7 and 2.8, it is clear that the volumetric heat and mass transfer coefficients for the liquid-phase are strong function of the desiccant inlet temperature. It is observed that at a given temperature, calcium

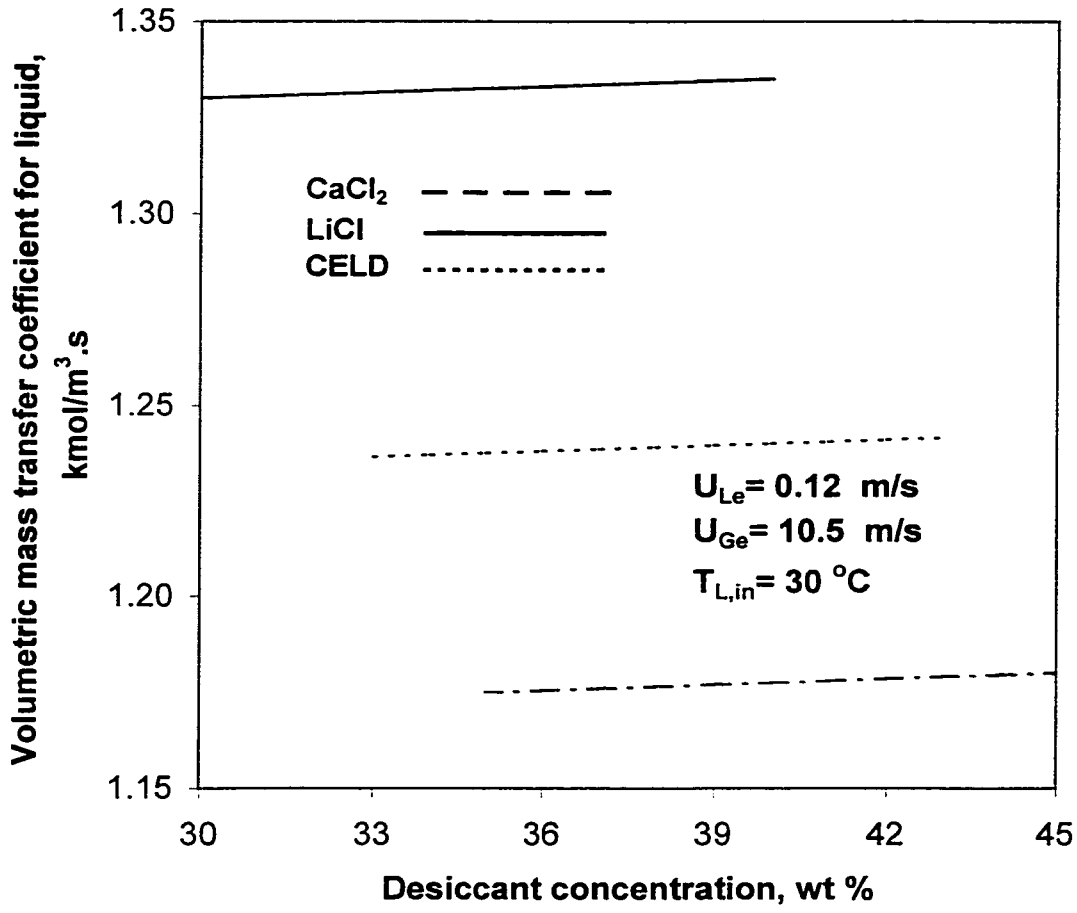

Fig. 2.6 Effect of desiccant concentration on liquid-phase mass transfer coefficient.

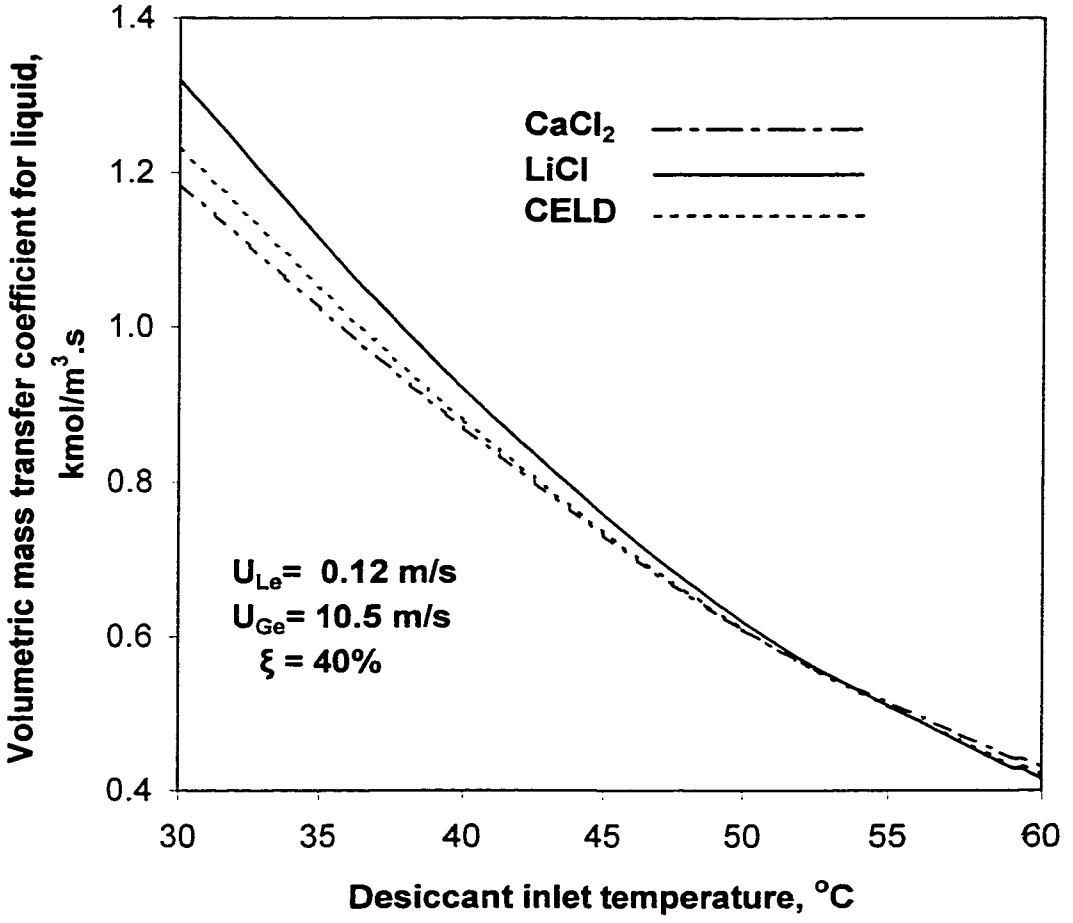

Fig. 2.7 Effect of desiccant inlet temperature on liquid-phase mass transfer coefficient.

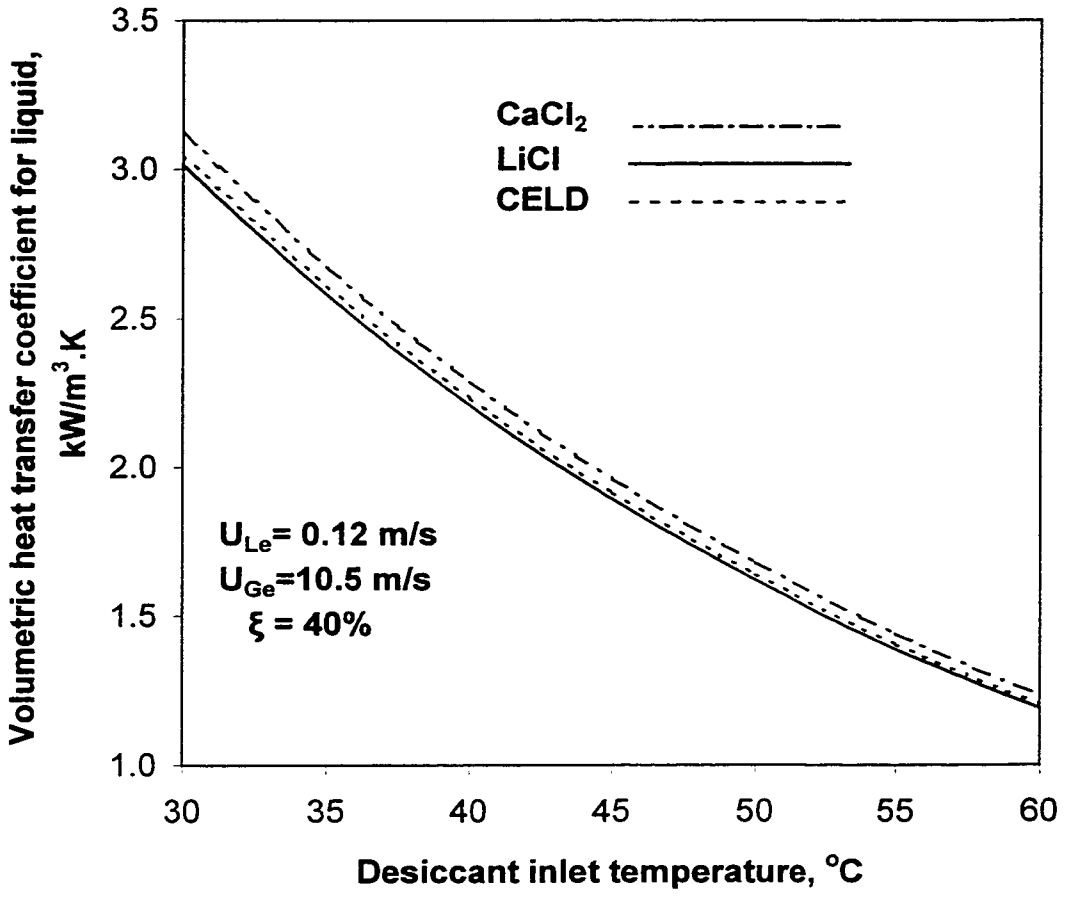

Fig. 2.8 Effect of desiccant inlet temperature on liquid-phase heat transfer coefficient.

chloride has higher heat transfer coefficient than other desiccants. This is due to the fact that for the given temperature and concentration, calcium chloride has higher vapor pressure than other desiccants. In other words, at a given temperature, heat transfer coefficient decreases with increase in the desiccant concentration. Hence, the desiccant concentration has an opposite effect on heat transfer coefficient than on mass transfer. The increase in viscosity of the desiccant due to its increase in concentration reduces the heat transfer.

The change of the liquid-phase heat transfer coefficient with effective liquid velocity is shown in Fig. 2.9. This figure indicates that the heat transfer coefficient is a strong function of the desiccant flow rate. However, the change of the heat transfer coefficients is almost the same for all three desiccants. This suggests that the solvent dominate the liquid-phase heat transfer coefficient rather than the solute.

The effects of desiccant concentration on the liquid-phase heat transfer coefficient are shown in Fig. 2.10. From the figure it is clear that the desiccant concentration has negligible effect on the heat transfer coefficient. Calcium chloride solution has the highest heat transfer coefficient for the same concentration due to its molecular weight, as represented in eqn. (2-28).

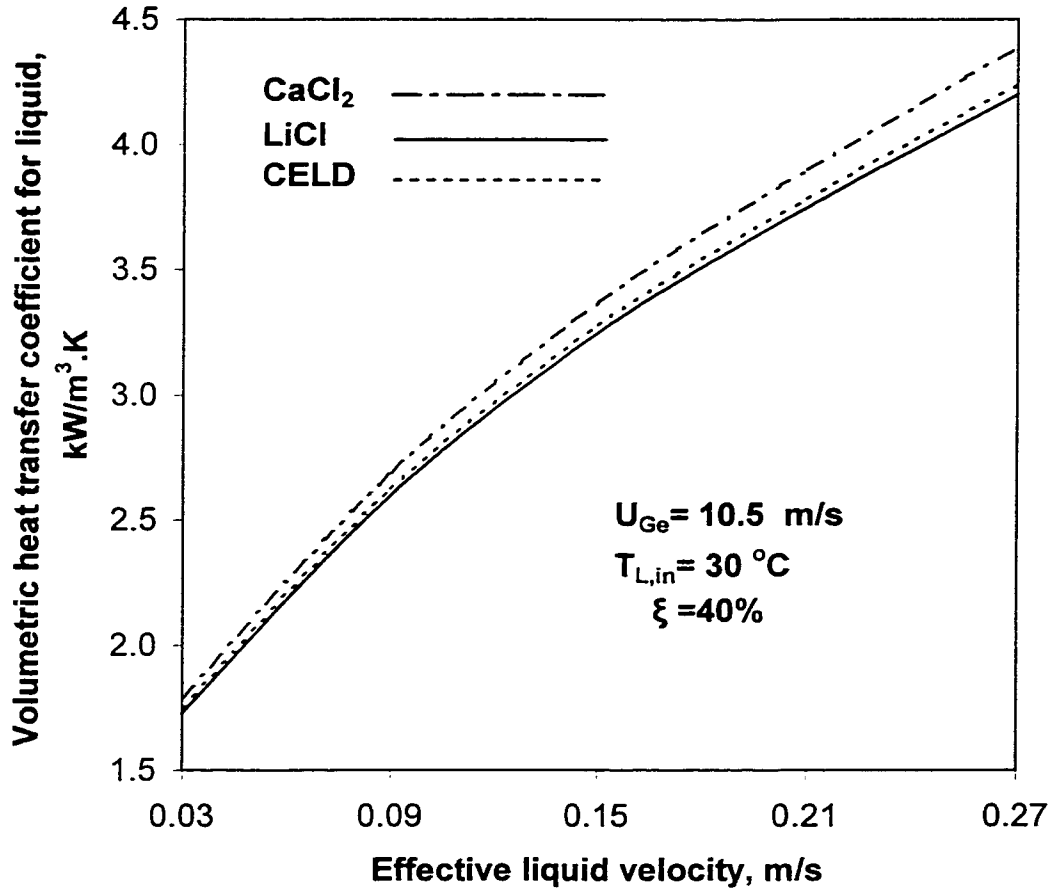

Fig. 2.9 Effect of desiccant velocity on liquid-phase heat transfer coefficient.

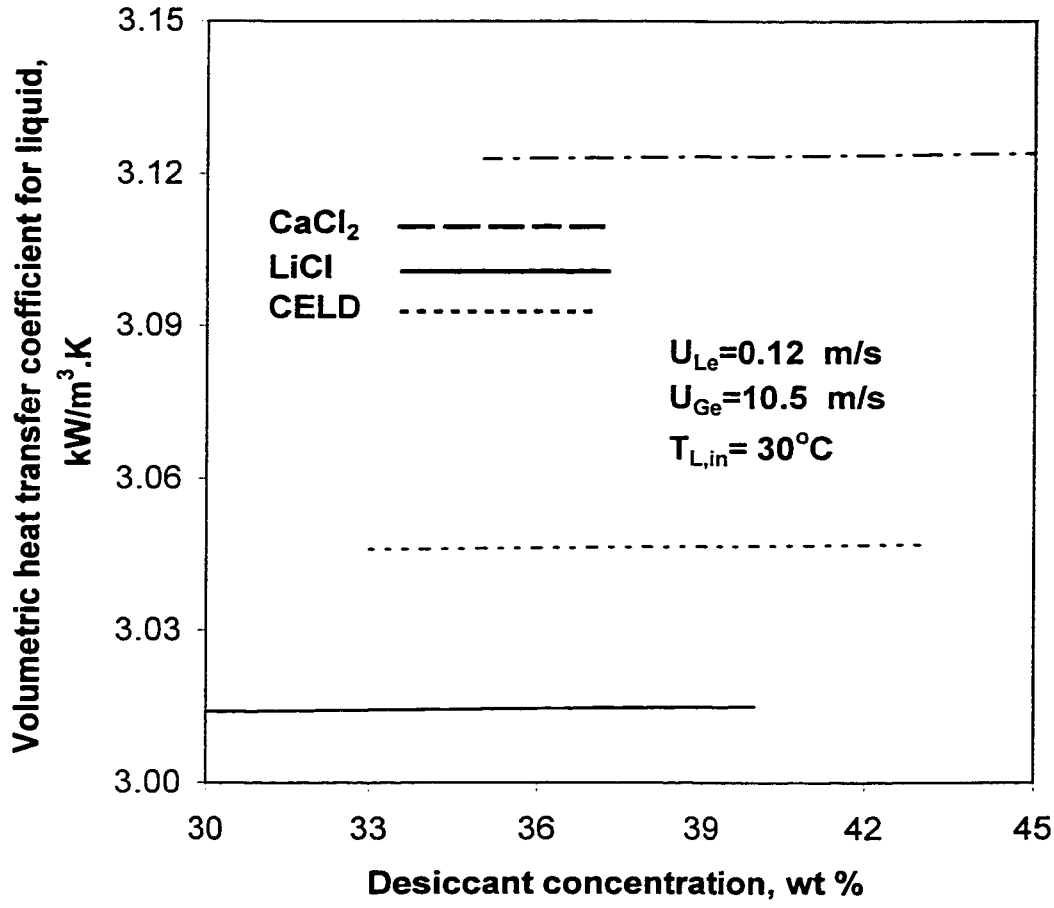

Fig. 2.10 Effect of desiccant concentration on liquid-phase heat transfer coefficient.

CHAPTER 3

HEAT AND MASS TRANSFER ANALYSIS OF THE STRUCTURED PACKING DEHUMIDIFIER

3.1 Introduction

The dehumidification process in a structured packing tower involves simultaneous heat and mass transfer. The driving potential is the difference in partial pressure of water vapor in the air and the desiccant at the interface. The interfacial condition is a function of the desiccant's concentration and temperature and also of the air absolute humidity and temperature. During the operation the composition and temperature of both streams vary from the bottom to the top of the tower. In this system, resistance to mass transfer in the liquid phase must also be considered because of the concentration of the desiccant [35]. The summary of the previous studies in the dehumidifier performance for the last ten years is given in Table 3.1. The table shows the parameters describing the performance, the desiccant used, the packing type used and whether experiments were conducted. The effect of various parameters on the dehumidification system's performance such as that of:

(i) inlet liquid temperature and concentration,

(ii) air humidity and temperature of air entering the tower,

TABLE 3.1: Packed Bed Dehumidifier Performance

Reference	Desiccant	Packing	Performance Parameter	Experiments
Öberg and Goswami (1998)	TEG	1 in Polyproplene Rauschert Hiflow rings	m_{cond} ε_Y	Yes
Potnis and Lenz (1996,1994)	LiBr	Random Polyproplene Tripack and structured Munter's CELDEK	m_{cond}	Yes
Khan (1996,1994)	LiCl	———	ε_Y, ε_H	No
Chung et al. (1995)	TEG	5/8 in Polyproplene flexi rings, ½ in ceramic Intalox saddles, 0.28 in structured cellulose and PVC	ε_Y K_Ga	Yes
Elsayed et al. (1993)	$CaCl_2$	25 mm Raching Rings	ε_h, ε_m	No
Chung et al. (1993)	LiCl	5/8 in Polyproplene flexi rings	ε_Y K_Ga	Yes
McDonald et al. (1992)	CELD	Intalox Snowflake	$T_{a,OUT}$ Y_{OUT}	Yes
Patnaik et al. (1990)	LiBr	Polyproplene Tripack no. ½	m_{cond}	Yes

(iii) air humidity leaving the tower, and

(iv) flow rates of liquid and air

have been considered in the present study and discussed in this chapter. Packing height will be calculated for different parameters as discussed above.

3.2 Modeling Considerations

Many theoretical models for packed bed absorption dehumidifiers have been developed. A finite difference model was developed by Factor and Grossman [36]. In this model, it was assumed that the resistance to heat and mass transfer in the liquid phase is negligible. However, some experimental findings suggest that the resistance to mass transfer in the liquid phase may be dominating [37]. The present study includes resistance to mass transfer in the liquid phase.

Stevens et al. [38] developed an effectiveness-NTU model analogous to an effectiveness-NTU model used in heat exchanger analysis. However, the number of transfer units (NTU) was based on the air flow rate rather than the minimum fluid capacity rate. Sadasivam and Balakrishnan [39] improved this effectiveness-NTU model by considering the minimum fluid capacity rate when calculating the number of transfer units. A linear relationship between saturated air enthalpy and temperature is introduced in this model. The main advantage of an effectiveness-NTU model is that the computational time is decreased although it needs iteration.

Aside from the above theoretical models, Khan [40] and Khan and Ball [41] presented formulations based on fitted algebraic equations. They are not very general

since the algebraic equations depend on system-dependent variables such as the ratio of liquid to air flow rate, the number units in the tower, and the desiccant used. To promote mass transfer in dehumidification process, it is desired that the liquid desiccant "wet" the packing and spread evenly over its surface. The packing should have a large surface area per unit volume and possess desirable hydraulic characteristics. Liquid desiccant dehumidification system with structured packing is proposed for this research.

3.3 Finite Difference Model

For the present study, a finite difference model based on the model by Treybal [42] is employed. The following assumptions are made in deriving a set of governing equations for an adiabatic desiccant mixture-air contact system:

(1) Heat loss through the tower wall is negligible.

(2) The interface temperature is equal to the temperature of the bulk liquid.

(3) The packing is adequately irrigated, that is, the interfacial surface is the same for heat and mass transfer.

(4) No axial dispersion occurs in the structured packing tower.

A schematic representation of a differential section of the packed bed is shown in Fig. 3.1. The governing equations are obtained by dividing the packed bed height Z into small segments, dZ. Mass and energy balances are then solved for each segment, from the bottom to the top of the tower.

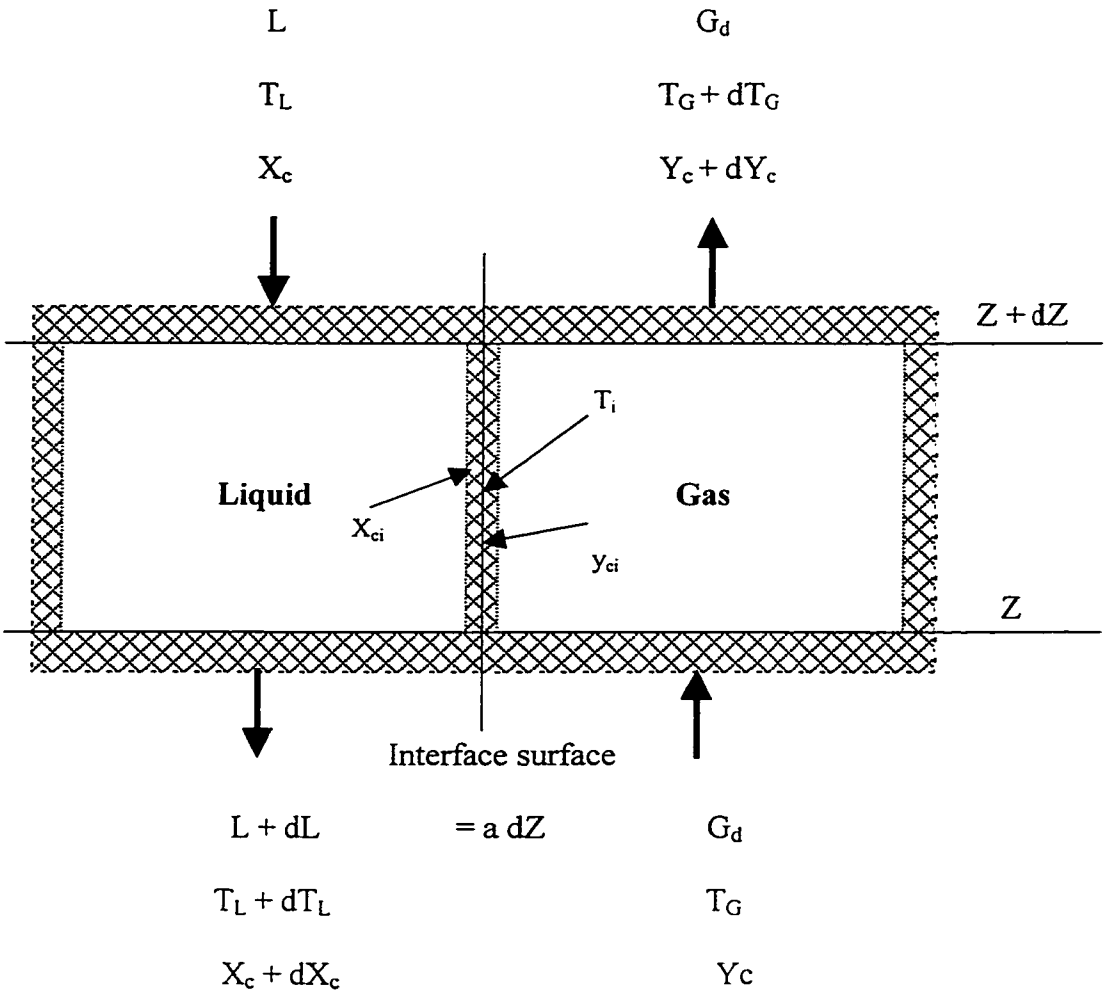

Fig. 3.1 Differential section of a structured packing tower.

A mass balance over the differential element yields,

$$dL = G_d dY \tag{3-1}$$

The mass flux of water vapor across the interface. taken positive from the air to liquid, is

$$N_C M_w a dZ = F_G M_w a dZ \ln\left(\frac{1-y_{ci}}{1-y_c}\right) = -G_d dY \tag{3-2}$$

Equation (3-2) gives the change in air humidity across the segment as

$$\frac{dY}{dZ} = -\frac{M_w F_G a}{G_d} \ln\left(\frac{1-y_{ci}}{1-y_c}\right) \tag{3-3}$$

The interfacial gas phase concentration is given by

$$y_{ci} = 1-(1-y_c)\left(\frac{x_c}{x_{ci}}\right)^{\frac{F_L}{F_G}} \tag{3-4}$$

Vapor-liquid equilibrium data for the desiccant solutions are used along with equation (3-3) to solve for the interface concentrations in the gas and liquid phases.

The heat transfer flux from the air to the interface is,

$$q_G a dZ = h_G' a(T_G - T_i) dZ \tag{3-5}$$

where h'_G is the heat transfer coefficient corrected for simultaneous heat and mass transfer as follows:

$$h_G^{'}a = \frac{-G_d C_v \dfrac{dY}{dZ}}{1-\exp\left(\dfrac{G_d C_v \dfrac{dY}{dZ}}{h_G a}\right)} \tag{3-6}$$

The specific enthalpy of moist air is

$$H_G = C_G(T_G - T_0) + Y[C_v(T_G - T_0) + \lambda_0] \tag{3-7}$$

Since this enthalpy is a function of the air temperature and humidity, the differential change in air enthalpy is found from the partial derivatives of H_G:

$$dH_G = (C_G + C_v)dT_G + [C_v(T_G - T_0) + \lambda_0]dY \tag{3-8}$$

The energy balance on the air side gives the air temperature gradient across the segment as,

$$\frac{dT_G}{dZ} = \frac{-h_G^{'}a(T_G - T_i)}{G_d(C_G + YC_v)} \tag{3-9}$$

Similarly the liquid temperature gradient can be derived and is given by,

$$\frac{dT_L}{dZ} = \frac{G_d}{C_L L}\left\{(C_G + YC_v)\frac{dT_G}{dZ} + [C_v(T_G - T_0) - C_L(T_L - T_0) + \lambda_0 - \Delta H_s]\frac{dY}{dZ}\right\} \tag{3-10}$$

Equation (3-4) must be solved simultaneously with the vapor-liquid equilibrium data for desiccants.

3.4 Vapor-Liquid Equilibrium Data

The following functional relation gives the equilibrium distribution for any desiccant:

$$y_{ci} = A' + B'T_i - \frac{C'}{x_{ci}} \tag{3-11}$$

where A', B' and C' are constants for the range of operating conditions of interest.

The interfacial gas phase concentration must be solved simultaneously with the vapor-liquid equilibrium data for liquid desiccants. The following functional relations are calculated and they give the equilibrium distribution for various liquid desiccants:

For calcium chloride solution:

$$y_{ci} = 0.040416 + 0.00091228T_i - \frac{0.030388}{x_{ci}} \tag{3.12}$$

For lithium chloride solution:

$$y_{ci} = 0.01912364 + 0.0003504T_i - \frac{0.012567}{x_{ci}} \tag{3.13}$$

For mixture of lithium chloride and calcium chloride (CELD) solution:

$$y_{ci} = 0.02977 + 0.00063134T_i - \frac{0.02147}{x_{ci}} \tag{3.14}$$

The interfacial condition x_{ci} and y_{ci} are determined by the incremental search method for every section of the dehumidifier. The analysis presented above will evaluate the performance of the dehumidifier with the following given parameters: liquid inlet temperature and concentration, air inlet temperature and the humidity, exiting air humidity or desired level of dehumidification and the flow rates of liquid and air. The output will be the height of the structured packing, exit air temperature and humidity, and exit liquid temperature and concentration. The calculation starts at the bottom of the tower where $Z = 0$.

3.5 Computational Procedure

The computation starts with reading the inlet conditions of air and liquid, and the exit humidity of the air. A reference temperature is assumed. Calculations start by assuming the exit temperature of the liquid. Then the structured packing height is divided into N sections and N is chosen as 100. The liquid and air exit conditions are calculated from the mass and energy balance in every section. The program is initialized from the bottom of the dehumidifier with the guessed liquid exit temperature. First the heat and mass transfer coefficients are calculated as given in the previous chapter and then interface moisture condition is calculated. The concentration and temperature gradients are calculated along the Z direction. After this step the incremental dehumidifier height is calculated for the given change in the absolute

humidity. Then for the next incremental dehumidifier section, the air and liquid properties are updated.

The same calculation of interface moisture conditions is repeated for each section. When the *(N+1)* cross section or N^{th} dehumidifier section is processed, the program reaches the top of the column. Here the calculated liquid inlet temperature is compared with the given value. If the difference of the two values is larger than a given error, a new appropriate liquid exit temperature is assumed and iterations are repeated until the convergence is reached. An over relaxation method is used for this iterative calculation.

The results are liquid and air temperatures, liquid concentration, air exit humidity and dehumidifier packing height. The liquid and air humidity profile can also be determined, if desired.

3.6 Results and Discussion

As explained in the procedures, the computer simulation gives the height of the structured packing as the output for the desired level of performance. The flow chart and the listing of the program is given in the Appendix II. The performance of the dehumidifier is analyzed in order to find the optimal design for the tower. An important criterion for the optimal column is the packing height.

3.6.1 Comparison between Random and Structured Packing

Structured packings have a regular geometric structure and, in contrast

to random packings, are fabricated and fitted carefully to the dimensions of the column. When placed in the column, successive elements are oriented at 90° to each other. Structured packings offer several advantages over random packings, including lower pressure drop and easy installation, but a detailed comparison between the two packing types is not available. Hence an attempt is made to compare the performance of the structured packing with the available random packing data [35]. The operating parameters of the dehumidifier that have been kept constant for the comparison are given in Table 3.2 and the physical characteristics of the packings are given in Table 3.3.

The effect of desiccant inlet temperature on the performance of the dehumidification process for both packing materials is shown in Fig.3.2. Decreasing the desiccant temperature causes decrease in the vapor pressure of the desiccant that results in a higher mass transfer rate for both packing materials. As the desiccant inlet temperature increases, the packing height also increases to obtain the required humidity ratio at the outlet. It is clear from the figure that the structured packing material outperforms the random packing material.

The effect of desiccant inlet concentration on the performance of the dehumidification process is shown in Fig.3.3 for both packing materials. As the desiccant concentration increases, the required packing height decreases. This is due to the fact that for the given temperature, as the desiccant concentration increases its vapor pressure decreases and thus the potential for mass transfer increases. This figure

TABLE 3.2: Dehumidifier Parameters for the Comparison of Packings

Desiccant	45% $Cacl_2$
Structured Packing	Gauze packing, type BXPFP
Random Packing	50 mm ceramic Raschig rings
Desiccant inlet temperature	25° C
Air inlet temperature	32°C
Desiccant flow rate	0.05 kmol/m^2s
Air flow rate	0.038kmol/m^2s
Humidity ratio of air at inlet	0.022 kg moisture/kg dry air
Humidity ratio of air at outlet	0.01723 kg moisture/kg dry air

TABLE 3.3: Geometric Information of the Random and Structured Packings

Properties	**50 mm Ceramic Raschig rings**
Surface area (m^2/m^3)	190
Void fraction	0.74
Properties	**Gauze-type structured packing**
Surface area (m^2/m^3)	470
Crimp height, h (m)	0.0067
Channel base, B (m)	0.011
Channel side, S (m)	0.0077
Equivalent diameter, d_{eq} (m)	0.0076
Void fraction	0.88
Crimp angle from vertical (deg)	30

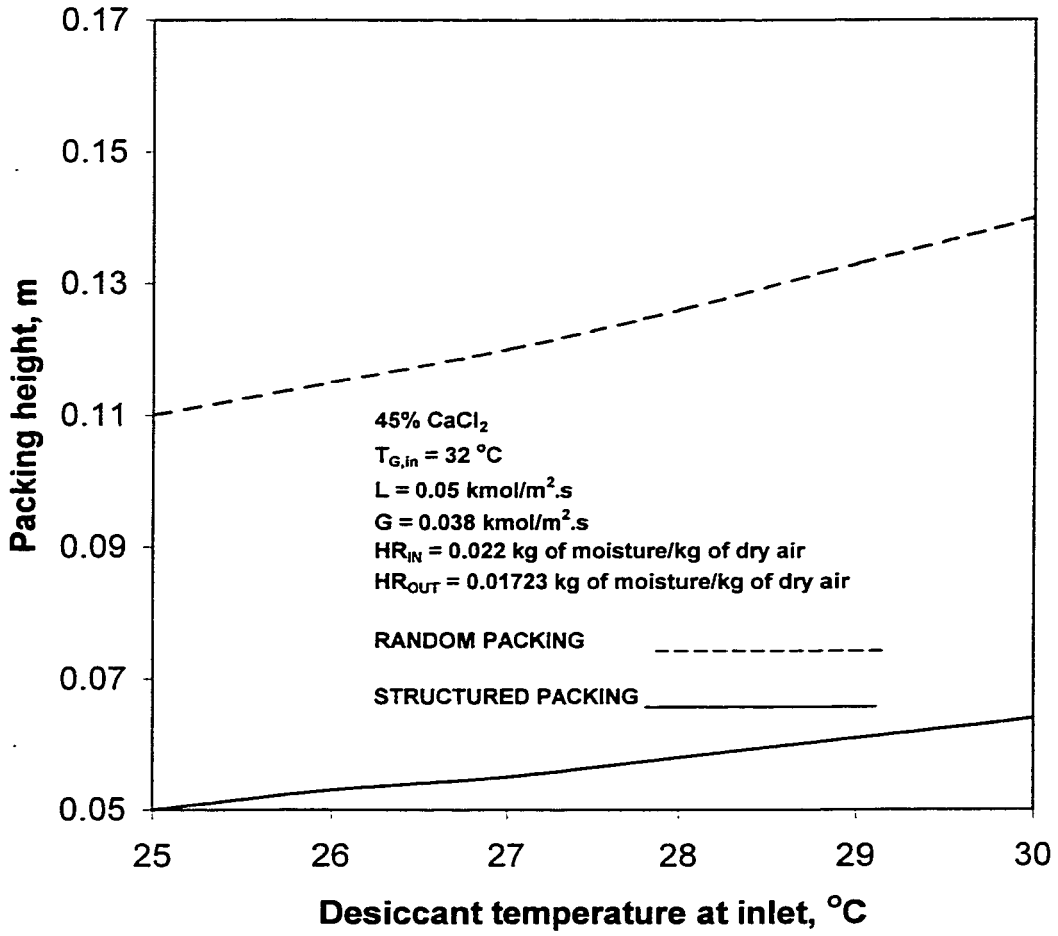

Fig. 3.2 Comparison of packing materials – Effect of desiccant inlet temperature.

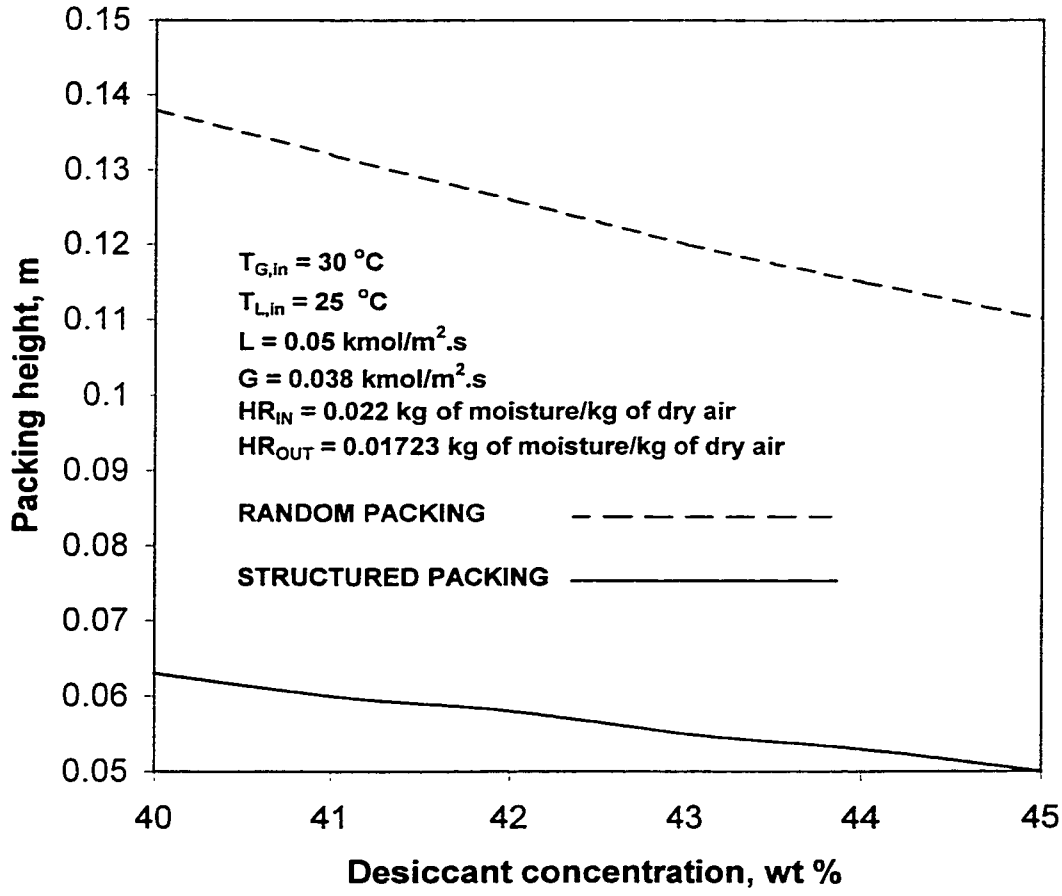

Fig. 3.3 Comparison of packing materials – Effect of desiccant inlet concentration.

also clearly indicates that structured packing requires less packing than random packing material for the same operating conditions.

3.6.2 Parametric Investigation of the Structured Packing Dehumidifier

As indicated in the procedure above, the simultaneous heat and mass transfer analysis in a structured packed tower is carried out and the results are shown in Figs. 3.4 to 3.13. Three different desiccants, namely calcium chloride, lithium chloride and the Cost Effective Liquid Desiccant (CELD, the mixture of 50% calcium chloride and 50% lithium chloride by weight) are considered and their performances are evaluated. The parameters of the structured packing dehumidifier that have been kept constant for the parametric investigation are shown in Table 3.4.

Figures 3.4 and 3.5 show the performance of the dehumidifier for different packing height. From the figures the following general observation can be made for the air inlet humidity of 0.03 kg of water per kg of dry air: As the packing height increases, the outlet humidity of the air decreases. However, the relationship between the two is not linear. As the packing height increases, the rate of decrease of humidity decreases. This is a result of a decrease of the vapor pressure of the air. When the dehumidifier reaches a certain height, the air that is close to the top of the tower will be dehumidified, and as a result of this, its vapor pressure will decrease. Even though the desiccant is strong, the driving force (that is difference in vapor pressure) will be very low. This will result in a lower mass transfer.

TABLE 3.4: Dehumidifier Parameters for the Parametric Investigation

Desiccant	45% $CaCl_2$, 45% LiCl, 45% CELD
Structured Packing	Gauze packing, type BXPFP
Liquid inlet temperature	25° C
Air inlet temperature	40° C
Effective desiccant velocity	0.24 m/s
Effective air velocity	12 m/s
Humidity ratio of air at inlet	0.03 kg moisture/kg dry air
Humidity ratio of air at outlet	0.011 kg moisture/kg dry air

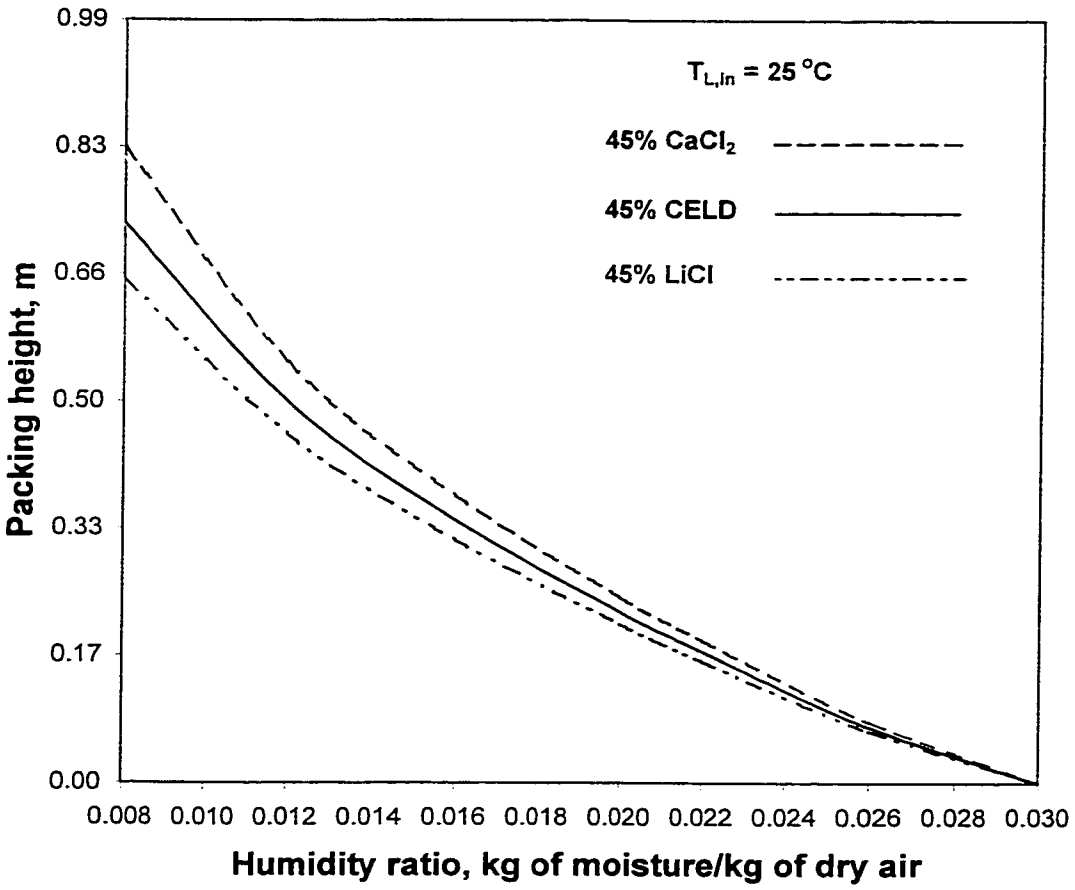

Fig. 3.4 Humidity ratio profile for the desiccant inlet temperature of 25 °C.

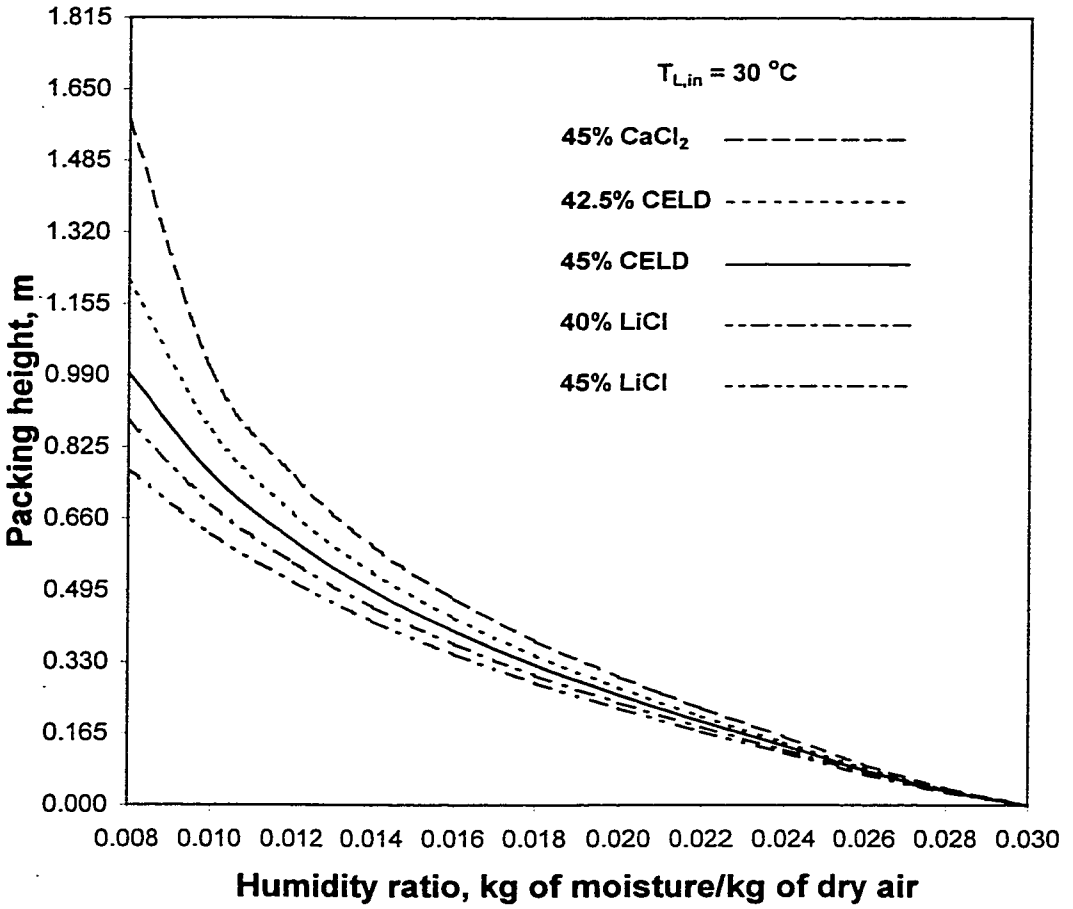

Fig. 3.5 Humidity ratio profile for the desiccant inlet temperature of 30 °C.

From the figures it is clear that lithium chloride needs the least packing height for the same operating conditions and calcium chloride needs the large packing height for the liquid inlet temperatures of 25 and 30° C. Since the desiccant is at low temperature (namely 25° C), the effect of different desiccants on the packing height is insignificant, especially at higher (say 0.012 kg of water per kg of dry air) exit humidity ratios.

Figure 3.5 shows the performance of the dehumidifier for different packing heights for the liquid inlet temperature of 30° C. The warm solution (say 30 °C) facilitates the dehumidification process resulting in a longer packing depth in comparison with a cool solution (say 25 °C as in fig. 3.4). It is interesting to note that in order to get very dry air (say 0.008 kg of water per kg of dry air), the dehumidifier using calcium chloride solution needs longer packing compared with CELD solution and lithium chloride solution.

Figure 3.6 shows the variation of air humidity ratio on the packing heights. For the three desiccants as the packing height increases, the humidity ratio decreases for all three different desiccants at the concentration of 45%. The removal of moisture is faster at the bottom range of the dehumidifier, whereas to remove the same amount of moisture at the top range of the dehumidifier more packing height is required since the potential for mass transfer is less. This may be attributed to the fact that at the top of the dehumidifier, the air is comparatively dry, which has a lower vapor pressure as explained earlier.

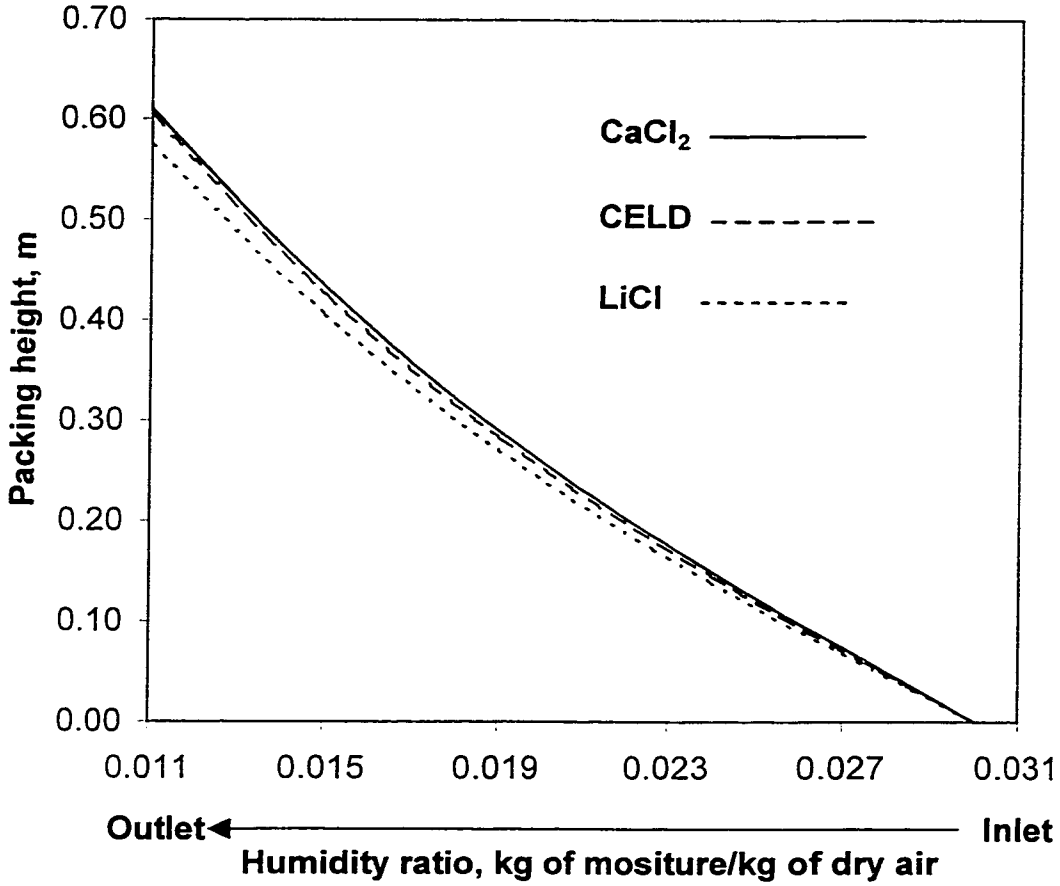

Fig. 3.6 Variation of humidity ratio on the packing height for three different desiccants.

Figure 3.7 shows the dehumidifier performance versus increasing desiccant inlet temperature for three different desiccants at 45% concentration. For a particular packing height, as the desiccant inlet temperature increases, the air outlet humidity also increases. Increasing desiccant temperature causes an increase in the vapor pressure of the desiccant, which results in a lower mass transfer rate. Even at higher desiccant temperatures (say 30° C) at inlet, the variation of packing height is linear for CELD and lithium chloride solutions whereas for calcium chloride it varies exponentially. This clearly indicates that calcium chloride is not suitable for dehumidification of air at higher inlet temperatures compared with the other two desiccants.

The effect of desiccant concentration at the inlet of the dehumidifier on its performance for three different desiccants is shown in Fig.3.8 for a given set of operating conditions. The strong desiccant at the inlet requires a smaller tower than does the weak desiccant. This is due to the fact that the strong desiccant has a lower vapor pressure at a given temperature that increases the potential for mass transfer. Hence, to obtain the same air humidity at the top of the dehumidifier, its height is less. However, this effect is insignificant for lithium chloride solution due to its good thermophysical properties. It is to be noted that when calcium chloride solution concentration decreases to less than 42%, a very high tower is required for a given set of operating conditions and virtually dehumidification is impossible when its concentration is less than 40%. However, even though CELD solution requires a taller tower than lithium chloride solution for the same given set of operating conditions,

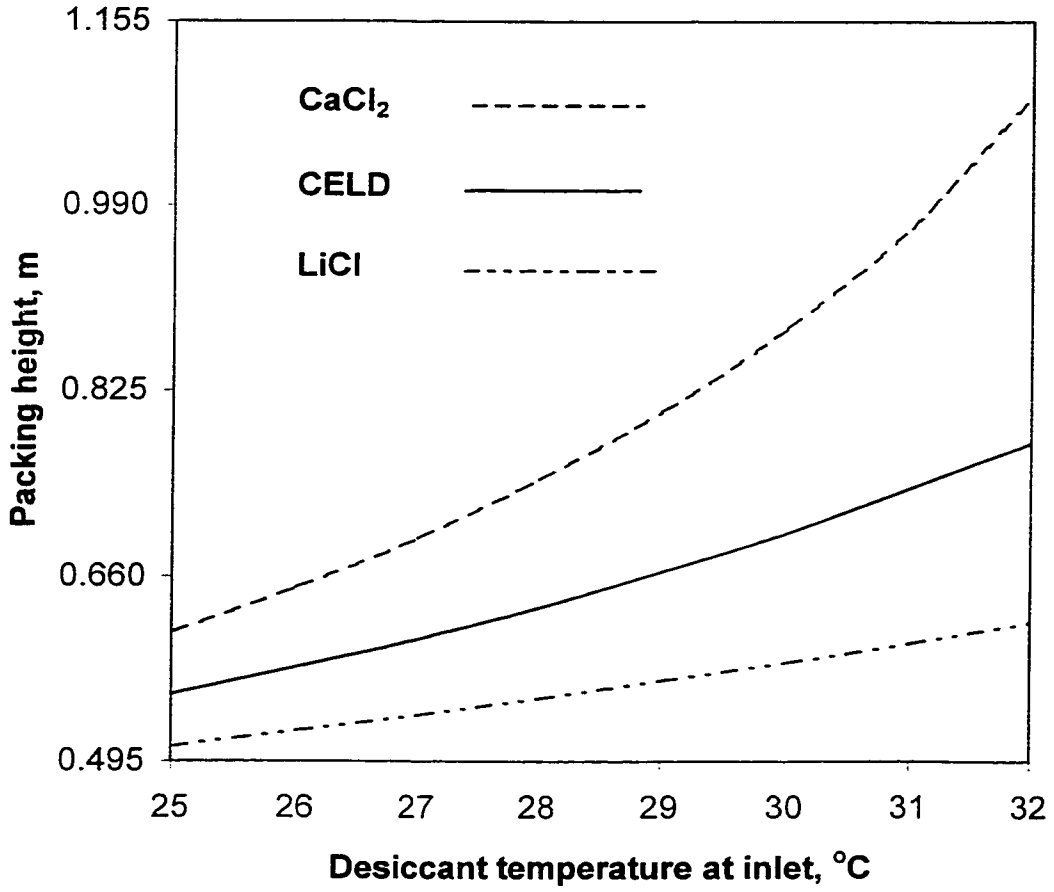

Fig 3.7 Effect of desiccant inlet temperature on the packing height.

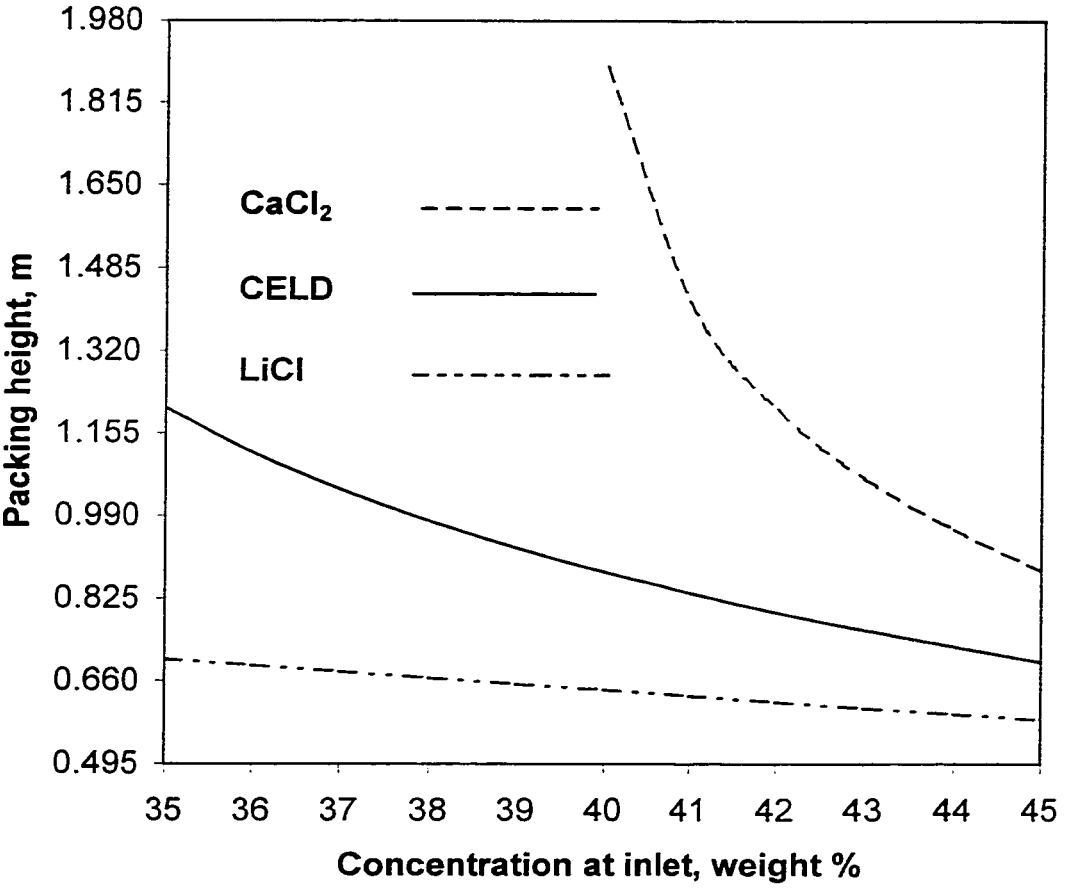

Fig. 3.8 Effect of desiccant inlet concentration on the packing height.

dehumidification is possible even when the concentration decreases to 35% at the top of the dehumidifier.

Another interesting aspect is the effect of air inlet temperature on the height of the packing. As shown in Fig.3.9, for a given set of operating conditions, the air inlet temperature has an effect on the packing height but virtually no bearing when the air inlet temperature is low. As air inlet temperature increases (say 40° C), the height of packing required to obtain the same air humidity at the top of the dehumidifier, increases since the warm air heats the desiccant. Due to this effect the vapor pressure of the desiccant increases and the potential for mass transfer decreases. When the air inlet temperature is low (that is, close to the desiccant temperature), virtually this will not affect the packing height.

The effect of air inlet humidity on the height of the packing is shown in Figs. 3.10 and 3.11 for two air humidities of 0.03 and 0.035 kg of water per kg of dry air and the air inlet temperature of 40° C. The liquid temperature profile is shown in Fig.3.10. As one to expect, a taller tower is needed to dehumidify the air of higher humidity ratio. When the desiccant enters the dehumidifier, it absorbs both heat and moisture from the air. The transferred heat and the heat generated by moisture absorption cause the desiccant temperature to increase. The highly humid air (0.035 kg of water per kg of dry air) causes the desiccant temperature to increase from 30 to 33.1° C, whereas the less humid air (0.03 kg of water per kg of dry air) increases the desiccant temperature from 30 to 32.4° C. The air temperature profile is shown in Fig. 3.11 for desiccant inlet temperature of 30° C. Since the air inlet temperature is higher than the desiccant inlet temperature, the air temperature decreases due to sensible heat transfer to the

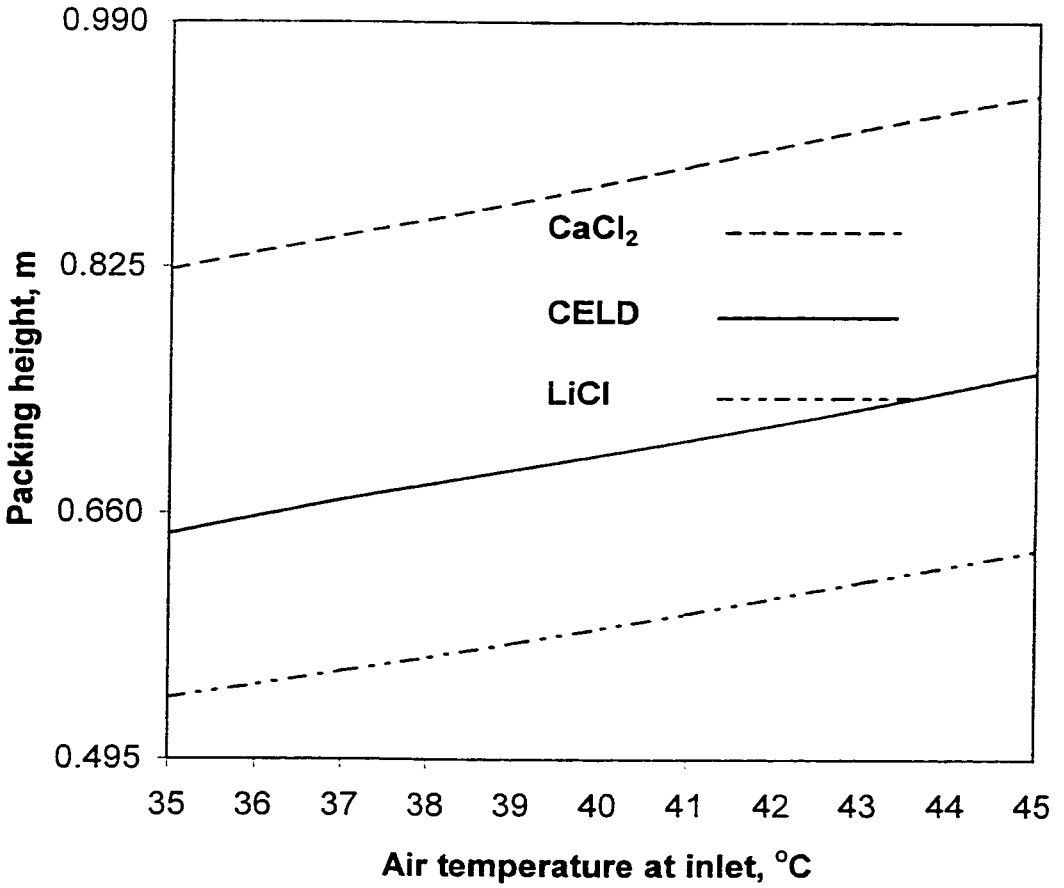

Fig. 3.9 Effect of air inlet temperature on the packing height.

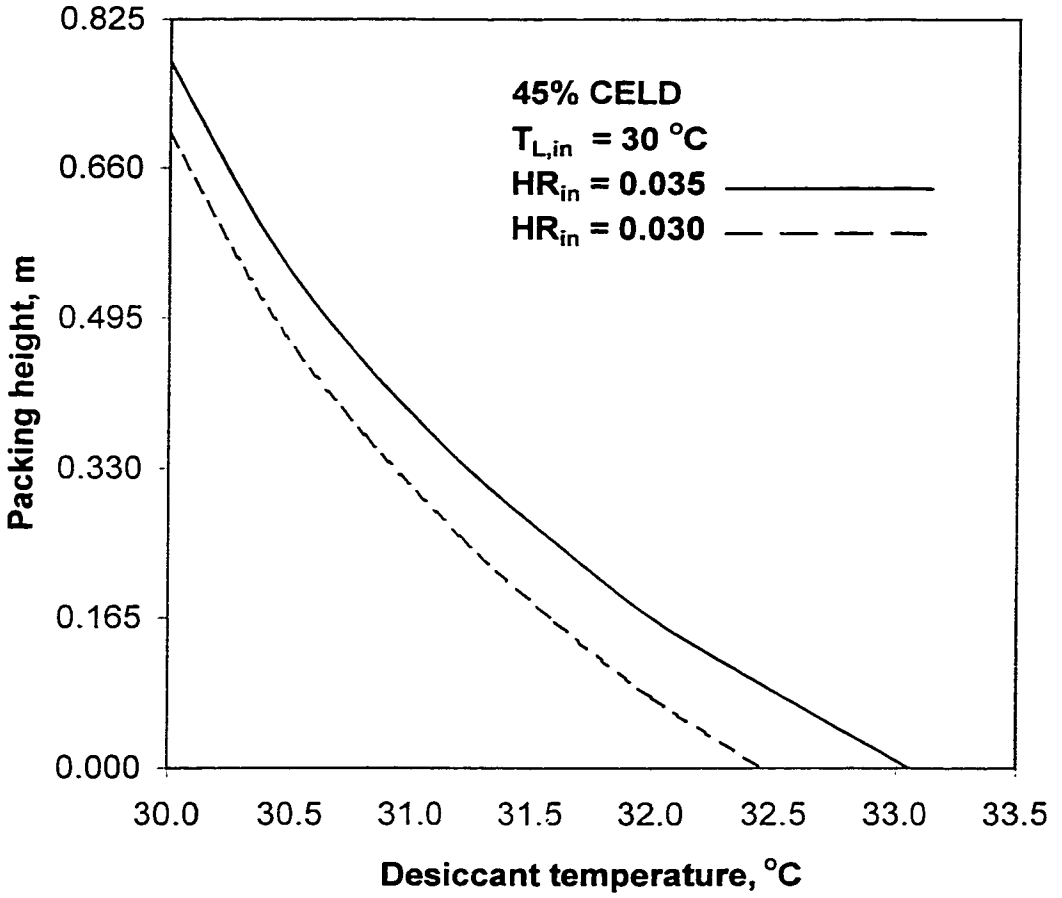

Fig. 3.10 Desiccant temperature profile for two different air inlet humidity ratios.

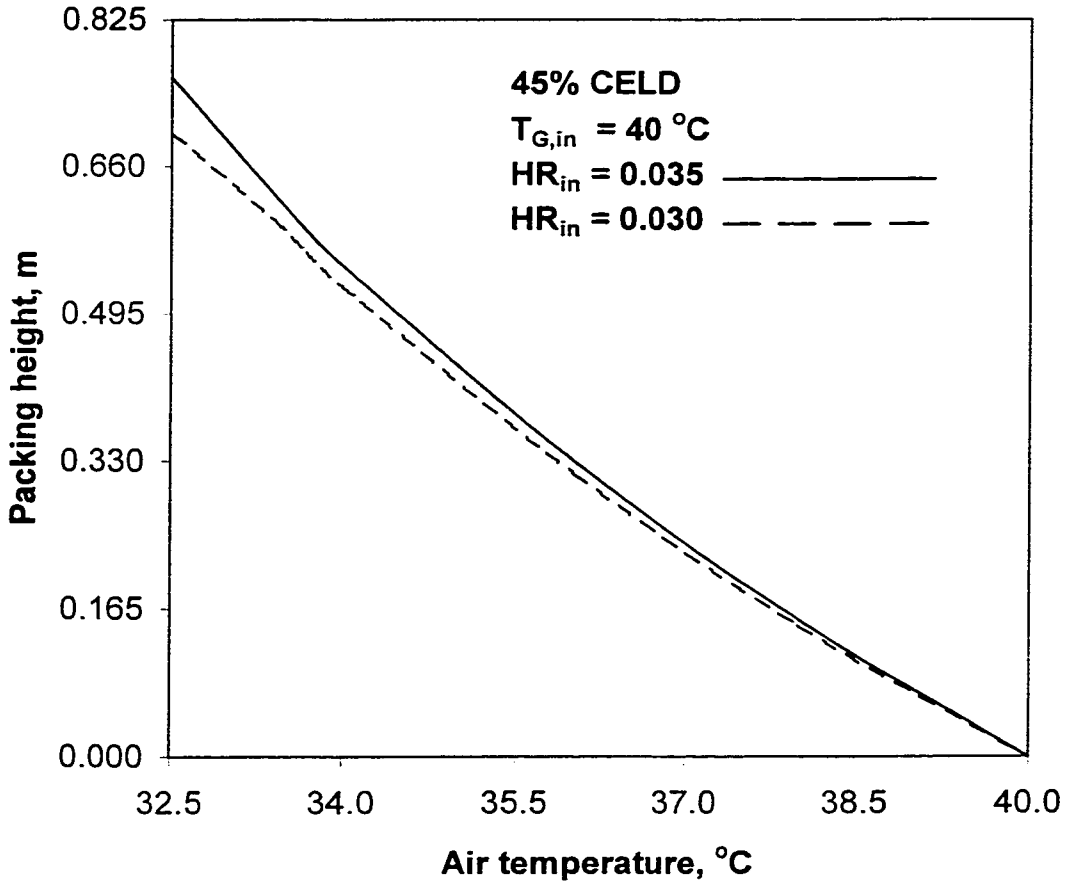

Fig. 3.11 Air temperature profile for two different air inlet humidity ratios.

desiccant for two different air inlet humidities but the effect of air inlet humidity is insignificant.

The effect of desiccant flow rate at the inlet of the dehumidifier is shown in Fig.3.12 for a given set of conditions of operation for three different desiccants. As the desiccant flow rate increases for a particular flow rate of air, the height of the packing decreases to achieve the same degree of dehumidification and this effect is insignificant as the flow rate increases for all three desiccants. Therefore, very high flow rate of desiccant is not required for dehumidification of air but a certain minimum flow rate of desiccant is needed for the desired level of dehumidification.

The effect of air flow rate at the inlet of the dehumidifier is shown in Fig.3.13. For a particular flow rate of desiccant, the low flow rate of air requires a smaller tower and the higher flow rate requires a taller tower. As the air flow rate increases to obtain the same level of dehumidification, more moisture must be removed from the air and hence, packing height is increased.

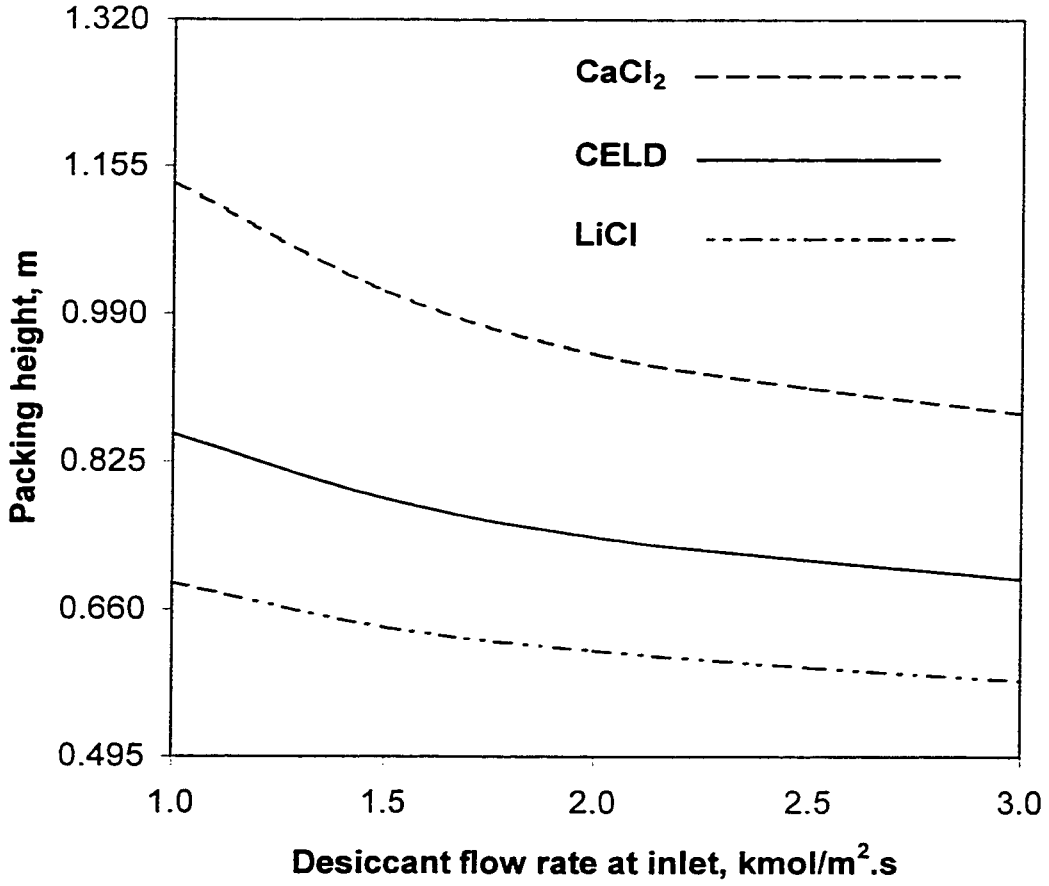

Fig. 3.12 Effect of desiccant inlet flow rate on the packing height.

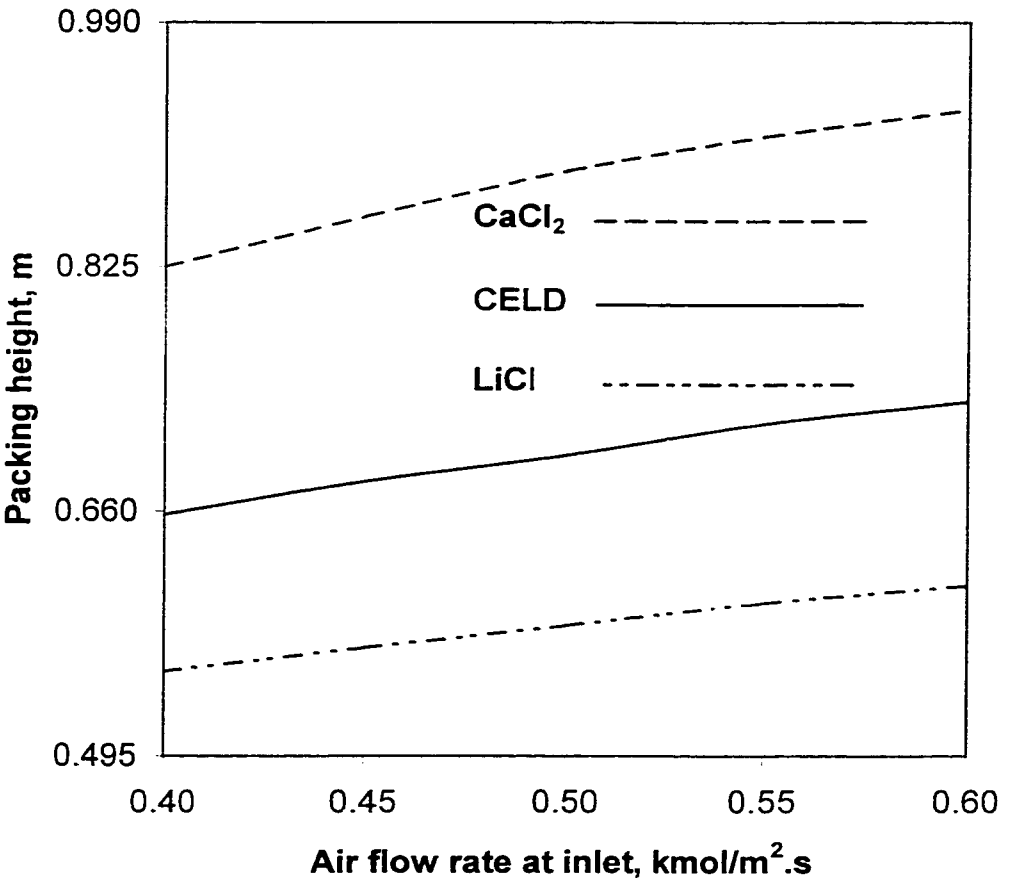

Fig. 3.13 Effect of air inlet flow rate on the packing height.

CHAPTER 4

REGENERATION PROCESS IN STRUCTURED PACKING TOWER

4.1 Regeneration of Weak Desiccants

In the dehumidification process, the strong desiccant that has been brought into contact with the air to be dehumidified, absorbs the moisture from the air during which process it gets diluted. In order to reuse the same desiccant in the process, the desiccant has to be regenerated to an acceptable level of concentration. This regeneration process is equally an important part of the desiccant cooling system.

The overall desiccant cooling system efficiency and reliability, in other words, the efficiency, reliability and feasibility of the regeneration process determine the feasibility of the desiccant cooling system. This is due to the fact that the latent load taken care of in the dehumidifier has to be evaporated from the weak liquid desiccant in the regenerator. Hence, the regenerator of a desiccant cooling system is the most critical component of it. The heat required for regenerating the weak desiccants can be supplied by fossil fuel, waste heat, or any form of low grade thermal energy, and most of the time, solar energy is used in such processes [43,44].

4.1.1 Solar Regeneration of Weak Desiccants

Since regeneration can be facilitated at lower temperatures, some studies have been conducted to use the energy from the sun. Regeneration of desiccants using solar energy can be brought about by different methods [45]. A solar air heater or water heater can either supply the heat required for the regeneration process. For example, Lof [46] proposed a space cooling system, in which the weak glycol is regenerated by solar heated air. Ko [47] proposed a hybrid air conditioning system, in which lithium chloride is heated by solar heated hot water to drive the moisture from the solution. It should be noted that in such a system the solar heat is first collected at air or water heating collectors and finally transferred to the desiccant.

On the other hand by using direct type solar regenerators where the desiccant is itself the heat collecting fluid, the regeneration process can be made more effective. The desiccant temperature is more or less equal to the collector plate temperature. Based on the methods of regenerating the weak desiccants, regenerators can be divided into different categories. The heat and mass transfer occurring in these regenerators have been studied well and are presented by Gandhidasan [48]. Among these regenerators, open regeneration system is the simplest one. It is a gently sloping black roof over which the weak desiccant is trickled. The roof is open to the atmosphere and exposed to direct solar radiation. Roof evaporation works well in a hot, low humidity atmosphere, but not in humid climates. Dilution of the solution by rainfall and dust contamination is additional problems. To alleviate these problems, a glass cover over the solution

regenerator has been proposed [49]. Both regenerators can conveniently use the collector area only for the specific purpose of solution concentration.

In humid climates, open regeneration system performance is poor due to low potential for mass transfer. Therefore, Gandhidasan and Al-Farayedhi [50] proposed a partly closed-open solar regenerator. In this regenerator the upper part of the open regenerator is covered with a single glazing where the desiccant can be heated up without evaporation of water. The evaporation starts at the beginning of the open surface. This design is more expensive than the simple sloped roof.

4.1.2 Regeneration in a Packed Column Using Solar Heated Air

The use of a packed column was investigated in a theoretical study by Leboeuf and Lof [51] in order to make the desiccant cooling system compatible with a conventional solar air heating system and to extend its application to more humid climates. In the column, solution flows by gravity over suitable packing while solar heated air is forced counter-current to it in direct contact. Reconcentrated solution is collected below the packing and humidified air is exhausted to the atmosphere. It was determined that packing depth of less than 30 cm and column diameter of less than a meter should be sufficient for approximately 3-ton of refrigeration system. The study considered wide range of air humidities and air temperatures of 70 to 90° C that could be obtained from a flat plate solar collector heating ambient air. To substantiate the theoretical analysis, an experimental investigation of a packed column regenerator was undertaken [52]. It is to be noted that approximately 70 m^2 solar air heating collector area is required for 3-ton

air conditioning capacity and storage must be provided to use the energy in the night. These make the system more expensive and the cooling system performance depends on climatic conditions.

4.1.3 Regeneration of Weak Desiccants by Mechanical Energy

Reverse osmosis (RO) process has been used for desalination of seawater in which saline water with some concentration of dissolved salts is concentrated to pure water when passed through a membrane, thereby concentrating the saline water to a higher degree. The reverse osmosis process is characterized by the use of pressure in excess of the osmotic pressure to force the solution of salt at the same temperature through a selective membrane capable of rejecting the dissolved salts. In a similar manner, weak liquid desiccants can also be regenerated by removing the water from the solution.

Membranes can be classified according to structure, production, essential transport mechanism and areas of application [53]. The most important membrane qualities for regeneration of liquid desiccants are high selectivity, high permeability, mechanical and temperature stability and chemical resistance. Recently an attempt has been made [54] to use reverse osmosis to concentrate the weak liquid desiccants and an analysis is developed to predict the pressure required to regenerate two weak desiccants, namely calcium chloride and lithium chloride, from a given concentration to a required concentration. It is concluded that the pressure required to regenerate

calcium chloride is less than that of lithium chloride for the same operating conditions. It is to be noted that one type of membrane is not sufficient to cover all possible applications of regeneration of weak liquid desiccants.

4.1.4 Regeneration of Weak Desiccants in a Structured Packing Tower

It is to be noted that most of the processes described above are either costly or a function of climatic conditions. Hence in this research, it is proposed to use conventional energy, namely electrical energy, to heat the air and structured packing column will be used for desiccant-air contact operation.

One of the key components in liquid desiccant cooling system is an air-desiccant contactor, which is used for regeneration. In the regenerator, the spent or weak desiccant is contact with hot air so as to transfer the humidity from the desiccant to the air. Such a contactor must provide as large as possible surface area exposure between the liquid and the air, in order to maximize heat and mass transfer. This can be done:

- by breaking the liquid into small droplets in a spray chamber.
- by breaking the liquid into small streams flowing through the air in a wetted wall column, or
- by passing the air and the liquid through a packed column where the packing serves to break the liquid into thin films.

The packed column enjoys several advantages over the other contactor systems as described in chapter 1. These advantages make the packed column a good candidate for this study and the metal gauze-type structured packing is chosen as the packing material

for regeneration purposes. The summary of the previous studies in the regenerator performance for the last ten years is given in Table 4.1. The table shows the parameters describing the performance, the desiccant used, the packing type used and whether experiments were conducted or not.

4.2 Simultaneous Heat and Mass Transfer Analysis of the Regeneration Process

When hot air and the weak desiccant comes in contact in the regeneration column, because of the difference in their vapor pressure, heat and mass transfer occurs, until a certain equilibrium is reached. As the hot air moves up in the column, it absorbs the moisture from the desiccant and its vapor pressure increases. In contrast, as the liquid falls down through the column, its vapor pressure decreases with its water vapor content. In the structured packing column, the regeneration process involves simultaneous heat and mass transfer. A step-wise heat and mass balance across the column is used to determine its performance. For the present study, a steady-state finite difference model is employed and the general assumptions made for the dehumidification process in a structured packing tower, as given in chapter 3, are valid for the regeneration process also.

A schematic of a differential section of the structured packing regenerator is shown in Fig. 4.1. The mathematical model is the same as the dehumidification process except for some minor changes described below and also in the

TABLE 4.1: Packed Bed Regenerator Performance

Reference	Desiccant	Packing	Performance Parameter	Experiments
Martin and Goswami (1999)	TEG	1 in Polyproplene Rauschert Hiflow rings	m_{evap} ε_Y	Yes
Khan (1996,1994)	LiCl	———	ε_Y, ε_H	No
Potnis and Lenz (1996,1994)	LiBr	Random Polyproplene Tripack and structured Munter's CELDEK	m_{evap}	Yes
Ertas et al. (1994)	CELD	Intalox Snowflake	$T_{L,OUT}$ X_{OUT}	Yes
Elsayed et al. (1993)	$CaCl_2$	25 mm Raching Rings	ε_h, ε_m	No
Patnaik et al. (1990)	LiBr	Polyproplene Tripack no. ½	m_{evap}	Yes
Gandhidasan (1990)	$CaCl_2$	1 in Rasching Rings	m_{evap}	No

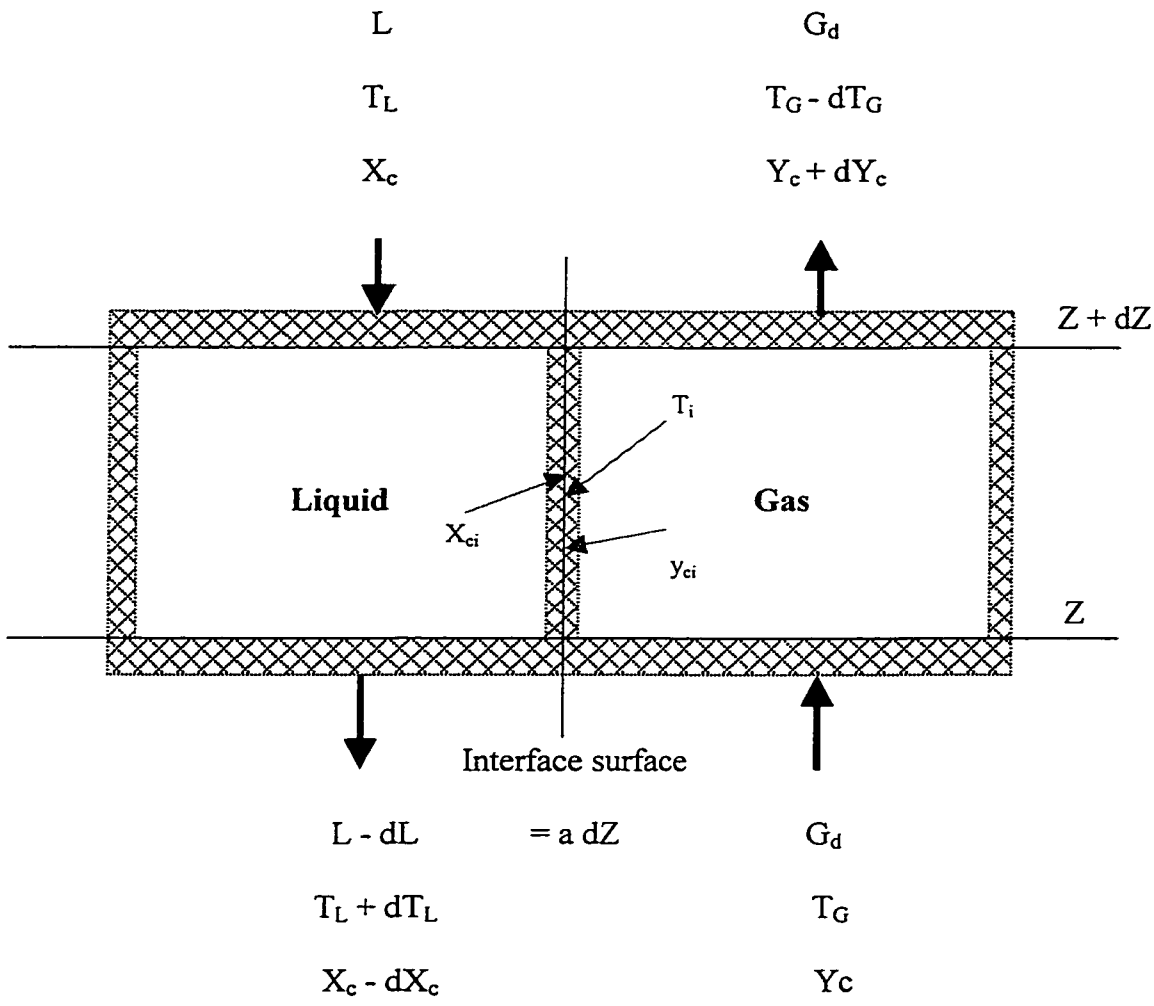

Fig. 4.1 Differential section of a structured packing regenerator.

specification of the inlet conditions of the air and desiccant. In this analysis, resistance to mass transfer in the liquid phase is also considered because of the concentration of the desiccant. When beginning the analysis, several quantities are selected, calculated from the dehumidifier analysis, or determined by the climatic conditions. Liquid inlet concentration is found from the dehumidifier analysis. The exit concentration of the liquid is chosen in conjunction with the dehumidifier. The mass of evaporated water from the desiccant can be evaluated by knowledge of desiccant concentration and its flow rate. During regeneration, desiccant concentration increases and the flow rate decreases. As the mass of desiccant in the solution is constant during regeneration, the following expression can be written:

$$L_i \xi_i = L_o \xi_o \tag{4-1}$$

Ambient weather conditions determine the entering inlet humidity of the air, while the air inlet temperature is chosen based on the electrical heater. Neither the solution exit nor air exit temperature is known; a trail and error solution must be applied.

Starting at the bottom of the bed, an outlet temperature for the solution is assumed, which will be checked later. Then a temperature for the interface between the air and the liquid is assumed for this section. The interfacial conditions are influenced by properties of the desiccant and air streams and vary from point to point in the regenerator. From the interface temperature and the liquid concentration, the concentration of water in the air (that is, air specific humidity) at the interface is found

from the vapor pressure curves of the desiccant for the range of interest of operating conditions. Humidity gradient, air temperature gradient and the desiccant temperature gradient equations are derived and they allow local gradients to be calculated in successive steps of tower height *(dZ)*, beginning from the bottom of the tower, $Z = 0$. Equation (4-2) must be solved simultaneously with the vapor-liquid equilibrium data for desiccants. For the regeneration of weak desiccants, the following functional relations give the equilibrium distribution for various liquid desiccants:

For calcium chloride solution:

$$y_{ci} = 0.0448 + 0.00112T_i - \frac{0.03576}{x_{ci}} \tag{4-2}$$

For lithium chloride solution:

$$y_{ci} = 0.06916 + 0.000423T_i - \frac{0.0412}{x_{ci}} \tag{4-3}$$

For mixture of lithium chloride and calcium chloride (CELD) solution:

$$y_{ci} = 0.05698 + 0.0007715T_i - \frac{0.03848}{x_{ci}} \tag{4-4}$$

As in the dehumidifier analysis, the interfacial condition x_{ci} and y_{ci} are determined by the incremental search method for every section of the regenerator. The analysis presented above will evaluate the performance of the regenerator with the following given parameters: liquid inlet temperature and concentration, air inlet temperature and the humidity, exiting desiccant concentration and the flow rates of liquid and air. The output will be the height of the packing, exiting air temperature and humidity, and exiting liquid temperature. The calculation starts at the bottom of the tower where $Z = 0$. The entire procedure is continued for succeeding sections of the regenerator until it agrees with the known desiccant inlet concentration and temperature. If not, the initial guess for the outlet desiccant temperature is incremented appropriately, and the entire process is repeated until agreement is reached. The value of Z at the last section is the required packing height for the given conditions.

Following this analysis, a computer program that simulates the performance of the regenerator was written and the listing is given in the Appendix III. The input parameters include flow rates, solution concentrations, inlet air temperature and humidity, desiccant inlet temperature and the heat and mass transfer coefficients. The outputs include desiccant exit temperatures, exit air temperature, packing height, and regenerator conditions such as temperatures and concentrations at each section.

4.3 Results and Discussion

The performance of the regenerator is analyzed in order to find the optimal design for the tower. An important criterion for the optimal column is the packing

height. With the REGENERATOR sizing program developed a more detailed study of the effects of operational and environmental parameters on the regenerator performance is carried out. As in the dehumidification analysis, three different liquid desiccants are considered and their performance is evaluated. The parameters of the structured packing regenerator that have been kept constant for the parametric investigation are given in Table 4.2. It is to be noted that the flow rates of desiccant and air need not be the same as for the dehumidification process. If the provisions are made, then the less flow rate of desiccant can be taken to the regenerator and it can be over-concentrated so that the dehumidifier concentration will be the same. Since higher temperatures are involved in the regeneration process compared with dehumidification process, stainless steel gauze-type structured packing is proposed for regeneration process. The geometric information of the packing selected for regeneration of weak desiccants is given in Table 4.3. The simultaneous heat and mass transfer analysis in a structured packing regenerator is carried out and the results of the computer runs are shown in Figs. 4.2 – 4.7.

Figure 4.2 shows the performance of the regenerator versus increasing air inlet temperature for three different desiccants. As air inlet temperature increases, the height of the packing required to obtain the same desiccant concentration at the bottom of the regenerator decreases. This is due to the fact that the hot air heats the desiccant and hence due to this effect the vapor pressure of the desiccant increases and the potential for mass transfer increases. It is interesting to note that calcium chloride-air system need less packing compared with other desiccants for the same operating

TABLE 4.2: Regenerator Parameters Used for the Parametric Investigation in the Regenerator Sizing Program

Desiccant	$CaCl_2$, LiCl, CELD
Structured Packing	Gauze packing, type BX
Desiccant inlet concentration	44.5%
Desiccant outlet concentration	45%
Desiccant inlet temperature	35°C
Air inlet temperature	65°C
Humidity ratio of air at inlet	0.01 kg moisture/kg dry air
Inlet desiccant flow rate	0.05 kmol/m^2s
Inlet air flow rate	0.5 kmol/m^2s

TABLE 4.3: Geometric Information of the Regenerator Packing

Properties	Gauze packing, type BX
Surface area (m^2/m^3)	500
Crimp height, h (m)	0.0065
Channel base, B (m)	0.0102
Channel side, S (m)	0.00735
Equivalent diameter, d_{eq} (m)	0.0072
Void fraction	0.90
Channel flow angle from horizontal (deg)	60

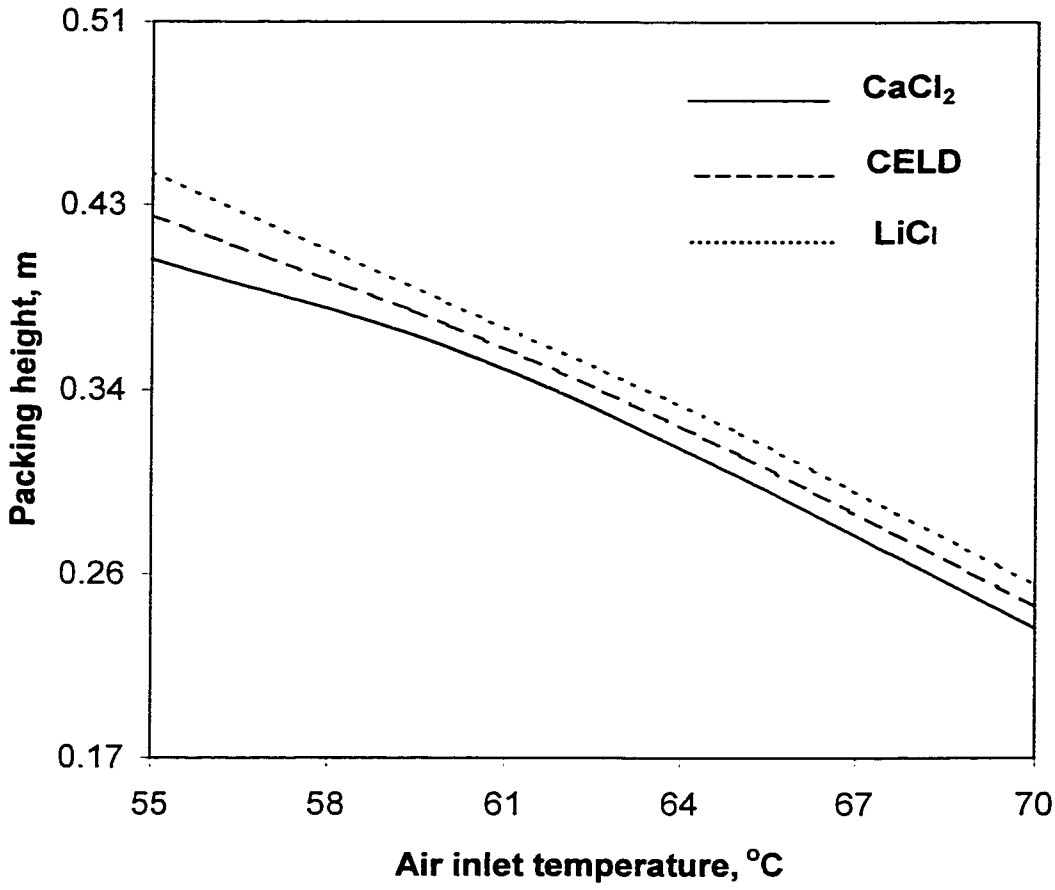

Fig. 4.2 Effect of air inlet temperature on the regenerator packing height.

conditions. At the given inlet conditions for the desiccant, the vapor pressure of calcium chloride solution is the greatest among the three desiccants. This increases the potential for mass transfer and hence less packing is required. However, the difference in packing height for three different desiccants is insignificant as inlet air temperature increases.

Figure 4.3 shows the effect of desiccant inlet temperature on the regenerator performance for three different desiccants. The entering desiccant meets humidified air that is at a temperature approximately 10 to 15°C lower than it enters. As the desiccant inlet temperature increases, the packing height decreases to obtain the required concentration of the desiccant at the outlet of the regenerator. The warm desiccant (say 35°C) facilitates the regeneration process resulting in a smaller packing height in comparison with relatively cool desiccant (say 30°C). Increasing the desiccant inlet temperature causes an increase in the vapor pressure of the desiccant, which results in a higher mass transfer rate. The difference in packing height for three different desiccants is insignificant as inlet desiccant temperature increases. This clearly indicates that preheating the desiccant improves the performance of the regeneration process. This can be achieved by adding a heat exchanger to preheat the weak desiccant leaving the dehumidifier before it enters the regenerator by using the hot, strong desiccant leaving the regenerator.

The effect of hot air humidity ratio at the inlet to the regenerator on its performance is shown in Fig. 4.4 for a given set of operating conditions for three different desiccants. The dry, hot air requires a smaller packing than does the hot, humid air. This is due to the fact that hot, dry air has a lower vapor pressure that

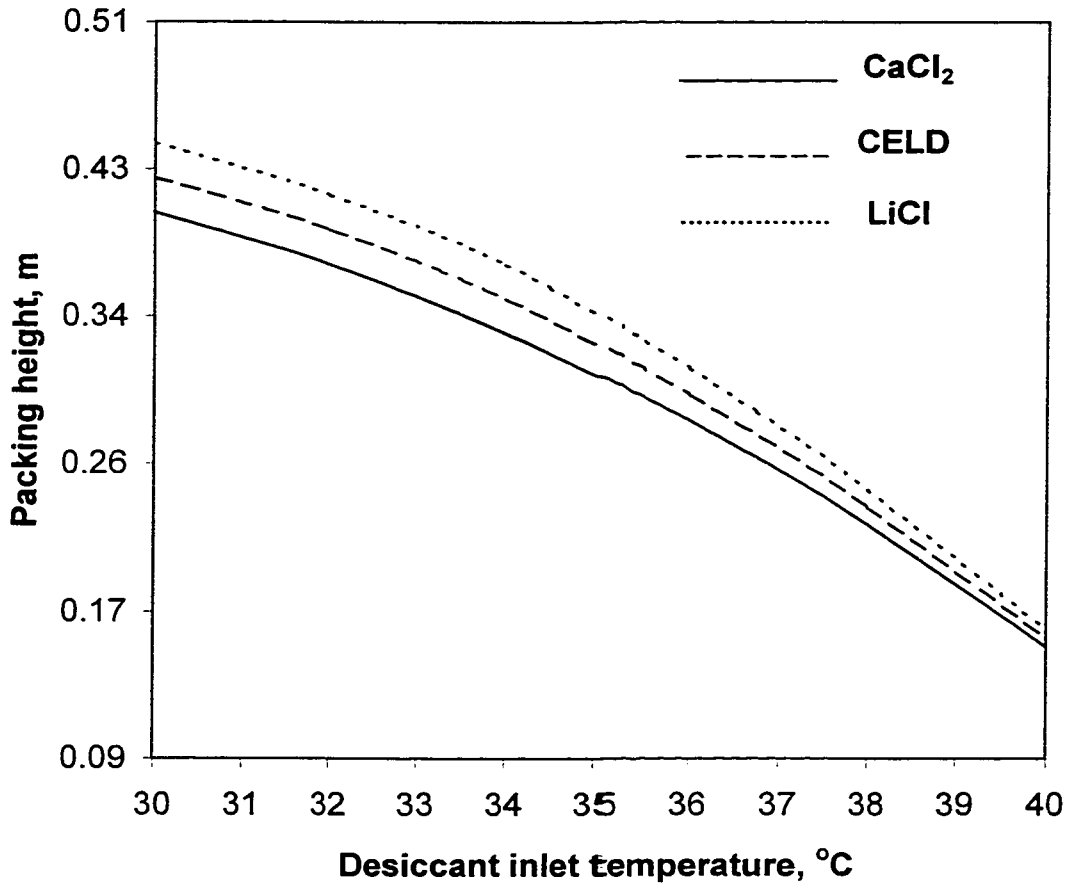

Fig. 4.3 Effect of desiccant inlet temperature on the regenerator packing height.

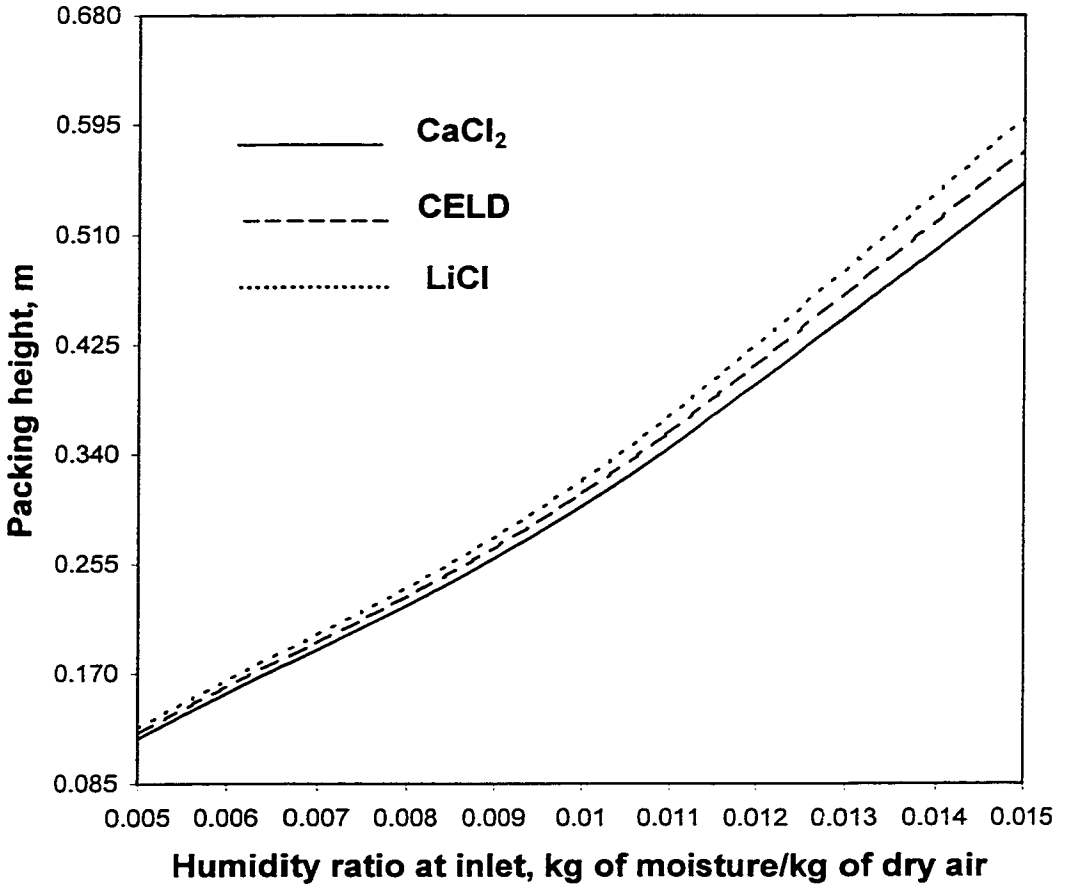

Fig. 4.4 Effect of inlet humidity ratio on the regenerator packing height.

increases the potential for mass transfer. Hence, to obtain the same concentration at the outlet of the regenerator its height is less. From the figure it is clear that all three desiccants require almost the same packing height if the entering hot air is dry. As the humidity ratio of the entering hot air increases, the packing height increases exponentially and hence, this is one of the most important controlling parameters for the performance of the regenerator.

The effect of desiccant concentration at the inlet to the regenerator on its performance for three different desiccants is shown in Fig. 4.5 for a set of given operating conditions. In order to obtain 45% concentration at the outlet of the regenerator, as one expected, the weak desiccant at the inlet (say 44% concentration) requires a taller tower than does the relatively strong desiccant (say 44.5% concentration). In order to concentrate the desiccant with 44% concentration to 45% at the outlet, more water must be removed from the solution and hence it needs more packing height.

The effect of air flow rate at the inlet to the regenerator is shown in Fig. 4.6. For a particular flow rate of desiccant, the high flow rate of air requires a smaller tower and lower flow rate requires a taller tower. As the air flow rate decreases to obtain the same level of regeneration, that is 45% concentration at the outlet of the regenerator, more water must be removed from the desiccant and hence, packing depth is increased.

The effect of desiccant flow rate at the inlet to the regenerator is shown in Fig. 4.7 for a given set of operating conditions for three different desiccants. As the desiccant flow rate decreases for a particular flow rate of air, the packing height

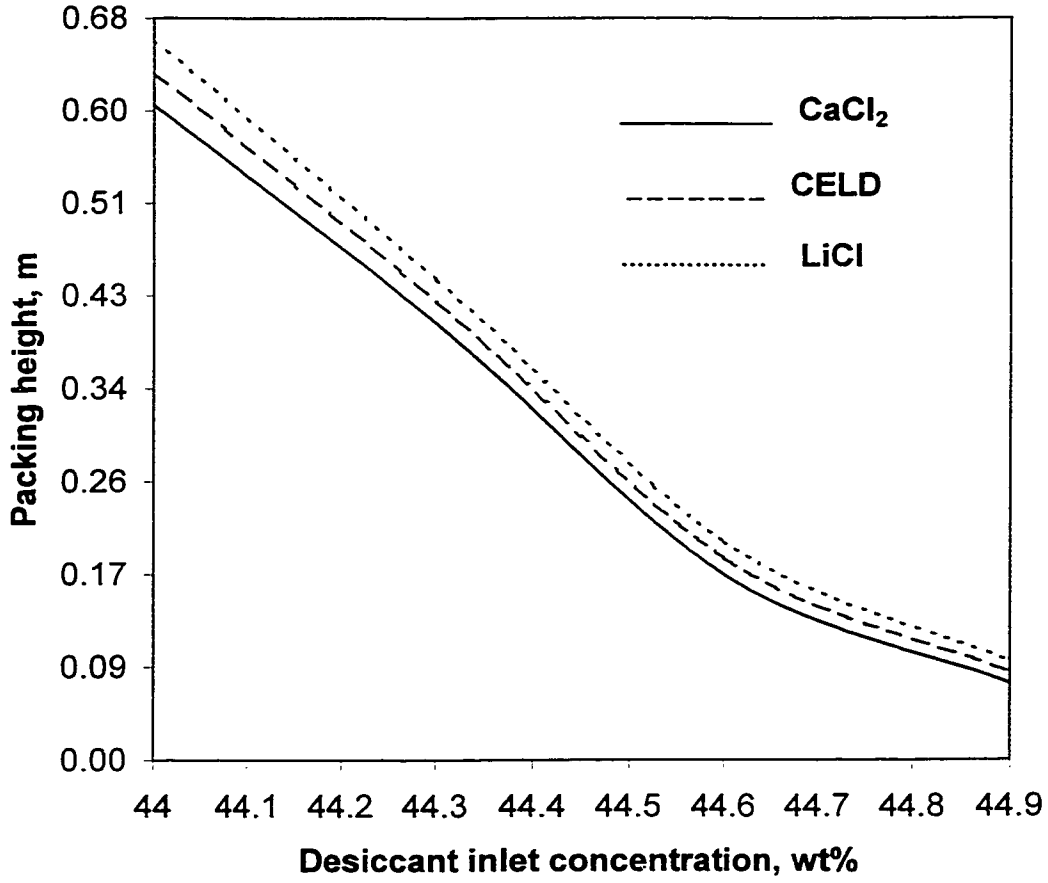

Fig. 4.5 Effect of desiccant inlet concentration on the regenerator packing height.

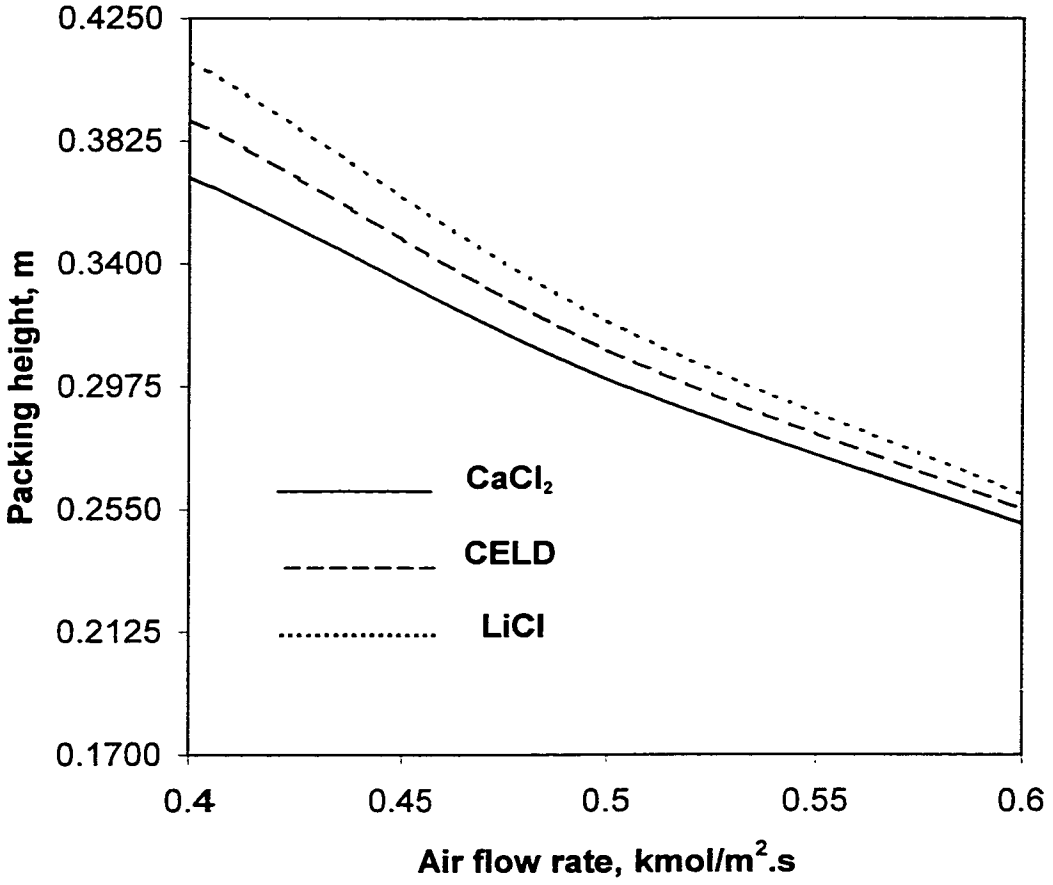

Fig. 4.6 Effect of air flow rate on the regenerator packing height.

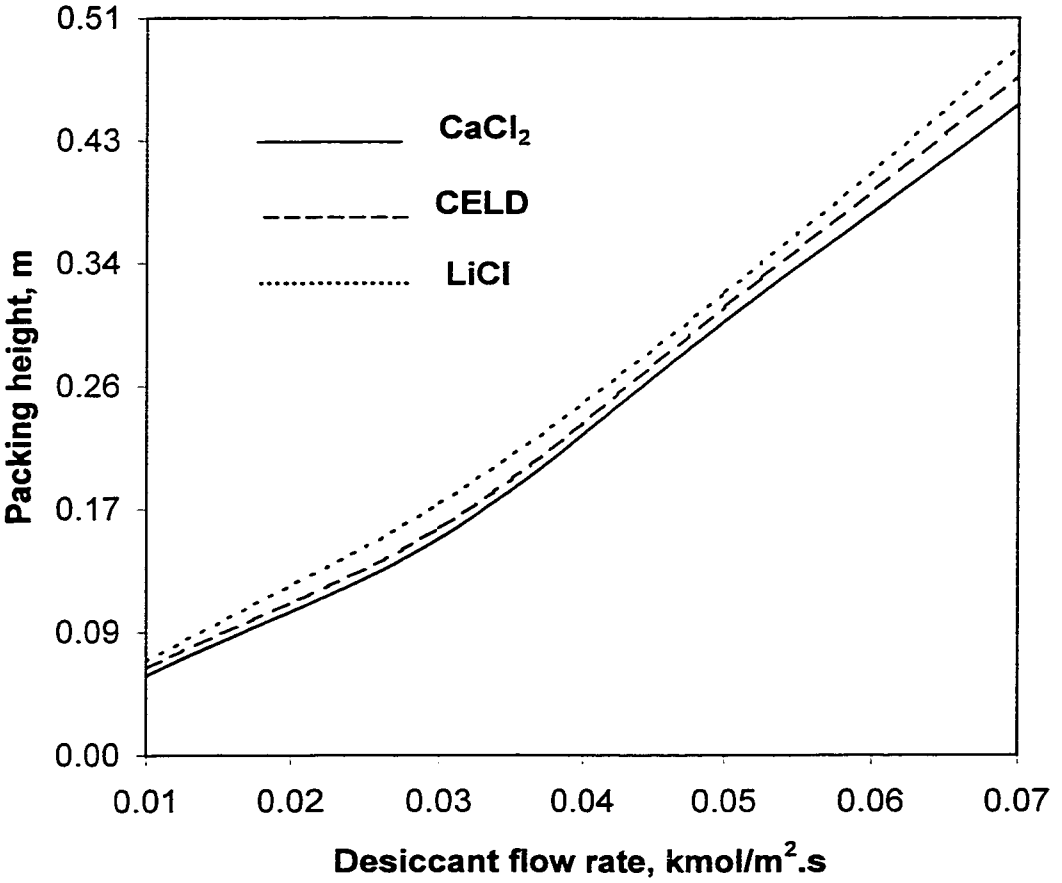

Fig. 4.7 Effect of desiccant flow rate on the regenerator packing height.

decreases to achieve the same level of regeneration and this effect is insignificant as the flow rate decreases for all three desiccants. However, care must be taken that the desiccant flow rate remains high enough for adequate wetting of packing. As the desiccant flow rate increases, more water must be removed from the solution to obtain 45% concentration and hence, more packing is needed.

CHAPTER 5

EFFECTIVENESS FOR AN ADIABATIC COUNTERFLOW STRUCTURED PACKING REGENERATOR

5.1 Introduction

The performance of structured packing tower operating as an air dehumidifier or liquid regenerator is influenced by many operating parameters and conditions such as desiccant fluid characteristics (viscosity, density, and surface tension), packing type (shape, size, and material), desiccant distribution over the packing, flow configuration (counter or co-current flow), tower height, fluid flow rates, and the inlet conditions of the desiccant (temperature and concentration) and the air (temperature and humidity). Efficiency or effectiveness defines the performance of any device. The performance of a pump, turbine, compressor, fan, etc. is evaluated by efficiency. Whereas the performance of an air washer, heat exchanger, packed bed dehumidifier, etc. are evaluated by effectiveness. Recently effectiveness of heat and mass transfer processes in a packed bed liquid desiccant dehumidifier/regenerator is defined [55] based on the experimental data. The effectiveness is defined in terms of humidity ratio as well as enthalpy of the air. They are applied for both dehumidification and regeneration processes. It is to be noted that the function of the dehumidifier is to remove the

moisture from the air whereas the moisture is removed from the desiccant in the regenerator.

5.2 Effectiveness for a Humidification/Dehumidification Process

Before one looks into regeneration process, it would be more appropriate to know more about the effectiveness for a humidification/dehumidification process. Humidification process means that the moisture content of the air is increased and this is just opposite to dehumidification process. This may easily be accomplished by passing air stream through a chamber in which water is sprayed. This device is called an air washer. There are several expressions to define the effectiveness of an air washer [56], some are based on the extent to which the dry bulb temperature of the entering moist air stream approaches its initial wet bulb temperature and others are based on the change of state undergone by the air. The effectiveness of a humidifier can be defined either in change in enthalpy, moisture content or temperature.

The definition of the effectiveness of a dehumidification process is not as simple as that of the humidification process. The purpose of the dehumidification process is to reduce the moisture content of the air. This process does not generally follow the line of constant wet bulb temperature. During the dehumidification process the moisture content of the air is reduced but the temperature or enthalpy of the air may be increased or decreased or remain the same. Hence the effectiveness of the dehumidifier can be defined in terms of change in moisture content of the air.

The effectiveness of a packed bed dehumidifier is defined [57] as the ratio of actual change in moisture content of air during the dehumidification process to the maximum possible change in moisture content of air. It is required to set a theoretical limit on the minimum humidity ratio at the air outlet, that is, the inlet air cannot be dehumidified below that limit under those conditions. For a counterflow packed bed dehumidifier, at the air outlet we have the liquid inlet (at the top of the packing). At this cross-section one finds the lowest liquid vapor pressure. Also the lowest air vapor pressure is at the top. As long as the air vapor pressure is higher than the liquid vapor pressure dehumidification can take place. Hence, the maximum possible dehumidification depends on the properties of the desiccant at the inlet. Therefore, the desiccant inlet conditions set a theoretical limit on the minimum vapor pressure, and therefore the minimum humidity ratio that air can achieve. The same definition is recently used [58] to define the absorption efficiency of the spray tower dehumidifier. It is to be noted that so far no attempt has been made to define the effectiveness for the regeneration process.

5.3 Need for the Definition of Packed Bed Regenerator Effectiveness

The packed bed regeneration process is described in chapter 4. First the volumetric heat and mass transfer coefficients of the gauze-type structured packing for a desiccant-air contact system, were evaluated and then the performance of the

structured packing regenerator was investigated. The computer program solves the heat and mass transfer equations for modeling packed bed regenerator.

For regenerating the weak desiccants in the regenerator, either the air can be heated [59] or the desiccant can be heated [40] and in some cases both can be heated [17]. In such conditions the enthalpy of the air at the inlet may or may not be greater than the enthalpy of the air at the outlet of the regenerator. In fact, Elsayed et al. [17] used the absolute values for defining the effectiveness. In the dehumidifier none of the fluids is heated and hence the enthalpy of the air at the inlet is always greater than the enthalpy of the air at the outlet of the dehumidifier. From the above discussion it is clear that the same effectiveness as given in [55] can be applied only for dehumidification process and/or regeneration process using heated air. The same effectiveness definition cannot be applied for the cases when the desiccant is heated for regeneration. Hence, in this chapter, an attempt is made to define the effectiveness for an adiabatic counterflow packed bed regenerator where either the air or the desiccant is heated.

5.3.1 Definition of Regenerator Effectiveness for a System Using Heated Air

The purpose of the regeneration process is to reduce the moisture content of the desiccant so that the same desiccant can be repeatedly used in the cycle. The regenerator is not only a heat exchanger but also a mass exchanger. The liquid desiccant has a certain vapor pressure at a given liquid temperature and desiccant

concentration. For regeneration to occur, the air vapor pressure must be lower than the desiccant vapor pressure. In a packed bed regenerator it is assumed that at each cross-section of the tower quasiequilibrium conditions exist. In order to increase the desiccant vapor pressure, either the desiccant can be heated or the hot air can be introduced into the tower.

In a desiccant cooling system, the air is heated by using the waste heat given out by the condenser, and any further heating, if necessary, will be provided by the auxiliary heat source. Depending upon the operating conditions of the regeneration process, the vapor pressure of the desiccant at the inlet may or may not be greater than its vapor pressure at the exit of the regenerator. Hence the definition of the regeneration process must be involved with desiccant concentration rather than its vapor pressure. In this study, the effectiveness of the packed bed regeneration process using heated air is defined as the ratio of actual change in concentration of the desiccant during the regeneration process to the maximum possible change in the concentration of the desiccant:

$$\varepsilon = \frac{\xi_{s,o} - \xi_{s,i}}{\xi_{s,\max} - \xi_{s,i}} \tag{5-1}$$

We are interested in setting a theoretical limit on the maximum desiccant concentration. This value is depending upon the application of the use of desiccant and the type of the desiccant used. For example, in the proposed study, the desiccant is

used for cooling operation and after the regeneration the desiccant will be sent to the dehumidifier. Hence, the maximum value of the desiccant concentration depends on the operating conditions of the dehumidifier. For the dehumidification process, if calcium chloride is chosen as the desiccant, then the maximum concentration will be 50% by weight. If desiccant concentration exceeds this value, then crystallization takes place. Similarly, if lithium chloride is selected, then the maximum concentration will be 45% by weight. Therefore, it can be written as,

$\xi_{s,max}$ = 50% for calcium chloride, by weight

$\xi_{s,max}$ = 45% for lithium chloride, by weight

and $\xi_{s,max}$ = 47.5% for CELD (for the mixture of 50% calcium chloride and 50% lithium chloride, by weight)

One can ultimately study the performance of the packed bed regenerator using heated air for the regeneration process based on the definition of the effectiveness set forth here.

5.3.2 Definition of Regenerator Effectiveness for a System Using Heated Desiccant

It is to be noted that in humid climates, regeneration process using heated air may not perform well since the potential for mass transfer is less. In this case, it is better to heat the desiccant and hence, the vapor pressure of the desiccant is always greater than that of the inlet air stream. In order to achieve this, the weak desiccant can

be preheated in a desiccant-to-desiccant heat exchanger with the strong desiccant leaving the regenerator. Auxiliary heating can be provided if further heating is necessary. Hence the effectiveness for the regeneration process using the heated desiccant is defined as the ratio of actual change in the vapor pressure of the desiccant to the maximum possible change in the vapor pressure. The desiccant can be regenerated until it reaches the vapor pressure of the air at the inlet. Let us define the effectiveness as,

$$\varepsilon = \frac{P_{L,in} - P_{L,out}}{P_{L,in} - P_{G,in}} \tag{5-2}$$

The above equation can be rewritten as,

$$\varepsilon = \frac{1 - \left(\frac{P_{L,out}}{P_{L,in}} \right)}{1 - \left(\frac{P_{G,in}}{P_{L,in}} \right)} \tag{5-3}$$

Air at the inlet of the regenerator has a certain humidity ratio at any given temperature, which can be converted to give the partial pressure of water vapor in the air. The weak desiccant at the inlet of the regenerator has a certain vapor pressure at a given desiccant temperature and concentration. For a counter-flow packed bed regenerator, at the desiccant outlet we have the air inlet (at the bottom of the tower). The ratio $P_{L,out}/P_{L,in}$

is called the regeneration factor. The air is humidified during the regeneration process and as long as the desiccant vapor pressure is higher than the air vapor pressure regeneration can takes place.

Because of the abundance of parameters involved in the regeneration process some sort of systematic approach is needed to be employed in order to retain only the most relevant ones in the definition of the effectiveness. Some parameters, such as air inlet vapor pressure and temperature, desiccant inlet temperature and concentration were quite apparent as viable parameters. The Buckingham-Pi theorem is used to indicate the relevant dimensionless parameters. As a result it is indicated that for a given height of packing material, the effectiveness might be expressed as,

$$\varepsilon = \varepsilon\left\langle \frac{P_{L,out}}{P_{L,in}}, P_{G,in}, \frac{T_{L,in}}{T_{G,in}}, \xi_{in}, \frac{G_{in}}{L_{in}} \right\rangle \tag{5-4}$$

Or for a given Z, $P_{G,in}$, L_{in}, and G_{in},

$$\varepsilon = \varepsilon\left\langle \frac{P_{L,out}}{P_{L,in}}, \frac{T_{L,in}}{T_{G,in}}, \xi_{in} \right\rangle \tag{5-5}$$

In other words,

$$\varepsilon = \varepsilon\left\langle T_{L,in}, P_{L,in}, \xi_{in}, P_{L,out}, T_{G,in} \right\rangle \tag{5-6}$$

It was decided that one could correlate ($P_{L,out}/P_{L,in}$) in terms of ($T_{L,in}/T_{G,in}$) and $\xi_{,in}$. $P_{L,in}$ can be correlated in terms of $T_{L,in}$ and ξ_{in}. Thus, the effectiveness can be correlated as,

$$\varepsilon = \varepsilon\left\langle T_{L,in}, \xi_{in}, T_{G,in} \right\rangle \tag{5-7}$$

for a given Z, $P_{G,in}$, L_{in}, and G_{in}.

In accordance with the definition of effectiveness,

$$\varepsilon = \frac{1 - \dfrac{P_{L,out}}{P_{L,in}}}{1 - P_{G,in}\left(\dfrac{1}{P_{L,in}}\right)} \tag{5-8}$$

where

$$\frac{P_{L,out}}{P_{L,in}} = \frac{P_{L,out}}{P_{L,in}}\left\langle \frac{T_{L,in}}{T_{G,in}}, \xi_{in} \right\rangle \tag{5-9}$$

and

$$P_{L,in} = P_{L,in}\left\langle T_{L,in}, \xi_{in} \right\rangle \tag{5-10}$$

for a given Z, $P_{G,in}$, L_{in}, and G_{in}.

In order to correlate Eqn. (5-9), the program REGENERATOR was run for a given packing height and a given desiccant inlet and air inlet flow rates and for a given $P_{G,in}$. The program was run several times; $P_{L,out}/P_{L,in}$ was plotted versus $T_{L,in}/T_{G,in}$ for a few desiccant inlet concentrations. Fig. 5.1 indicates that $P_{L,out}/P_{L,in}$ varies exponentially with $T_{L,in}/T_{G,in}$ for several ξ_{in}. This plot was fed into a regression routine, and the following correlation was obtained,

$$\frac{P_{L,out}}{P_{L,in}} = C_1 e^{C_2\left(\frac{T_{L,in}}{T_{G,in}}\right)} e^{C_3\xi_{in}} \tag{5-11}$$

The next step was to correlate Eqn. (5-10) with the help of existing calcium chloride data [32]. Regression was performed on the calcium chloride vapor pressure data, with an exponential model and the following curve fit was obtained,

$$P_{L,in} = C_4 e^{C_5 T_{L,in}} e^{C_6 \xi_{in}} \tag{5-12}$$

Thus the expression for effectiveness becomes,

$$\varepsilon = \frac{1 - C_1 e^{C_2\left(\frac{T_{L,in}}{T_{G,in}}\right)} e^{C_3\xi_{in}}}{1 - \frac{P_{G,in}}{C_4 e^{C_5 T_{L,in}} e^{C_6\xi_{in}}}} \tag{5-13}$$

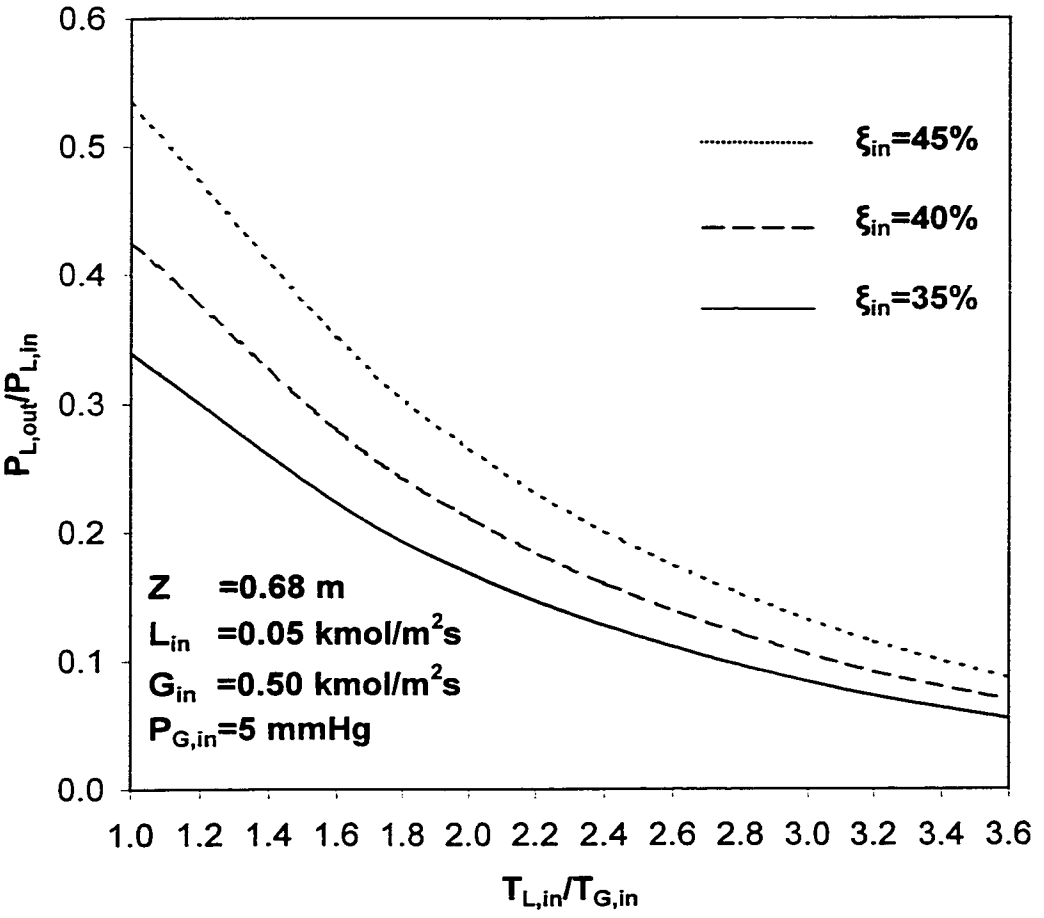

Fig. 5.1 Variation of regeneration factor with inlet temperature ratio for different concentrations.

for a given Z, $P_{G,in}$, L_{in}, G_{in} and geometry/desiccant. It may be noted that the regression coefficients C_4, C_5, and C_6 are independent of the tower geometry and operating conditions; they only depend on the liquid desiccant substance. The regression coefficients C_1, C_2, and C_3 are dependent on the tower height, Z, the partial pressure of water vapor in the regeneration air at the inlet of the regenerator, $P_{G,in}$, and the flow rates L_{in}, and G_{in}. The geometry coefficients C_1, C_2, and C_3 have been calculated for two different packing heights: Z = 0.34 and 0.68 m, for L_{in}= 0.05 kmol/m^{2}s, G_{in} = 0.5 kmol/m^{2}s, and are given in Table 5.1. The above coefficients are valid for the following operating ranges: $T_{L,in}$ = 40 to 90°C, $T_{G,in}$ = 25 to 40°C, ξ_{in} = 35 to 45% of calcium chloride solution as the desiccant.

5.4 Results and Discussion.

An expression for regenerator effectiveness using heated desiccant was obtained in terms of air and desiccant inlet conditions. The effectiveness obtained in Eqn. (5-13) is plotted versus the air inlet temperature in Fig. 5.2. This figure illustrates the general effect of $T_{G,in}$ on ε. For a given air inlet temperature, the regenerator effectiveness increases as the desiccant temperature increases. However, for a given desiccant inlet temperature, the effectiveness decreases as the air inlet temperature increases. This is due to the fact that as the air inlet temperature increases, the desiccant outlet temperature also increases for the same operating conditions. Due to the higher outlet temperature of the desiccant in the regenerator, the vapor pressure of the desiccant at the outlet also increases for the same concentration of the desiccant and

TABLE 5.1: The Geometry Coefficients

Z, m	$P_{G,in}$, mmHg	C_1	C_2	C_3
0.34	05	0.28	-0.700	4.53
	15	0.06	-0.763	4.78
	25	0.80	-0.800	4.90
0.68	05	0.14	-0.700	4.53
	15	0.40	-0.763	4.78
	25	0.06	-0.800	4.90

For $CaCl_2$: C_4=15.044, C_5=0.0476, C_6=-3.70

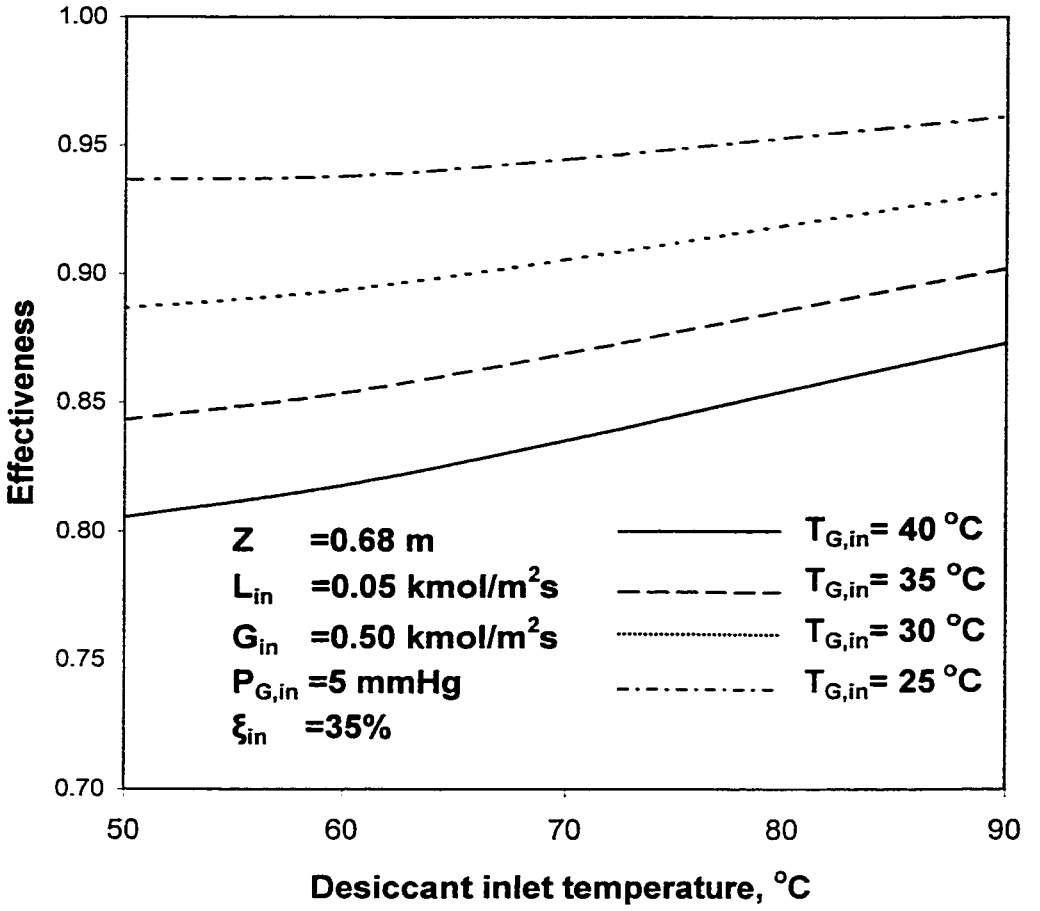

Fig. 5.2 Effect of regeneration air inlet temperature on effectiveness.

for the same $P_{G,in}$. Therefore, the actual change in the vapor pressure of the desiccant in the regenerator decreases and hence, the effectiveness decreases.

The effect of the desiccant concentration at the inlet of the regenerator on the effectiveness for different desiccant inlet temperatures is shown in Fig. 5.3. As the desiccant concentration increases the effectiveness decreases. This is due to the fact that for a given desiccant temperature as the concentration increases, the vapor pressure decreases. Therefore, the potential for mass transfer decreases and hence, the effectiveness also decreases.

The effect of partial pressure of water vapor (that is, humidity ratio) in the regeneration air on the effectiveness is shown in Figs. 5.4 and 5.5. As the partial pressure of water vapor in the regeneration air decreases, the potential for mass transfer increases and hence, the effectiveness increases as shown in Fig. 5.4. Figure 5.5 shows the effect of temperature ratio $T_{L,in}/T_{G,in}$ on the regeneration factor $P_{L,out}/P_{L,in}$ for different $P_{G,in}$. From the figure it is clear that as the regeneration air humidity ratio (say 25 mm Hg) increases the desiccant inlet temperature must be at least 1.5 times greater than the regeneration air inlet temperature.

The influence of tower packing height has been studied and is presented in Fig. 5.6 for the same operating conditions. The effect of using a larger tower is to increase the regenerator effectiveness. Two different packing heights are compared on the same scale. Theoretically, one could achieve an effectiveness of 100% if a tall enough tower is used. For the given conditions, the average effectiveness of a packing height of 0.34 m is about 85%; increasing the packing height to 0.68 m increases the average

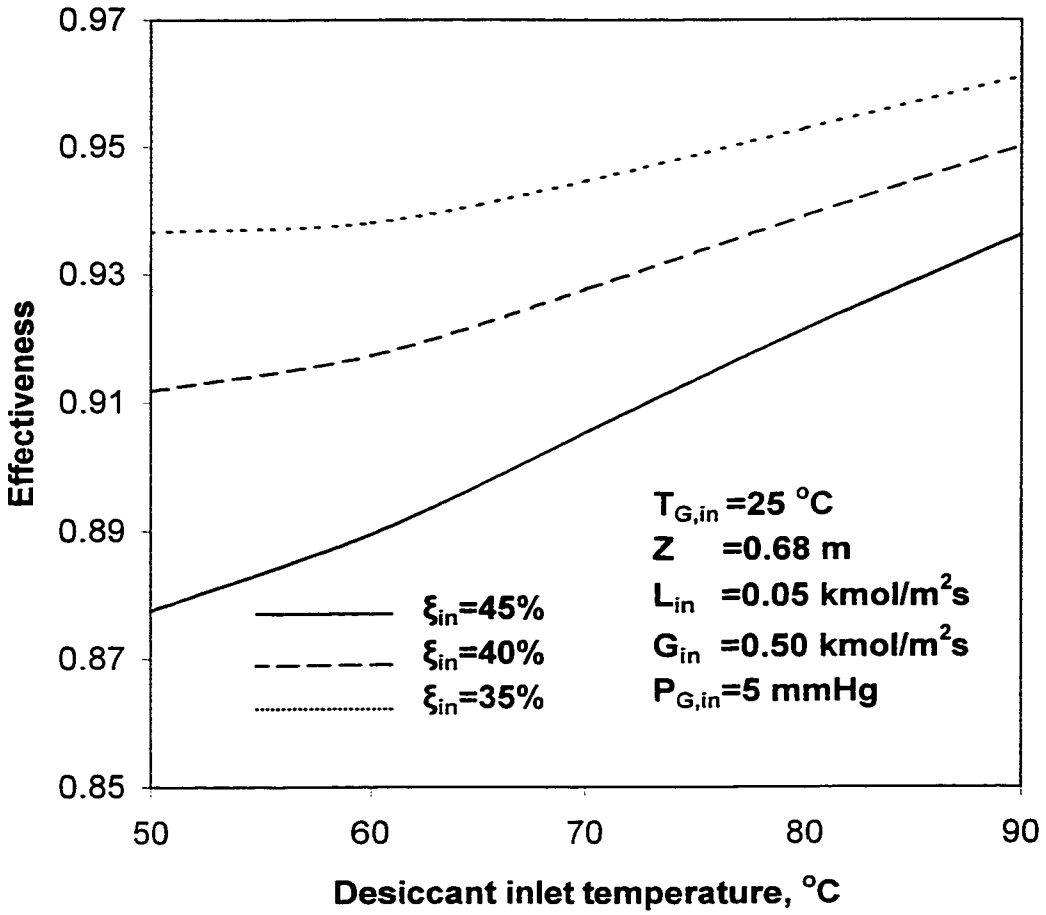

Fig. 5.3 Effect of desiccant inlet concentration on effectiveness.

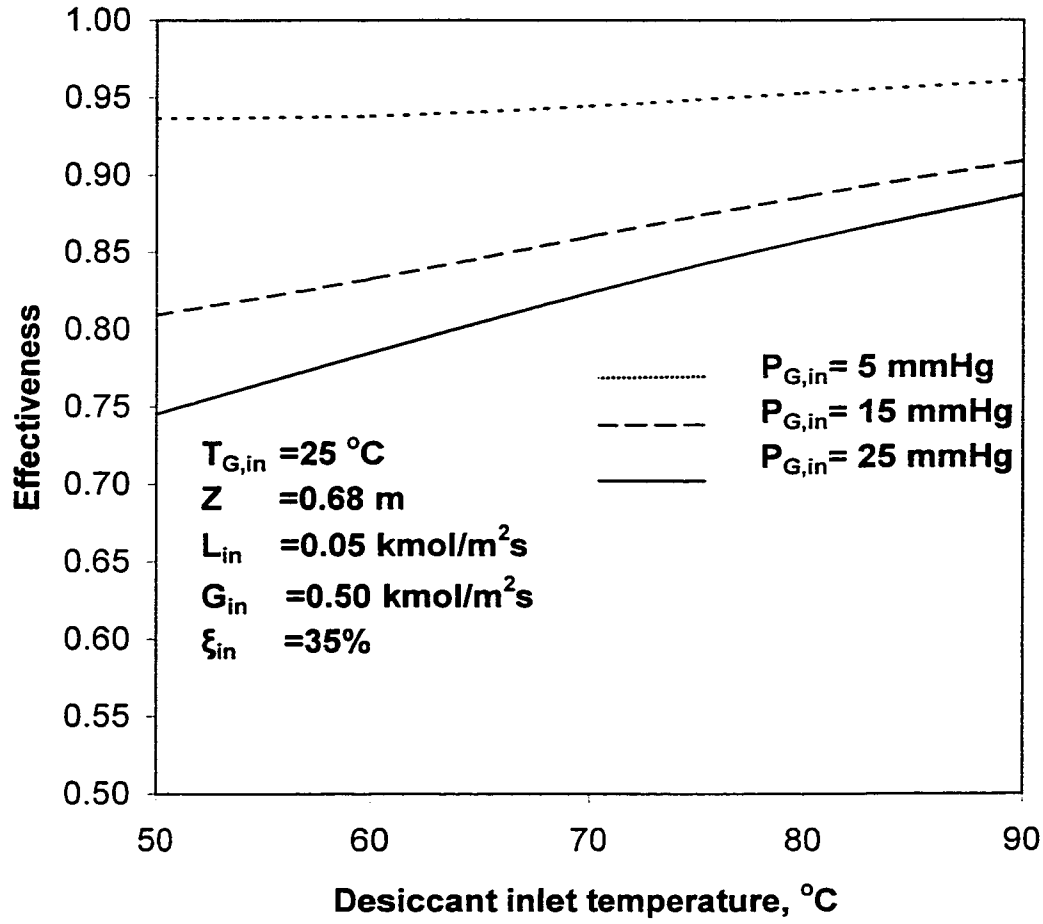

Fig. 5.4 Effect of regeneration air humidity ratio (vapor pressure) on effectiveness.

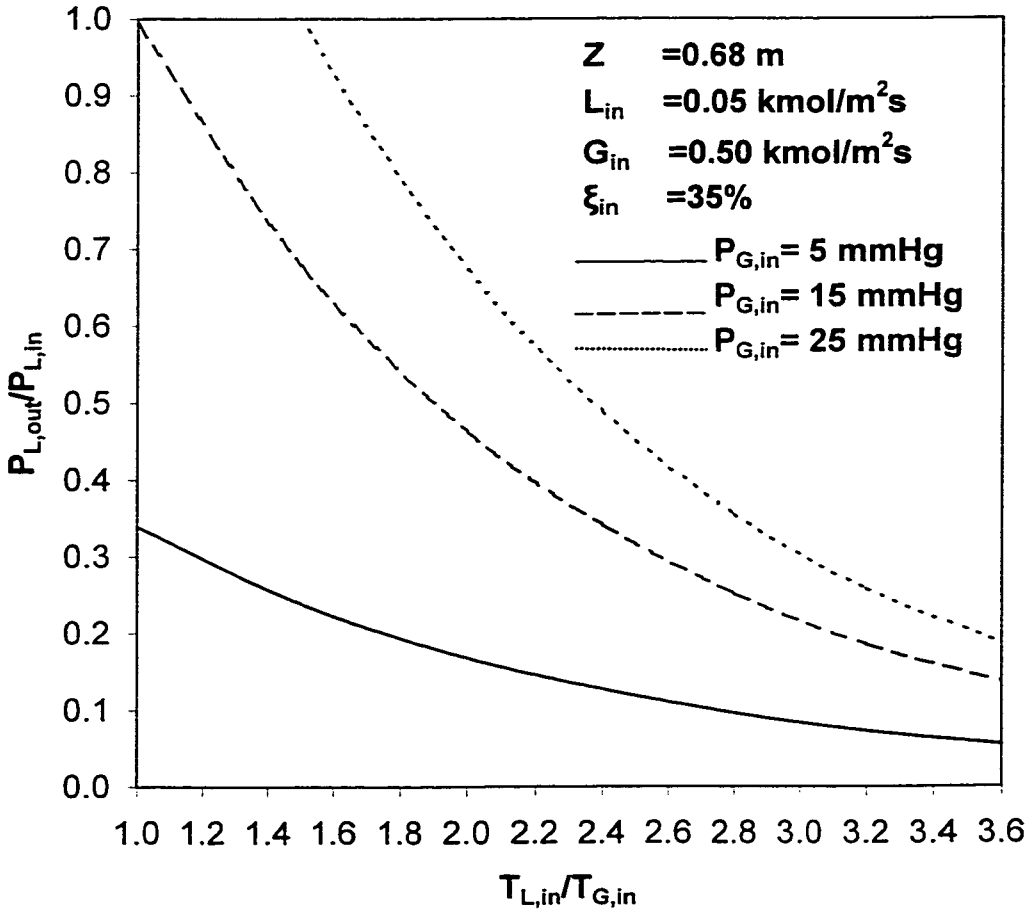

Fig. 5.5 Variation of regeneration factor with inlet temperature ratio for several $P_{G,in}$.

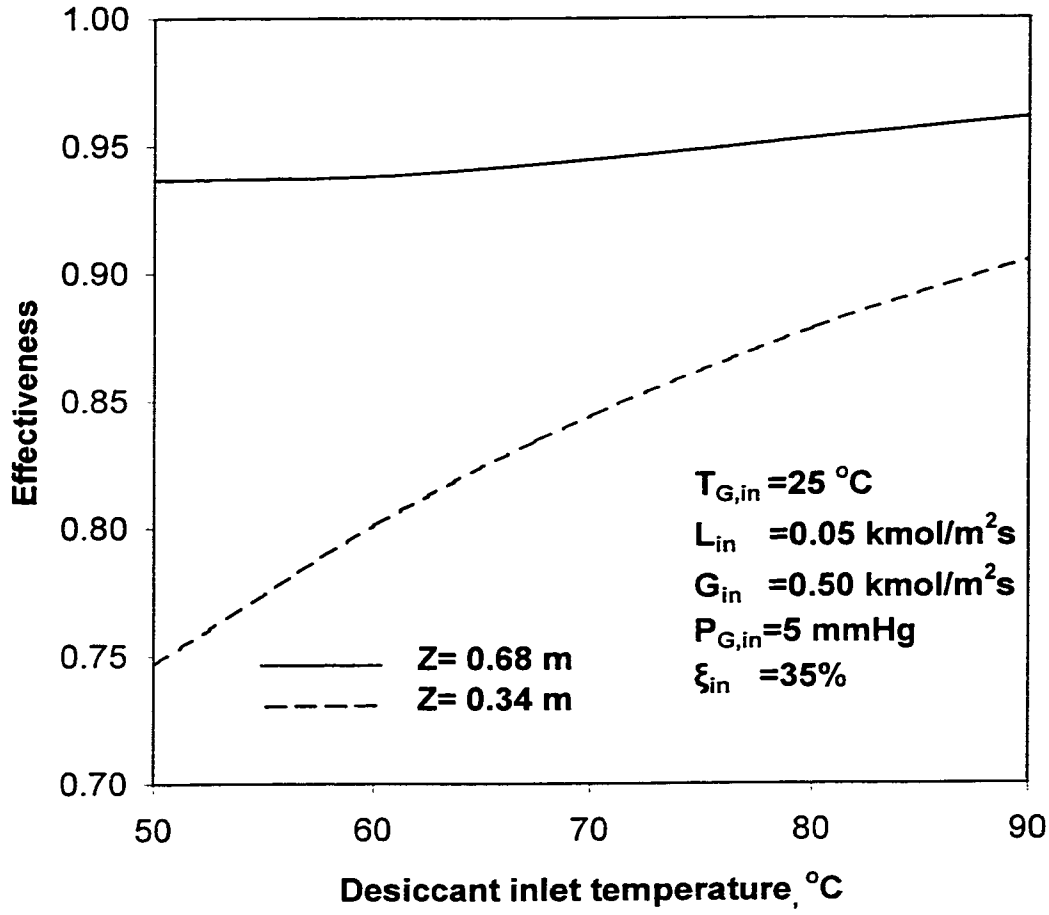

Fig. 5.6 Effect of packing height on effectiveness.

effectiveness to nearly 94.5%. At this rate is would take a packing height not larger than about 1 m to achieve a 100% effectiveness for the regeneration process. That is to say that making a packing height larger than 1 m would not increase its regeneration power, unless some other parameter, such as $T_{L,in}$, is also altered. Therefore knowledge of effectiveness could be useful in setting a limit for the optimum packing height.

CHAPTER 6

PRESSURE DROP IN THE STRUCTURED PACKING DEHUMIDIFIER/ REGENERATOR

6.1 Introduction

Knowledge of the maximum hydraulic capacity and pressure drop of packing are important because in many cases it provides a rational basis for design. On the other hand, many investigators acknowledge the disadvantage of a high-pressure drop through the packed bed dehumidifier/regenerator since the pressure drop directly relates the power consumed by a fan needed to pass the air through a packed bed by,

$$Power = \frac{m_G \Delta P}{\rho_G \eta_f} \tag{6-1}$$

The primary factors that influence the pressure drop are [60] the percentage of void space in the packed tower, packing size and shape, and the densities and mass velocities of the air and the desiccant solution. A part of this pressure drop can be attributed to the packing support, but most of the loss is due to the packing material. The pressure drop through the random packing is several times greater than through structured packing. Structured packings have recently found their use in desiccant-air

desiccants. When designing such systems, the principles of fluid mechanics must be considered for selection of the tower cross-sectional area. At lower values of liquid flow rate, the pressure drop is affected mostly by air flow rate because the air, due to its low density, needs more cross-sectional area between packing pieces in which to flow. At higher liquid flow rate values, the pressure drop increases rapidly due to choking of packing interstices by the liquid.

Figure 6.1 typifies how the pressure drop per height varies with the volumetric flow rate of air for structured packing. There are three flow domains. At low flow rate of air, for a constant desiccant flow rate, the pressure drop increases with increasing air flow rate, as if the packing were dry. It is only mildly dependent on the desiccant flow rate since the liquid adheres to the packing surface and the void space in the packing is nearly constant. The primary effect of the desiccant flow rate is to fill the void space and thus decrease the space available for air flow. The desiccant solution retained in the voids of packing is called the dynamic holdup. If the air flow rate becomes sufficiently large, a region is reached in which a significant holdup of desiccant solution on the packing occurs. This is defined as the region of loading. At a particular value of the air flow rate called the loading point, portions of liquid become airborne, the packing void space becomes smaller, and the slope of the curve becomes steeper. As the liquid desiccant flow rate increases, the air flow rate at the loading point decreases. At values of air flow rate above the loading point, large amounts of liquid remain airborne and may even accumulate at the top of the packing. The packed

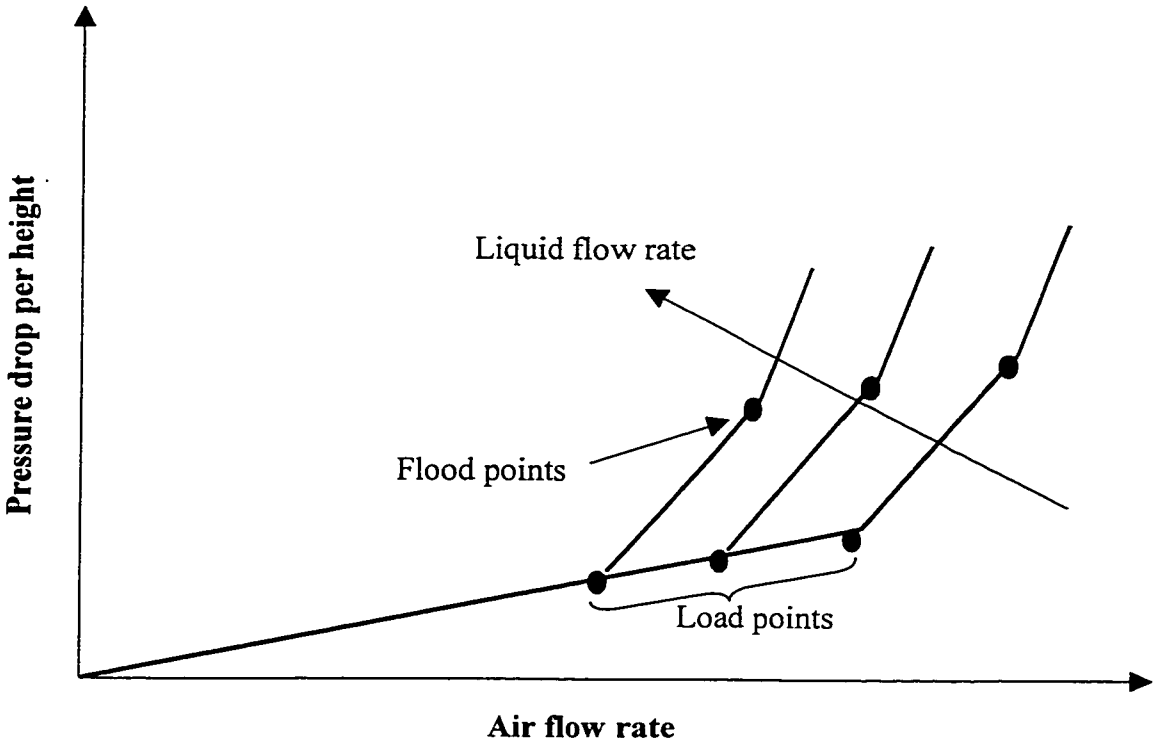

Fig. 6.1 Variation of pressure drop per height with volumetric flow rate of air for structured packing.

bed is now said to be flooded. The value of air flow rate at which flooding occurs is called the flooding point.

This condition is undesirable and should be avoided for successful operation of the tower. After reaching the loading point in the tower, the pressure drop increases more rapidly with increasing the air flow rate until the flooding point is reached. Structured packing towers are typically operated at a superficial air velocity that corresponds to about 50 to 80% of the flooding velocity. This condition is usually near the loading point.

6.2 Models for Predicting Pressure Drop in a Liquid-Gas Contact System

There are two models to describe the hydrodynamics of a liquid-gas contact system containing structured packings. They are the channel model and the particle model. In the channel model, the gas is assumed to be flowing upward inside the numerous small channels having some characteristic dimension; as the liquid flows down the walls of the same channels it reduces the available cross-sectional area for gas flow, thus causing increased pressure drop. In the particle model, the gas is assumed to flow around a packing particle having a characteristic dimension and the liquid acts to increase this dimension by its adherence to the particle surface. The presence of the liquid also reduces the void fraction of the packing.

Rocha et al. [26] and Bravo et al. [61] developed a channel model to describe the pressure drop in structured packing for water-air system. Stichlmair et al. [62] used

particle model for prediction of pressure drop in structured packing as well as random packing columns.

6.2.1 Channel Model

The structured packing incorporates corrugated sheet metal or wire gauze that may or may not be perforated and is arranged such that liquid desiccant flows in thin films along the packing surface. The air flows upward, contacting the desiccant solution as might be expected in a wetted wall arrangement. This type of packing eliminates much of the form drag associated with conventional random type packings and yet preserves much of the intrinsic mass transfer capability of wetted wall devices. Hence, this model is based on the wetted wall column analogy [61] and is proved to be reliable at low pressure drops and at conditions below the loading point since the liquid holdup is not influenced by air velocity. The pressure drop is calculated by,

$$\left(\frac{\Delta P}{\Delta Z}\right)=\left(\frac{\Delta P_d}{\Delta Z}\right)\left[\frac{1}{1-C_1 Fr_l^{0.5}}\right]^5 \tag{6-2}$$

where $\Delta P_d/\Delta Z$ is the dry pressure drop per unit height which is correlated by a conventional Fanning or Darcy relationship and is given by,

$$\left(\frac{\Delta P_d}{\Delta Z}\right)=f\left(\frac{\rho_g U_{ge}^{\ 2}}{S}\right) \tag{6-3}$$

where the friction faction f is given by,

$$f = C_2 + \frac{C_3}{\mathrm{Re}_g} \tag{6-4}$$

$$\mathrm{Re}_g = \frac{SU_{ge}\rho_g}{\mu_g} \tag{6-5}$$

$$U_{ge} = \frac{U_g}{\varepsilon Sin\theta} \tag{6-6}$$

$$Fr_l = \frac{U_l^2}{Sg} \tag{6-7}$$

The constants C_2 and C_3 were determined from dry bed pressure drop data and the constants were found to be $C_2 = 0.177$ and $C_3 = 88.774$. The constant C_1 was found to vary with nominal size of the packing. For example, gauze-type structured packing of channel angle of 60° and the equivalent diameter of 0.353" (9 mm), the value of $C_1 = 3.38$ was assumed.

The above model is modified by Rocha et al. [26] that allows predictions within the loading region and provides determination of the maximum hydraulic capacity of structured packing. This model requires only a knowledge of the packing dimensions and useful only for structured packings. It is to be noted that this model calculates the

pressure drop for the value of flooding pressure drop of 1025 Pa/m, as used for water-air system holdup. However, for desiccant-air contact system containing gauze-type structured packing, the flooding pressure drop is expected to be higher and it is needed to be found.

6.2.2 Particle Model

Stichlmair [62] formally applied the particle model for a two-phase flow. This approach is based on the determination of the dry bed pressure drop followed by a correction for the presence of liquid. The dry bed pressure drop based on fluidized bed analogy is given by,

$$\frac{\Delta P_d}{\Delta Z} = 0.75 f_o \left(\frac{1-\varepsilon}{\varepsilon^{4.65}}\right)\left(\frac{\rho_g U_g^{\ 2}}{d_p}\right) \tag{6-8}$$

where the friction factor f_o is given by,

$$f_o = \frac{D_1}{\mathrm{Re}_g} + \frac{D_2}{\mathrm{Re}_g^{\ 0.5}} + D_3 \tag{6-9}$$

$$\mathrm{Re}_g = \frac{U_g \rho_g d_p}{\mu_g} \tag{6-10}$$

$$d_p = \frac{6(1-\varepsilon)}{a_p} \tag{6-11}$$

The constants D_1, D_2 and D_3 vary with packing type. These constants for random as well as for structured packing materials are given by Stichlmair et al. [62].

The pressure drop of an irrigated bed is higher than that of a dry bed. This increase of pressure drop is caused by liquid being held up in the bed and this liquid change the effective structure of the bed. Porosity of the bed is decreased and the particle diameter is increased due to the liquid flow. The increase in pressure drop in irrigated packing is a function of the dry packing void fraction and the liquid holdup. The pressure drop in irrigated packing is valid below as well as above the loading point provided that the liquid holdup is known. Below the loading point, the holdup is a function of the liquid rate and above the loading point the holdup depends on the liquid as well as the gas rate.

The holdup below the loading point is given by,

$$h_o = 0.555\left(\frac{U_l^{\,2} a_p}{g\varepsilon^{4.65}}\right)^{0.333} \tag{6-12}$$

The holdup above the loading point is given by,

$$h = h_o\left[1+20\left(\frac{\Delta P_{irr}}{Z\rho_l g}\right)^2\right] \tag{6-13}$$

The pressure drop in irrigated packing is given by,

$$\frac{\Delta P_{irr}}{\Delta Z} = \frac{\Delta P_d}{\Delta Z}\left\{\frac{1-\varepsilon\left(1-\frac{h}{\varepsilon}\right)}{1-\varepsilon}\right\}^{\left(\frac{2+c}{3}\right)}\left[1-\frac{h}{\varepsilon}\right]^{-4.65} \tag{6-14}$$

where

$$c = -\frac{\left(\frac{D_1}{\mathrm{Re}_g}+\frac{D_2}{2\mathrm{Re}_g^{0.5}}\right)}{f_o} \tag{6-15}$$

The above equation is implicit in pressure drop and requires a numerical solution. Since this model accounts for the effect of gas velocity on liquid holdup, it is applicable well into the loading region. This model can be applied for both random packing and the structured packing.

6.3 System Analysis for Desiccant-Air System

Flooding does not necessarily occur at the same pressure drop for all liquid loading [63]. The value of the flooding pressure drop depends on the value of the flow parameter and the size of the packing. It is to be noted that for the sake of simplicity, a value of 1025 Pa/m was selected as the flooding pressure drop [26]. They reported that for structured packings, this pressure drop should lie between values of 900 and 1200 Pa/m and this is valid only for the air/water system. However, for desiccant-air contact system containing structured packing materials the flooding pressure drop would be higher than water-air system. This is due to the fact that the viscosity of the desiccant increases as concentration increases. Further, as desiccant temperature decreases its viscosity increases for a particular value of concentration. Hence, it is necessary to calculate the flooding pressure drop and then, channel model can be used to calculate the irrigated pressure drop for desiccant-air contact system. This approach is adopted here to calculate the pressure drop in a desiccant-air contact system containing gauze-type structured packing.

The model presented here is the combination of channel model and particle model. The particle model for desiccant-air contact system is used to find the pressure drop at the flood point and this flooding pressure drop is used in the channel model to calculate the irrigated pressure drop. At the flood point the pressure drop increases infinitely with increasing gas load. If the gas load is represented by the dry pressure drop, the flooding condition is represented by setting the derivative of the pressure

drop with respect to gas velocity at constant liquid velocity equal to infinity, as given by Stichlmair et al. [62].

$$\frac{\partial \Delta P_{irr}}{\partial \Delta P_d} = \infty \tag{6-16}$$

In other words, the reciprocal is equal to zero as,

$$\frac{\partial \Delta P_d}{\partial \Delta P_{irr}} = 0 \tag{6-17}$$

This must be solved for the pressure drop at the flood point. Equation (6-14) is used to determine the appropriate flooding velocities. A particular combination of gas velocity and pressure drop exists for every liquid velocity at the flood point, and the pressure drop at the flood point is not necessarily constant for every pair of gas and liquid flood velocities. Differentiation of Eqn. (6-17) yields the pressure drop at the flood point, which is given by

$$\left(\frac{\Delta P_{irr}}{Z\rho_L g}\right)_f^{-2} - \frac{40\left(\frac{2+c}{3}\right)h_o}{1-\varepsilon+h_o\left[1+20\left(\frac{\Delta P_{irr}}{Z\rho_L g}\right)_f^2\right]} - \frac{186h_o}{\varepsilon-h_o\left[1+20\left(\frac{\Delta P_{irr}}{Z\rho_L g}\right)_f^2\right]} = 0 \tag{6-18}$$

6.4 Results and Discussion

As mentioned earlier, Rocha et al. [26] used 1025 Pa/m as the flooding pressure drop for the air-water system containing structured packings. However, it is expected that the flooding pressure drop for desiccant-air contact system to be higher than water-air system because of the high viscosity and high surface tension of the desiccant. Knowledge of flood point is essential for tower dimensioning in that the flooding condition establishes the theoretical minimum tower diameter [62]. In order to calculate the flood point for a desiccant-air contact system, first the superficial air velocity is assumed and the dry pressure drop is calculated using the Eqn. (6-8). For the same air velocity and a fixed desiccant superficial velocity, the irrigated pressure drop is calculated from Eqn. (6-14). A check has been made with Eqn. (6-18) to see whether the assumed superficial air velocity gives a closure value. Otherwise, a new value is assumed and the calculation is repeated till to get the closure value. Figure 6.2 shows the comparison of calculated values of pressure drop for this work with those obtained using Rocha et al. [26] and Stichlmair et al. [62] data for the same operating conditions. The figure gives confidence to this work because it's pressure drop lies between the pressure drop obtained by Rocha et al. and Stichlmair et al.. Figure 6.3 illustrates the flooding superficial air velocity versus superficial desiccant velocity. Three different desiccant-air contact systems, namely calcium chloride–air, lithium chloride–air, and CELD-air were considered and the results are compared with water-air system. It can be seen that the desiccant-air system needs the higher flooding superficial gas velocity than water-air system. For a given superficial liquid velocity, the changes in superficial gas velocity for different desiccant-air system are insignificant.

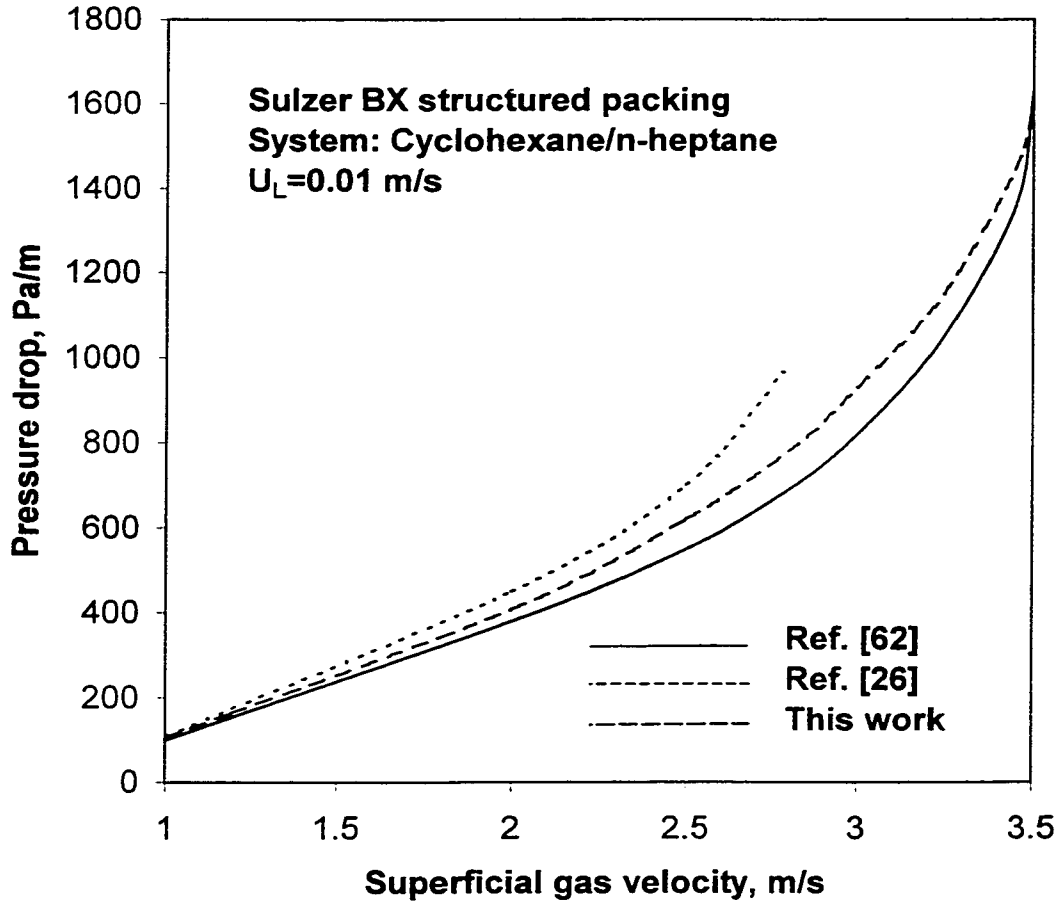

Fig. 6.2 Comparison of calculated values of pressure drop for this work with those obtained using Rocha et al. and Stichlmair et al.

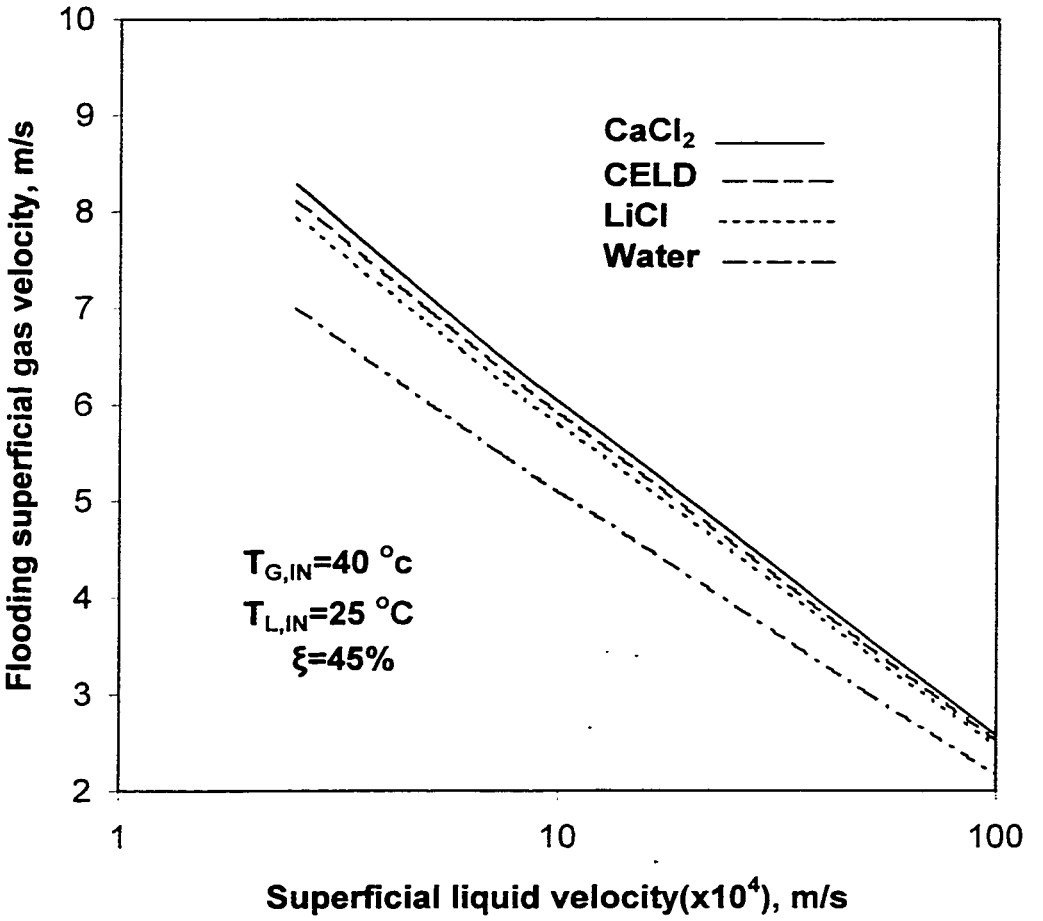

Fig. 6.3 Effect of superficial liquid velocity on flooding superficial gas velocity for different desiccants.

Figure 6.4 shows the variation of flooding pressure drop for different desiccant velocity. As the liquid superficial velocity (that is, liquid flow rate) decreases the flooding pressure drop increases. It is clear that the flooding pressure drop for desiccant-air system is always higher than water-air system. Among the desiccant-air systems and at a particular liquid superficial velocity, calcium chloride-air system has the highest flooding pressure drop and lithium chloride-air system has the least flooding pressure drop. The above study shows that the flooding pressure drop must be calculated before one finds the pressure drop of the bed.

Figure 6.5 shows the variation of structured packing pressure drop for different desiccant-air system and is compared with water-air system for various superficial air velocities. As one expected, water-air system has the lowest pressure drop for the given operating conditions and lithium chloride-air system has the highest pressure drop due to its viscosity. However, at low flow rates of air, the variation of pressure drop is insignificant among desiccant-air systems.

The study is extended to compare the pressure drop of gauze-type structured packing with random packing materials for a desiccant-air system. Raschig Rings and Berl saddles are widely used in the process industries and hence this study considers only these two packing materials. The physical characteristics of packing materials extracted from Stichlmair [62] are given in Table 6.1 and the results are shown in Fig. 6.6. In general, for any packing materials as the superficial air velocity increases the pressure drop also increases. The figure clearly demonstrates the structured packing has the lowest pressure drop and has wider operating ranges compared with random packing materials. Berl Saddles are more costly to produce than Raschig Rings but they give a lower pressure drop as illustrated in the figure.

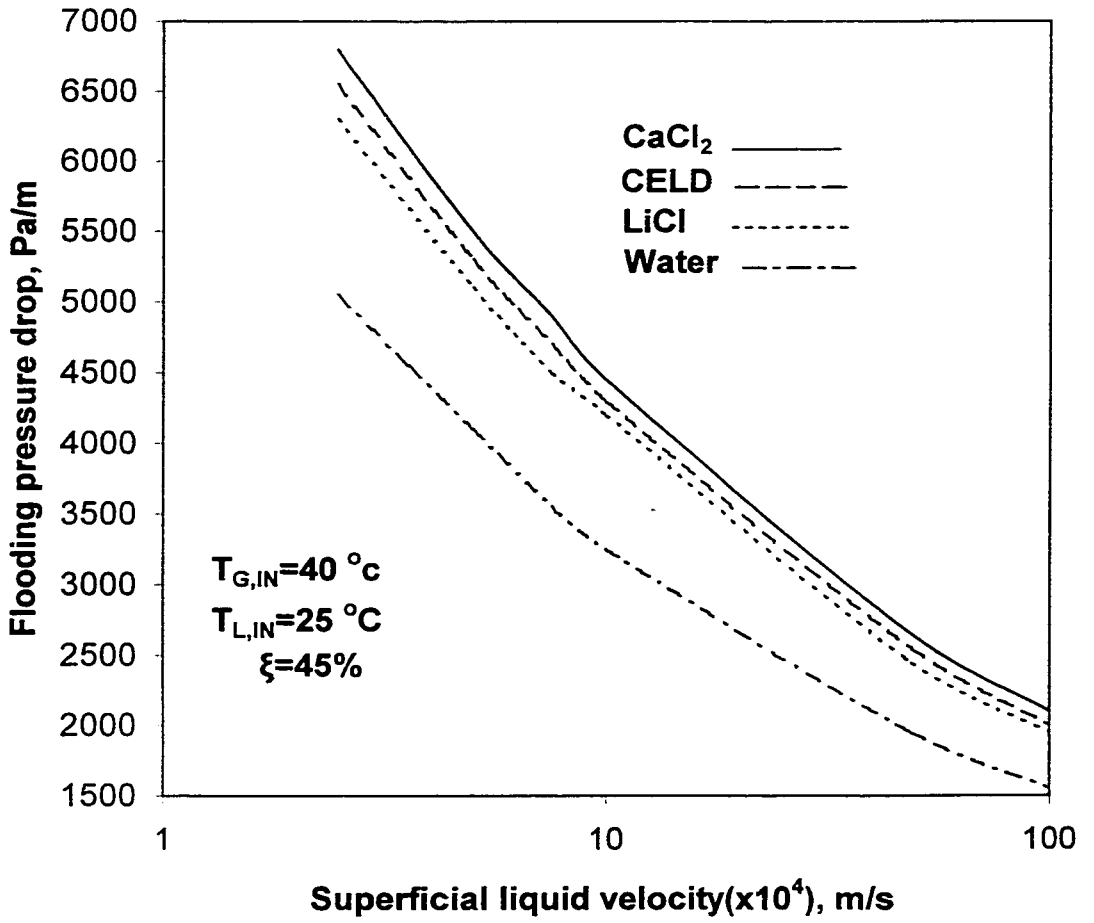

Fig. 6.4 Effect of superficial liquid velocity on flooding pressure drop for different desiccants.

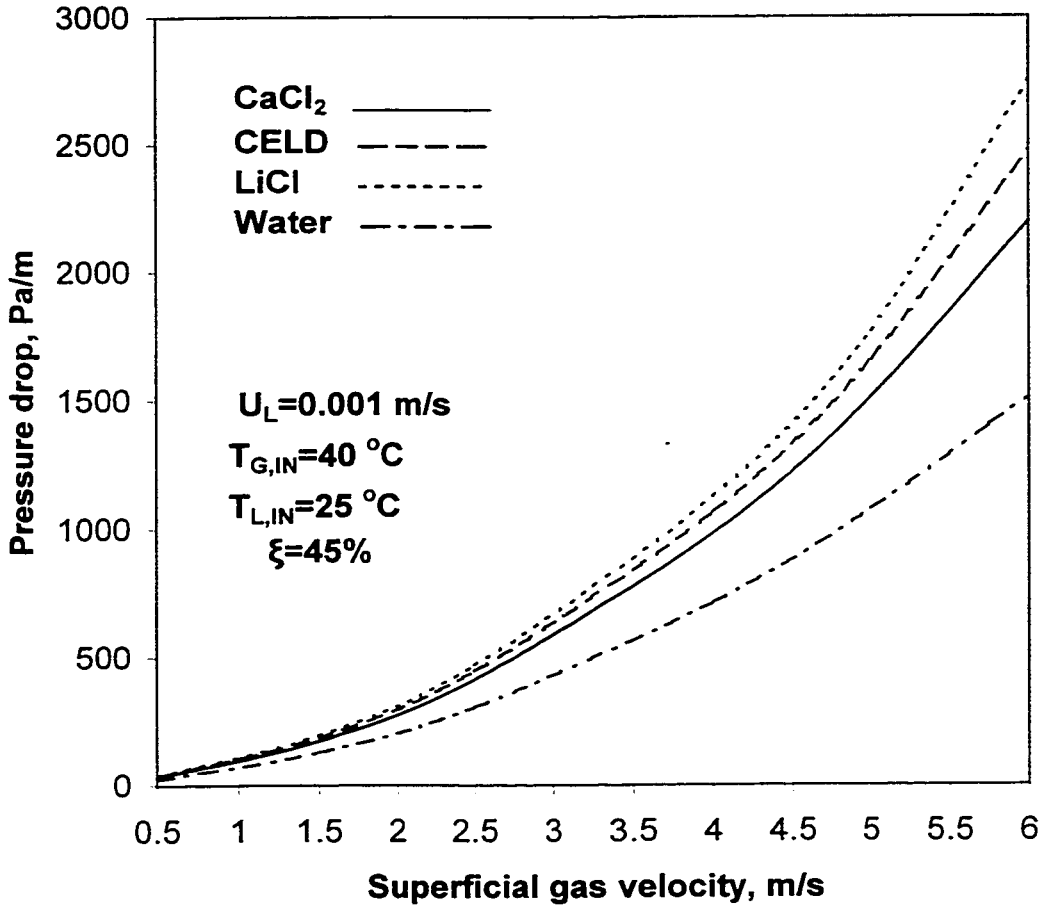

Fig. 6.5 Effect of superficial gas velocity on pressure drop for different desiccants.

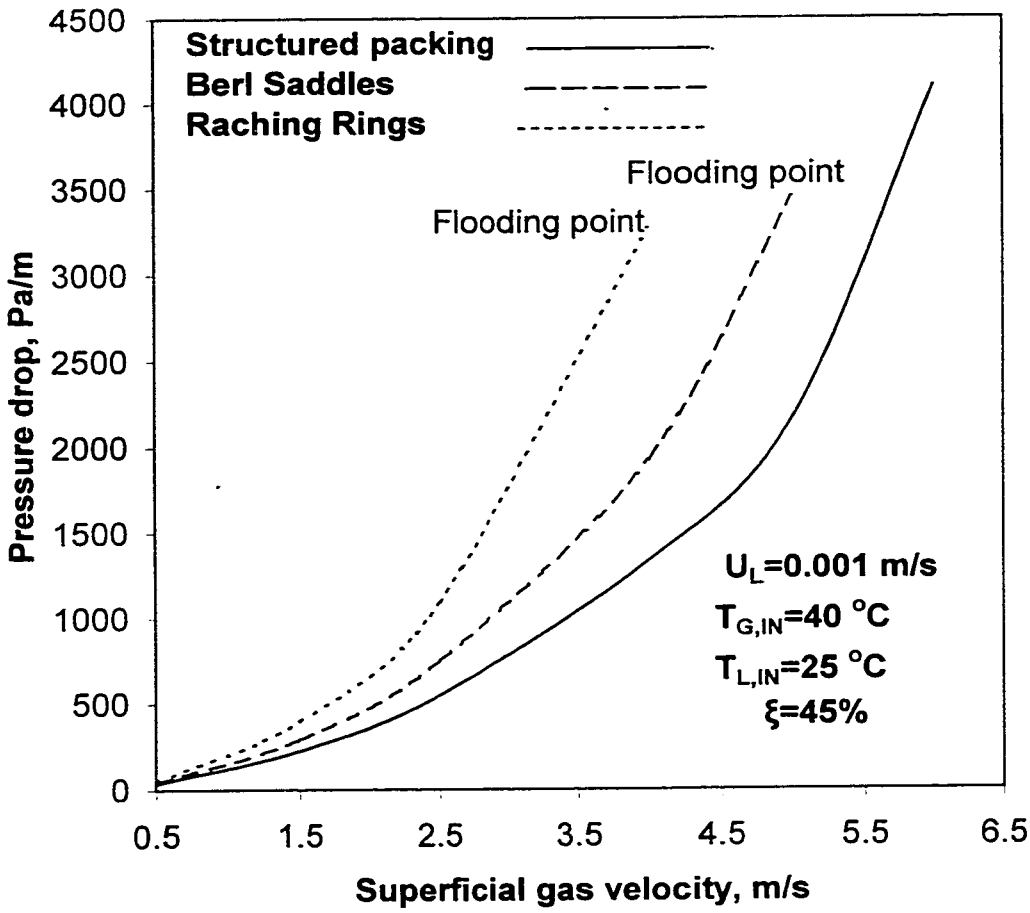

Fig. 6.6 Pressure drop for different packing materials.

TABLE 6.1: The Physical Characteristics of Packing Materials Extracting from [62]

Packing	Type/Size	a, m^2/m^3	ε	D_1	D_2	D_3
Structured Packing	Sulzer – BX type	450	0.86	115	2	0.35
Ceramic Raschig Rings	30 mm	137	0.775	48	8	2
Ceramic Berl Saddles	35 mm	133	0.75	53	14	1

CHAPTER 7

CONCLUSIONS AND RECOMMENDATIONS

7.1 Conclusions

The following conclusions can be drawn from the study:

- The lithium chloride has the highest rate of liquid-phase mass transfer coefficient when compared with the other two desiccants namely calcium chloride and the mixture of these two desiccants.
- The mixture of calcium chloride and lithium chloride solution has a considerable increase in liquid-phase mass transfer coefficient compared with calcium chloride solution.
- The structured packing materials outperform the random packing materials. The structured packing has the lowest pressure drop and has wider operating ranges compared with random packing materials.
- In the dehumidification process, the lithium chloride needs the least packing height for the same operating conditions and calcium chloride needs the largest packing height.

- ❖ In the regeneration process, the calcium chloride-air system need less packing compared with other desiccants for the same operating conditions. However, the difference in packing height for three different desiccants is insignificant.
- ❖ Preheating the desiccant improves the performance of the regeneration process.
- ❖ In humid climates, regeneration process using heated air may not perform well since the potential for mass transfer is less. In this case, it is better to heat the desiccant and hence, the vapor pressure of the desiccant is always greater than that of the inlet air stream.
- ❖ Water-air system has the lowest pressure drop for the given operating conditions and lithium chloride-air system has the highest pressure drop due to its viscosity. However, at low flow rates of air, the variation of pressure drop is insignificant among desiccant-air systems.

7.2 Recommendations:

- Further study is needed to find different combination of mixtures of two or more liquid desiccants in order to get better absorption performance without sacrificing the absorption properties and cost.
- Economic analysis must be carried out to find the suitable packing material for any particular application.

APPENDICES

APPENDIX I: THE PROPERTY DATA EQUATIONS FOR DIFFERENT DESICCANT SOLUTIONS AND AIR:

1. Air-properties equations

$$\rho_G = 1.2521 - 0.003\ T_G$$
$$\mu_G = 1.72\times10^{-5} + 4.63\times10^{-8}\ T_G$$
$$C_p = 1004.8 + 0.0696\ T_G$$
$$\kappa = 0.0242 + 7.0\times10^{-5}\ T_G$$
$$\sigma = 1.85\times10^{-5} + 1.54\times10^{-7}\ T_G$$
$$Pr_G = 0.7133 - 0.000167\ T_G$$

2. $CaCl_2$-properties equations

$$\rho_L = 990.857\xi - 0.5T_L + 937.425$$
$$\mu_L = 0.0122\xi - 4.3\times10^{-5}T_L - 1.37\times10^{-4}$$
$$C_p = -3.4\xi + 0.0027T_L + 3.735$$
$$\kappa = -1.7\times10^{-4}\xi + 1.25\times10^{-6}T_L + 0.00058$$

3. LiCl-properties equations

$$\rho_L = 636\xi - 0.275T_L + 989.578$$
$$\mu_L = 0.0307\xi - 7.78\times10^{-5}T_L - 3.36\times10^{-3}$$
$$C_p = -2.43\xi + 3.693$$
$$\kappa = -9.8\times10^{-5}\xi + 1.23\times10^{-6}T_L + 0.000545$$

4. CELD-properties equations

$$\rho_L = 813.43\xi - 0.388T_L + 963.5$$
$$\mu_L = 0.02146\xi - 6.1\times10^{-5}T_L - 1.75\times10^{-3}$$
$$C_p = -2.92\xi + 0.00135T_L + 3.714$$
$$\kappa = -1.34\times10^{-4}\xi + 1.24\times10^{-6}T_L + 0.0005625$$

The above property data equations are valid for:

T_L = 30 to 60 °C

ξ = 35 to 45% for $CaCl_2$

ξ = 30 to 40% for LiCl

ξ = 32.5 to 42.5% for CELD

APPENDIX II: FLOW CHART AND LISTING OF PROGRAM FOR THE DEHUMIDIFIER ANALYSIS.

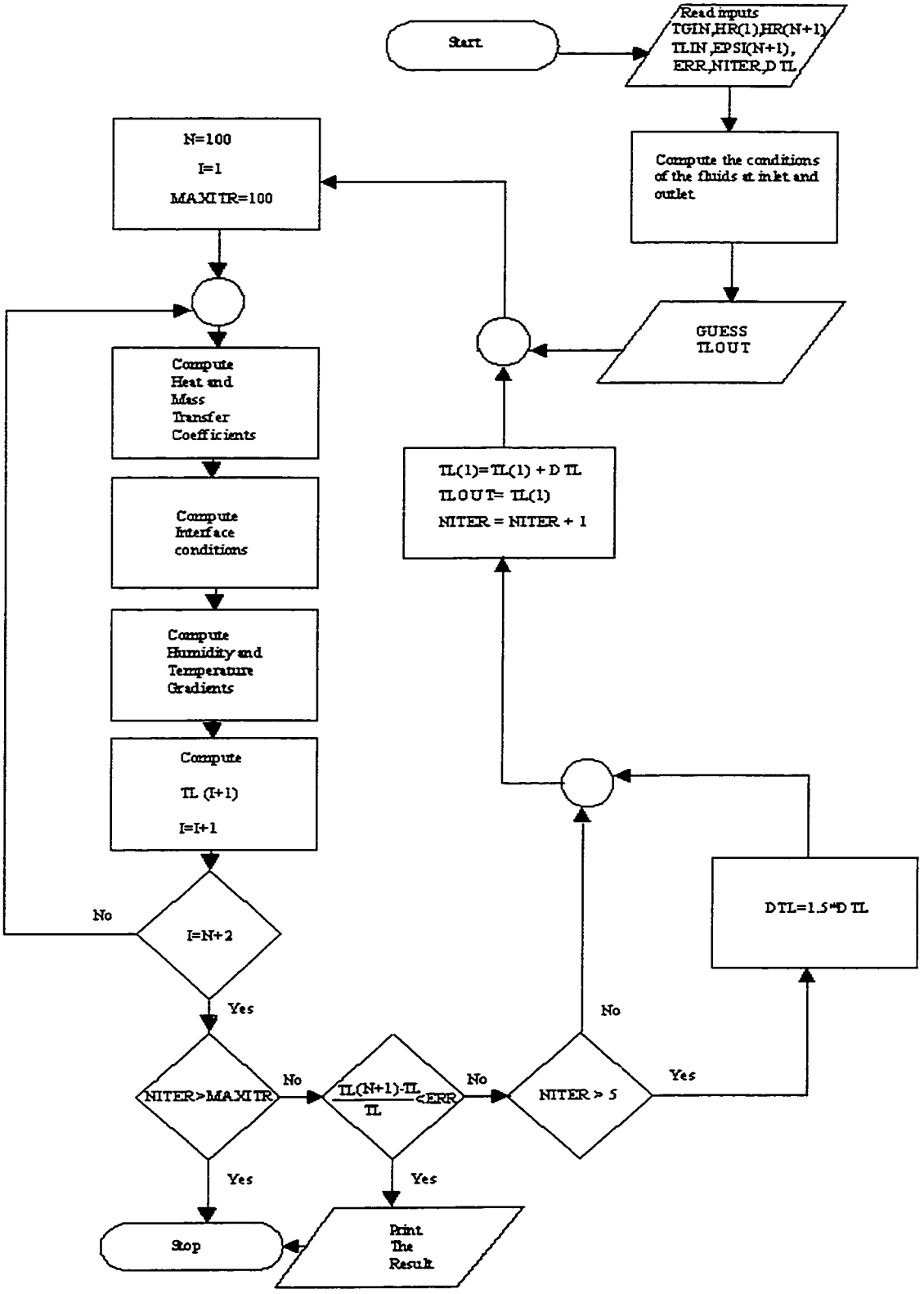

```
C       STRUCTURED PACKING DEHUMIDIFIER ANALYSIS
************************************************
C       DESICCANT - CALCIUM CHLORIDE
************************************************
C
        REAL Z(300),TG(300),TL(300),EPSI(300),HR(300)
        REAL LAMDAO,LIN,LOUT,L,LPRM,MWAIR,MWLIQ
        OPEN(6,file='m.txt')
C
        TGIN=39
        DO 362 IK=1,1
        TGIN=TGIN+1.0
        WRITE(6,274)TGIN
274     FORMAT(20X,'TGIN=',F10.4)
        DEHUMF=0.3405
        DO 182 JK=1,1
        DEHUMF=DEHUMF+0.005
    WRITE(6,756)DEHUMF
756     FORMAT(18X,'DEHUMF=',F10.4)
        LIN=0.01
        DO 543 K=1,1
        LIN=LIN+0.004
        G=0.22
        DO 564 KK=1,1
        G=G+0.02
        WRITE(6,544)LIN
544     FORMAT(21X,'LIN=',F10.3)
        WRITE(6,545)G
545     FORMAT(23X,'G=',F10.4)
C       READ THE INPUT DATA
        N=100
        CA=2.75E5
        CB=29145.0
        CC=33912.0
        LAMDAO=43.68E6
        TO=30
        DELHS=-8.18789E7
        EPSI(N+1)=0.45
        HR(1)=0.01213
        GB=G*(1.-HR(1))
        TLIN=25
        TLOUTA=30
        ERR=0.05
```

```
      MWAIR=28.97
      MWLIQ=110.99
      NITER=0
      MAXITR=100
      DTL=0.01
      BIGOUT=1
C
C     CONDITIONS OF GAS AT INLET (BOTTOM OF THE TOWER)
C
      PW=HR(1)*760.0/(0.622+HR(1))
      SYCIN=PW/760.0
      CYCIN=SYCIN/(1.-SYCIN)
      SXCIN=1.-EPSI(N+1)
      GBPRM=GB*MWAIR/1.2
C
C     CONDITIONS OF GAS AT THE OUTLET (TOP OF THE TOWER)
C
      CYCOUT=(1.-DEHUMF)*CYCIN
C
C     CONDITION OF LIQUID AT OUTLET (BOTTOM OF THE TOWER)
C
      LOUT=LIN+GB*(CYCIN-CYCOUT)
      WTOUT=LIN*SXCIN+GB*(CYCIN-CYCOUT)
      SXCOUT=WTOUT/LOUT
      EPSI(1)=1.-SXCOUT
C
C     GUESS LIQUID OUTLET TEMPERATURE
C
      TL(1)=TLOUTA
      TLOUT=TLOUTA
C
1000  CONTINUE
C
C     INITIALIZE AT THE BOTTOM OF THE TOWER
C
      I=1
      L=LOUT
      TG(1)=TGIN
      LPRM=L*MWLIQ/1350
      CYC=CYCIN
      EPSI(1)=1.-SXCOUT
      SXC=SXCOUT
      SYC=SYCIN
```

```
      Z(1)=0.0
C
2000  CONTINUE
C
C     CALCULATION OF HEAT & MASS TRANSFER COEFFICIENTS
C     STRUCTURED PACKING
C
   HGA=12963.21*(LPRM**0.1)*(GBPRM**0.79)*EXP(-0.026*TG(I))
   FGA=0.55*(LPRM**0.1)*(GBPRM**0.79)*EXP(-0.0293*TG(I))
      FLA=6.27*(LPRM**.4)*GBPRM**.07*EXP(-
.033*TL(I))*EXP(.0066*EPSI(I))
      FLAFGA=FLA/FGA
      CALL INFACE (SXC,SYC,TL(I),FLAFGA.SXCI,SYCI)
C
C     CALCULATE GRADIENTS AT SECTION I:
C
      DCYCDZ=-(FGA/GB)*ALOG((1.-SYCI)/(1.-SYC))
      HGACOR=(-GB*CC*DCYCDZ)/(1.-EXP((GB*CC*DCYCDZ)/HGA))
      DTGDZ=-(HGACOR*(TG(I)-TL(I)))/(GB*(CB+CYC*CC))
      DTLDZ=(1./(L*CA))*(GB*(CB+CYC*CC)*DTGDZ+GB*(CC*(TG(I)-TO)+
   1  LAMDAO)*DCYCDZ-GB*(CA*(TL(I)-TO)+DELHS)*DCYCDZ)
C
      DELCYC=(CYCOUT-CYCIN)/FLOAT(N)
C
C     UPDATE PARAMETERS FOR NEXT SECTION, I+1:
C
      DELZ=DELCYC/DCYCDZ
      Z(I+1)=Z(I)+DELZ
      CYC=CYC+DELCYC
      SYC=CYC/(1.+CYC)
      HR(I+1)=0.622*CYC
      FL=L
      L=L+GB*DELCYC
      LPRM=L*MWLIQ/1350
      SXC=(FL*SXC+GB*DELCYC)/L
      EPSI(I+1)=1.-SXC
      TG(I+1)=TG(I)+DELZ*DTGDZ
      TL(I+1)=TL(I)+DELZ*DTLDZ
C
      I=I+1
C
C     CHECK IF ALL N SECTIONS HAVE BEEN SCANNED, IF SO CHECK
FOR
```

```
C       ACCURACY OF THE GUESSED VALUE:
C
        IF(I.EQ.(N+2)) GO TO 50
        GO TO 2000
50      IF(NITER.EQ.MAXITR)GO TO 302
        IF(ABS((TL(N+1)-TLIN)/TLIN).LT.ERR)GO TO 201
        IF(TL(N+1)-TLIN)101,201,301
101     IF(NITER.GT.5) DTL=1.5*DTL
        TL(1)=TL(1)+DTL
        TLOUT=TL(1)
        NITER=NITER+1
        GO TO 1000
301     IF(NITER.GT.5)DTL=1.5*DTL
        TL(1)=TL(1)-DTL
        TLOUT=TL(1)
        NITER=NITER+1
        GO TO 1000
302     WRITE(6,3021)
3021    FORMAT(' MAX ITERATIONS PERFORMED, COULD NOT
CONVERGE')
        STOP
201     CONTINUE
C
C       PRINT OUT THE RESULTS:
C
        TGOUT=TG(N+1)
        HROUT=0.622*CYC
        WRITE(6,10) TL(N+1),TL(1),TG(N+1),TG(1),HR(N+1),HR(1),
     1  Z(N+1)
10      FORMAT(///,10X,'RESULTS FOR A PACKED TOWER DEHUMIDIFIER:'
        1               /10X,'-----------------(CACL2)-------------'
     2  /16X,'LIQ.TEMP.AT TOP , TL=',F10.3,3X,'(MODIFIED)'
     3  /10X,'LIQ.TEMP. AT BOTTOM, TLOUT=',F10.3,3X,'(FOUND)'
     4  /13X,'AIR TEMP. AT TOP, TGOUT=',F10.3,3X,'(FOUND)',
     5  /11X,'AIR TEMP. AT BOTTOM, TGIN=',F10.3,3X,'(GIVEN)',
     6  /13X,'HUM.RATIO AT TOP, HROUT=',F10.5,3X,'(GIVEN)',
     7  /11X,'HUM.RATIO AT BOTTOM, HRIN=',F10.5,3X,'(GIVEN)',
     8  //10X,'HEIGHT OF PACKING MATERIAL',
     9  '(TOWER HEIGHT)', 'Z=',F10.3,1X,'m'////)
c       IF(DEHUMF.GT.0.5333) GO TO 111
C
C       IF YOU WANT TO OBTAIN VARIOUS DISTRIBUTIONS, THEN ASSIGN
C       BIGOUT=1(NEAR THE BEGINNING OF THE PROGRAM).  IF YOU
```

```
C       DO NOT WANT ANYMORE OUTPUT THEN PUT BIGOUT=0.
C
        IF(BIGOUT.EQ.0.)GO TO 564
        WRITE(6,20)
20      FORMAT(//10X,'TEMPERATURE & CONCENTRATION DISTRIBUTION
ALONG',1X,
     1  'THE TOWER',/10X,57('-'),//23X,'Z',5X,'TL',5X,'EPSI',5X,
     1  'TG',6X,'HR')
        NP1=N+1
        DO 400 J=1,NP1
        I=N+2-J
        WRITE (6,30) Z(I),TL(I),EPSI(I),TG(I),HR(I)
30      FORMAT(20X,F5.3,2X,F6.3,2X,F5.3,3X,F6.3,2X,F5.3)
400     CONTINUE
564     CONTINUE
543     CONTINUE
182     CONTINUE
362     CONTINUE
        END
C
C       ***********************************************
C       SUBROUTINE INFACE
C       ***********************************************
C
        SUBROUTINE INFACE(SXC,SYC,TL,FLAFGA,X,SYCI)
        DXI=0.01
        EPSI=0.0001
        X=0.10
        XMAX=0.98
        T=TL
5       DELTX=DXI
        FX=0.040416+0.00091228*T-(0.030388/X)-1.+(1.-SYC)*
     1  (((1.-SXC)/(1.-X))**FLAFGA)
6       X=X+DELTX
        FX1=0.040416+0.00091228*T-(0.030388/X)-1.+(1.-SYC)*
     1  (((1.-SXC)/(1.-X))**FLAFGA)
        IF(ABS(FX1).GT.1./EPSI)GO TO 7
        GO TO 9
7       WRITE(6,8)X
8       FORMAT(' ','FUNCTION APPROACHING INFINITY FOR X=',F7.4)
        X=X+DXI
        GO TO 5
9       IF(FX*FX1)11,13,10
```

```
10      IF(X.GT.XMAX)RETURN
        FX=FX1
        GO TO 6
11      IF(DELTX-EPSI)13,13,12
12      X=X-DELTX
        DELTX=DELTX/10.
        GO TO 6
13      CONTINUE
        SYCI=0.040416+0.00091228*TL-(0.030388/X)
        X=X+EPSI
        GO TO 5
        END
```

APPENDIX III: LISTING OF PRORAM FOR THE REGENERATOR ANALYSIS.

```
C       STRUCTURED PACKING REGENERATOR ANALYSIS
************************************************
C       DESICCANT - CALCIUM CHLORIDE
************************************************
C
        REAL Z(300),TG(300),TL(300),EPSI(300),HR(300)
        REAL LAMDAO,LIN,LOUT,L,LPRM,MWAIR,MWLIQ
        OPEN(6,file='s.txt')
C
        TGIN=60
        DO 362 IK=1,1
        TGIN=TGIN+5.0
        WRITE(6,274)TGIN
274     FORMAT(20X,'TGIN=',F10.3)
    LIN=0.0108
        DO 543 K=1,1
        LIN=LIN+0.01
        G=0.192
        DO 564 KK=1,1
        G=G+0.004
        WRITE(6,544)LIN
544     FORMAT(21X,'LIN=',F10.3)
        WRITE(6,545)G
545     FORMAT(23X,'G=',F10.3)
C       READ THE INPUT DATA
        N=100
        CA=2.75E5
        CB=29218.0
        CC=33912.0
        LAMDAO=43.68E6
        TO=50.0
        DELHS=-8.18789E7
        EPSI(N+1)=0.44
        HR(1)=0.028
        EPSI(1)=0.45
        GB=G*(1.-HR(1))
        TLIN=45
        WRITE(6,583)TLIN
583     FORMAT(20X, 'TLIN=',F10.3)
        TLOUTA=50
```

```
      ERR=0.02
      MWAIR=28.97
      MWLIQ=110.99
      NITER=0
      MAXITR=500
      DTL=0.2
      BIGOUT=1
C
C     CONDITIONS OF GAS AT INLET (BOTTOM OF THE TOWER)
C
      PW=HR(1)*760.0/(0.622+HR(1))
      SYCIN=(PW/760.0)
      CYCIN=SYCIN/(1.-SYCIN)
      SXCIN=1.-EPSI(N+1)
      GBPRM=(GB*MWAIR)/1.2

C
C     CONDITION OF LIQUID AT OUTLET (BOTTOM OF THE TOWER)
C
      SXCOUT=1.-EPSI(1)
      LOUT=(LIN*EPSI(N+1))/EPSI(1)
      CYCOUT=CYCIN+((LIN-LOUT)/GB)
C
C     GUESS LIQUID OUTLET TEMPERATURE
C
      TL(1)=TLOUTA
      TLOUT=TLOUTA
C
1000  CONTINUE
C
C     INITIALIZE AT THE BOTTOM OF THE TOWER
C
      I=1
      L=LOUT
      TG(1)=TGIN
      LPRM=(L*MWLIQ)/1350.0
      CYC=CYCIN
      EPSI(1)=1.-SXCOUT
      SXC=SXCOUT
      SYC=SYCIN
      Z(1)=0.0
C
2000  CONTINUE
```

```
C
C       CALCULATION OF HEAT & MASS TRANSFER COEFFICIENTS
C
        HGA=850*(LPRM**0.04)*(GBPRM**0.8)*EXP(0.02*TG(I))
        FGA=0.011*(LPRM**0.04)*(GBPRM**0.8)*EXP(0.03*TG(I))
        FLA=7.3*(LPRM**0.46)*(GBPRM**0.075)*EXP(-0.035*TL(I))
        1*EXP(0.0097*EPSI(I))
        FLAFGA=FLA/FGA
        CALL INFACE (SXC,SYC,TL(I),FLAFGA,SXCI,SYCI)
C
C       CALCULATE GRADIENTS AT SECTION I:
C
        DCYCDZ=-(FGA/GB)*ALOG((1.-SYCI)/(1.+SYC))
        HGACOR=(-GB*CC*DCYCDZ)/(1.-EXP((GB*C C*DCYCDZ)/HGA))
        DTGDZ=-(HGACOR*(TL(I)-TG(I)))/(GB*(CB+CYC*CC))
        DTLDZ=(1./(L*CA))*(GB*(CB+CYC*CC)*DTGDZ+GB*(CC*(TG(I)-TO)+
    1   LAMDAO)*DCYCDZ-GB*(CA*(TL(I)-TO)+DELHS)*DCYCDZ)
C       WRITE(6,2107)DTLDZ,DTGDZ
2107    FORMAT(3X,'DTLDZ=',F10.3,3X,'DTGDZ=',F10.3)
C
C
C
        DELCYC=(CYCOUT-CYCIN)/FLOAT(N)
C
C       UPDATE PARAMETERS FOR NEXT SECTION, I+1:
C
        DELZ=DELCYC/DCYCDZ
C
C
C       WRITE(6,2101)DTGDZ,DTLDZ,DELCYC,DELZ
2101    FORMAT(1X,'DTGDZ=',F10.3,1X,'DTLDZ=',
        1F10.3,1X,'DELCYC=',F6.5,1X,'DELZ=',F6.3)

        Z(I+1)=Z(I)+DELZ
        CYC=CYC+(DELCYC)
        SYC=CYC/(1.+CYC)
        HR(I+1)=0.622*CYC
        FL=L
        L=L+GB*(DELCYC)
        LPRM=(L*MWLIQ)/1350.0
        SXC=(FL*SXC+GB*(DELCYC))/L
        EPSI(I+1)=1.-SXC
        TG(I+1)=TG(I)+DELZ*DTGDZ
```

```
      TL(I+1)=TL(I)+DELZ*DTLDZ
C
      I=I+1
C
C     CHECK IF ALL N SECTIONS HAVE BEEN SCANNED, IF SO CHECK
FOR
C     ACCURACY OF THE GUESSED VALUE:
C
      IF(I.EQ.(N+2)) GO TO 50
      GO TO 2000
50    IF(NITER.EQ.MAXITR)GO TO 302
      IF(ABS((TL(N+1)-TLIN)/TLIN).LT.ERR)GO TO 201
      IF(TL(N+1)-TLIN)101,201,301
101   IF(NITER.GT.5) DTL=1.5*DTL
      TL(1)=TL(1)+DTL
      TLOUT=TL(1)
      NITER=NITER+1
2102  FORMAT(3X,'NITER=',F4.2)
      GO TO 1000
301   IF(NITER.GT.5)DTL=1.5*DTL
      TL(1)=TL(1)-DTL
      TLOUT=TL(1)
      NITER=NITER+1
2103  FORMAT(3X, 'NITER=',I4.2)
      GO TO 1000
302   WRITE(6,3021)
3021  FORMAT(' MAX ITERATIONS PERFORMED, COULD NOT
CONVERGE')
      STOP
201   CONTINUE
C
C     PRINT OUT THE RESULTS:
C
      TGOUT=TG(N+1)
      HROUT=0.622*CYC
      WRITE(6,2105)PW,SYCIN,CYCIN,SXCIN,GBPRM
2105 FORMAT(1X,'PW=',F10.5,2X,'SYCIN=',F10.5,2X,'CYCIN=',
      1F10.5,2X,'SXCIN=',F10.5,2X,'GBPRM=',F10.5)
      WRITE(6,2104)SYCI,SYC,DCYCDZ
2104  FORMAT(3X,'SYCI=',F10.5,3X,'SYC=',F10.5,3X,'DCYCDZ=',F10.5)
      WRITE(6,2100)DTGDZ,DTLDZ,DELCYC,DELZ
2100 FORMAT(1X,'DTGDZ=',F10.5,1X,'DTLDZ=',
      1F10.5,1X,'DELCYC=',F8.7,1X,'DELZ=',F6.5)
```

```
      WRITE(6,10) EPSI(N+1),EPSI(1),TL(N+1),TL(1),TG(N+1),TG(1),
     1     HR(N+1),HR(1),
     1  Z(N+1)
10    FORMAT(///,10X,'RESULTS FOR A PACKED TOWER REGENERATOR:'
     1           /10X,'---------------------------------------'
     1     /20X,'LIQ.CONC.AT TOP =',F10.3,3X,'(GIVEN)'
     1     /17X,'LIQ.CONC.AT BOTTOM =',F10.3,3X,'(GIVEN)'
     2  /16X,'LIQ.TEMP.AT TOP , TL=',F10.3,3X,'(MODIFIED)'
     3  /10X,'LIQ.TEMP. AT BOTTOM, TLOUT=',F10.3,3X,'(FOUND)'
     4  /13X.'AIR TEMP. AT TOP, TGOUT=',F10.3,3X,'(FOUND)',
     5  /11X.'AIR TEMP. AT BOTTOM, TGIN=',F10.3,3X,'(GIVEN)',
     6  /13X,'HUM.RATIO AT TOP, HROUT=',F10.5,3X,'(FOUND)',
     7  /11X,'HUM.RATIO AT BOTTOM, HRIN=',F10.5,3X,'(GIVEN)',
     8  //10X,'HEIGHT OF PACKING MATERIAL',
     9  '(TOWER HEIGHT)', 'Z=',F10.3,1X,'m'////)
C
C     IF YOU WANT TO OBTAIN VARIOUS DISTRIBUTIONS, THEN ASSIGN
C     BIGOUT=1(NEAR THE BEGINNING OF THE PROGRAM).  IF YOU
C     DO NOT WANT ANYMORE OUTPUT THEN PUT BIGOUT=0.
C
      IF(BIGOUT.EQ.0.)GO TO 564
      WRITE(6,20)
20    FORMAT(//10X,'TEMPERATURE & CONCENTRATION DISTRIBUTION
ALONG',1X,
     1  'THE TOWER',/8X,57('-'),//24X,'Z',6X,'TL',6X,'EPSI',5X.
     1  'TG',6X,'HR')
      NP1=N+1
      DO 400 J=1,NP1
      I=N+2-J
      WRITE (6,30) Z(I),TL(I),EPSI(I),TG(I),HR(I)
30    FORMAT(20X,F7.4,2X,F6.3,2X,F6.5,3X,F6.3,2X,F6.5)
400   CONTINUE
564   CONTINUE
543   CONTINUE
182   CONTINUE
362   CONTINUE
      END
C
C     ***********************************************
C     SUBROUTINE INFACE
C     ***********************************************
C
      SUBROUTINE INFACE(SXC,SYC,TL,FLAFGA,X,SYCI)
```

```
      DXI=0.01
      EPSI=0.0001
      X=0.10
      XMAX=0.98
      T=TL
5     DELTX=DXI
      FX=0.0448+0.00112*T-(0.03576/X)-1.+(1.-SYC)*
     1(((1.-SXC)/(1.-X))**FLAFGA)
6     X=X+DELTX
      FX1=0.0448+0.00112*T-(0.03576/X)-1.+(1.-SYC)*
     1(((1.-SXC)/(1.-X))**FLAFGA)
      IF(ABS(FX1).GT.1./EPSI)GO TO 7
      GO TO 9
7     WRITE(6,8)X
8     FORMAT(' ','FUNCTION APPROACHING INFINITY FOR X=',F7.4)
      X=X+DXI
      GO TO 5
9     IF(FX*FX1)11,13,10
10    IF(X.GT.XMAX)RETURN
      FX=FX1
      GO TO 6
11    IF(DELTX-EPSI)13,13,12
12    X=X-DELTX
      DELTX=DELTX/10.
      GO TO 6
13    CONTINUE
      SYCI=0.0448+0.001-*12*TL-(0.03576/X)
      X=X+EPSI
      GO TO 5
      END
```

NOMENCLATURE

a	- effective interfacial area, m^2/m^3
a_p	- packing surface area, m^2/m^3
B	- channel base dimension, m
C_1, C_2, C_3.....	- constants as defined in Eqns. (5-11) and (5-12)
C_G, C_L	- specific heat for air and liquid, respectively, J/kg K
C_p	- specific heat, J/kg K
C_v	- specific heat for water vapor, J/kg K
d	- equivalent diameter of channel, m
D_G, D_L	- diffusion coefficient for air and liquid, respectively, m^2/s
Fr_L	- Froude number for the liquid, dimensionless
F_o, F_s', F_t	- correction factor for operating, static, and total holdups, respectively, dimensionless
F_G, F_L	- mass transfer coefficient for air and liquid, respectively, $kmol/m^2s$
F_Ga, F_La	- volumetric mass transfer coefficient for air and liquid, respectively, $kmol/m^3s$
g	- gravitational constant, m/s^2
g_{eff}	- effective gravity, m/s^2
G	- molar gas mass velocity of air, $kmol/m^2s$
G_d	- molar gas mass velocity of dry air, $kmol/m^2$ s

h - height of channel, m

h_G, h_L - heat transfer coefficient for air and liquid, respectively, kW/m^{2}K

h_Ga, h_La - volumetric heat transfer coefficient for air and liquid, respectively, kW/m^{3}K

$h_G^{'}a$ - volumetric heat transfer coefficient for air corrected for mass transfer (Ackermann correction), kW/m^{3}K

h_{op}, h_{stat}, h_t - operating, static, and total holdups, respectively, dimensionless

H_G - molar enthalpy of the gas stream, kJ/kmol

L - molar liquid mass velocity, kmol/m^{2}s

m - mass flow rate, kg/s

M_G, M_L - molecular mass for air and liquid, respectively, kg/kmol

M_w - molecular mass for water, kg/kmol

p - partial pressure of water vapor, mm Hg

P - pressure, mm Hg

Pr_G, Pr_L - Prandtl number for air and liquid, respectively, dimensionless

q_G - heat transfer flux for the gas, kJ/m^{2}s

r_{hd}, r_{ht} - hydraulic radius for diamond shaped and triangular shaped channel, respectively, m

Re_G, Re_L - Reynolds number for air and liquid, respectively, dimensionless

RH - relative humidity of air, %

s,S - specific and total entropy respectively, J/kg K and J/K

S - side dimension of corrugation, m

Sc_G, Sc_L - Schmidt number for air and liquid, respectively, dimensionless

Sh_G - Sherwood number for air. dimensionless

t - sheet thickness, m

t_e - exposure time, s

T - temperature, °C or K

T_G, T_L - temperature for air and liquid, respectively, °C

T_i - interface temperature, °C

T_0 - reference temperature, °C

u, U - specific and total internal energy respectively, J/kg and J

U_G, U_L - superficial velocity for air and liquid, respectively, m/s

U_{Ge}, U_{Le} - effective velocity for air and liquid, respectively, m/s

U_r - relative velocity, m/s

We_L - Weber number for the liquid, dimensionless

x_c - concentration of water in the liquid phase, kmol H_2O/kmol liquid mixture

x_{ci} - value of x_c at the interface, kmol H_2O/kmol liquid mixture

x_i - mole fraction for the component i

y - mole fraction in the gas phase

y_c - concentration of water in the gas phase, kmol H_2O/kmol gas mixture

y_{ci} - value of y_c at the interface, kmol H_2O/kmol gas mixture

Y - concentration of water in the gas phase, kmol H_2O/kmol gas mixture

Z - height of packing from the bottom, m

Greek letters

λ_0 - molar latent heat of vaporization of water at the reference temperature, kJ/kmol

ΔH_s - integral heat of solution per mole of solution, kJ/kmol

γ - contact angle between solid and liquid film, deg

κ - Thermal conductivity, W/mK

μ_G, μ_L - viscosity for air and liquid, respectively, mPa.s

δ_{op}, δ_{stat} - thickness of film for operating and static holdups, respectively, m

ΔP - pressure drop, Pa

ΔZ - incremental height, m

ε - void fraction of packing, OR effectiveness

θ - angle with horizontal for falling film or corrugation channel, deg

ξ - concentration of the desiccant by weight, %

ρ_G, ρ_L - density for air and liquid, respectively, kg/m^3

η - efficiency, %

σ - surface tension, N/m

Superscripts

l - liquid

o - at reference state

v - vapor

Subscript

a	- air
cond	- water condensation
evap	- water evaporation
i or in	- inlet
f	- fan
G	- gas
L	- desiccant
max	- maximum value
o or out	- outlet
Y	- humidity

REFERENCES

1. S. Jain, P. L. Dhar and S. C. Kaushik, "Evaluation of Liquid Desiccant Based Evaporative Cooling Cycles for Typical Hot and Humid Climates", *Heat Recovery Systems & CHP*, **14**, 621-632, 1994.

2. M. Meckler, "Desiccant-Assisted Air Conditioner Improves IAQ and Comfort", *Heating/Piping/Air conditioning*, **66**, 75-84, 1994.

3. W. C. Griffiths, "Use of Liquid Sorption Dehumidification to Improve Energy Utilization of Air System", *In Desiccant Cooling and Dehumidification, ASHRAE*, 33-39, 1992.

4. V. Öberg and D. Y. Goswami, "Experimental Study of the Heat and Mass Transfer in a Packed Bed Liquid Desiccant Air Dehumidifier", *Trans. of ASME Journal of Solar Energy Engineering*, **120**. 289-297, 1998.

5. T. F. N. Thoruwa, C. .M. Johnstone, A. D. Grant and J. E. Smith, "Novel, Low Cost $CaCl_2$ Based Desiccants for Solar Crop Drying Applications", *Renewable Energy*, **19**, 513-520, 2000.

6. S. B. Heath and F. R. Minger; U.S. Patent 2, **143**, 007, 1939.

7. N. Isshiki, "Storage and Generation of Power and Heat by Aqueous Solution of Salts", *Proc. of the Int. seminar on Thermochemical Energy Storage*, Stockholm, 301-326, 1980.

8. A. Ertas, E. E. Anderson and I. Kiris, "Properties of a New Liquid Desiccant Solution-Lithium Chloride and Calcium Chloride Mixture", *Solar Energy*, **49**, 205-212, 1992.

9. T. A. Ameel, K. G. Gee and B. D. Wood, "Performance Prediction of Alternative, Low Cost Absorbents for Open-Cycle Absorption Solar Cooling", *Solar Energy*, **54**, 65-73, 1995.

10. R. W. James, Desiccants and Humectants. Noyes Data Corporation, New Jersey, U.S.A, 1973.

11. S. Younus Ahmed, P. Gandhidasan and A. A. Al-Farayedhi, "Thermodynamic Analysis of Liquid Desiccants", *Solar Energy*, **62**, 11-18, 1998.

12. P. R. Armstrong and G. H. Brusewitz, "Design and testing of a liquid desiccant dehumidifier", *Trans. of the ASAE*, **27**, 169-172, 1984.

13. G. C. So'Brien and S. Sactunanthan, "Performance of a novel liquid desiccant dehumidifier/regenerator system", *Trans. of ASME Journal of Solar Energy Engineering*, **111,** 345-352, 1989.

14. N. C. Turner, U.S. Patent No. 4, 171, 620.

15. A. G. Queiroz, A. F. Orlando, and F. E. M. Saboya, "Performance analysis of an air drier for a liquid dehumidifier solar air conditioning system", *Trans. of the ASME Journal of Solar Energy Engineering*, **110**, 120-124, 1988.

16. A. M. Radhwan, H. N. Gari and M. M. Elsayed, "Parametric Study of a Packed Bed Dehumidifier/Regenerator Using $CaCl_2$ Liquid Desiccant", *Renewable Energy*, **3**, 49-60, 1993.

17. M. M. Elsayed, H. N. Gari and A. M. Radhwan, "Effectiveness of Heat and Mass Transfer in Packed Beds of Liquid Desiccant System", *Renewable Energy*, **3**, 661-668, 1993.

18. "Structured Packing", *The Chemical Engineer*, 25-30, 1988.

19. G. O. G. Lof, et al., "Coefficients of heat and mass transfer in a packed bed suitable for solar regeneration of aqueous lithium chloride solutions", *Trans. of ASME Journal of Solar Energy Engineering*. **106, 4**, 387-392, 1984.

20. P. Gandhidasan, C. F. Kettleborough, and M. R. Ullah, "Calculation of heat and mass transfer coefficients in a packed tower operating with a desiccant-air contact system", *Trans. of ASME Journal of Solar Energy Engineering*, **108, 2**, 123-128, 1986.

21. A. Ertas et al., "Comparison of mass and heat transfer coefficients of liquid desiccant mixtures in a packed column", *Trans. of ASME Journal of Energy Resources Technology*,**113, 1**,1-6, 1991.

22. S. V. Potnis, and T. G. Lenz, "Dimensionless mass-transfer correlations for packed-bed liquid-desiccant contactors", *Ind. Eng. Chem. Res.*, **35, 11**, 4185-4193, 1996.

23. T. W. Chung, T. K. Ghosh, and A. L. Hines, "Comparison between random and structured packings for dehumidification of air by lithium chloride solutions in a packed column and their heat and mass transfer correlations", *Ind. Eng. Chem. Res.*, **35, 1**, 192-198, 1998.

24. J. L. Bravo, J. A. Rocha, and J. R. Fair, "Mass transfer in gauze packings", *Hydrocarbon Processing*, **64, 1**, 91-95, 1985.

25. F. Kreith and D. Bharathan, "Heat transfer research for ocean thermal energy conversion", Paper presented at the *Second ASME/JSME Thermal Engineering Conference*, Hawaii, March 1987.

26. J. A. Rocha, J. L. Bravo, and J. R. Fair, "Distillation columns containing structured packings: A comprehensive model for their performance. 1. Hydraulic models", *Ind. Eng. Chem. Res.*, **32**, 641-651. 1993.

27. J. A. Rocha, J. L. Bravo, and J. R. Fair, "Distillation columns containing structured packings: A comprehensive model for their performance. 2. Mass transfer model", *Ind. Eng. Chem. Res.*, **35**, 1660-1667, 1996.

28. M. G. Shi, and A. Mersmann, "Effective interfacial area in packed columns", *Ger. Chem. Eng.*, **8**, 87-96, 1985.

29. E. R. Gilliland, and T. K. Sherwood, *Ind. Eng. Chem.*, **26**, 516, 1934.

30. R. E. Treybal, Mass Transfer Operations, 3rd Edition, McGraw-Hill, New York. 1980.

31. L. Spiegel and W. Meier, "Correlations of the performance characteristics of the various Mellapak types (Capacity, pressure drop, efficiency)", *Ind. Chem. Eng. Symp. Ser.*, **104**, p. A203, 1987.

32. Calcium Chloride Handbook. Dow Chemical Company, Michigan, U.S.A., 1999.

33. T. Uemura, "Studies on the lithium chloride-water absorption refrigerating machines", *Tech Report, Kansai University*, **9**, 71-88, 1967.

34. K. G. Mahmoud and H. D. Ball, "Liquid desiccant systems for cooling applications", *Proc. of the 23rd IECEC*, edited by D. Y. Goswami, ASME, New York, **4**, 149-152, 1988.

35. P. Gandhidasan, M. R. Ullah and C. F. Kettleborough, "Analysis of heat and mass transfer between a desiccant-air system in a packed tower", *Trans. of ASME J. of Solar Energy Engineering*, **109**, 89-93, 1987.

36. H. M. Factor and G. Grossman, "A packed bed dehumidifier/regenerator with liquid desiccants", *Solar Energy*, **24**, 541-550, 1980.

37. S. V. Potnis and T. G. Lenz, "Mass transfer studies for a solar assisted liquid desiccant cooling system", Solar Engineering – 1994, *Proc. of the 12th Annual ASME Solar Energy Conference*, San Francisco, CA, 359-365, 1994.

38. D. I. Stevens, J. E. Braun and S. A. Klein, "An effectiveness model of liquid-desiccant system heat/mass exchangers", *Solar Energy*, **42**, 449-455, 1989.

39. M. Sadasivam and A. R. Balakrishnan, "Effectiveness-NTU method for design of packed bed liquid desiccant dehumidifiers", *Chem. Eng. Research & Design*, **70**, 572-577, 1992.

40. A. Y. Khan, "Sensitivity analysis and component modeling of a packed-type liquid desiccant system at partial load operating conditions", *Int. J. of Energy Research*, **18**, 643-655, 1994.

41. A. Y. Khan and H. D. Ball, "Development of a generalized model for performance evaluation of packed-type liquid sorbent dehumidifiers and regenerators", *ASHRAE Trans.* **98**, 525-533, 1992.

42. R. E. Treybal, "Adiabatic gas absorption and stripping in packed tower", *Ind. Eng. Chem.*, **61**, 7, 36-41, 1969.

43. C. S. P. Peng and J. R. Howell, "Optimization of liquid desiccant systems for solar/geothermal dehumidification and cooling", *J. of Energy*, **5**, 401-408, 1981.

44. H. I. Robison, "Operational experience with a liquid desiccant heating and cooling system", *Proc. of the 18th IECEC*, 1952-1957, 1983.

45. C. S. P. Peng and J. R. Howell, "The performance of various types of regenerators for liquid desiccants", *Trans. of ASME Journal of Solar Energy Engineering*, **106**, 133-141, 1984.

46. G. O. G. Lof, "Home heating and cooling with solar energy", Solar Energy Research, University of Wisconsin Press, Madison, 33-46, 1955.

47. S. M. Ko, U. S. Patent No. 4,205,529.

48. P. Gandhidasan, "Heat and mass transfer in solar regenerators", in Handbook of Heat and Mass Transfer, ed. N. P. Cheremisinoff, Gulf Publishing Company Book Division, Houston, 1986.

49. P. Gandhidasan, "Closed-type solar regenerator: Analysis and simulation", *Trans. of ASME Journal of Energy Resources Technology*, **117**, 58-61, 1995.

50. P. Gandhidasan and A. A. Al-Farayedhi, "Thermal performance analysis of a partly closed/open solar regenerator", *Trans. of ASME Journal of Solar Energy Engineering*, **117**, 151-153, 1995.

51. C. Leboeuf and G. O. G. Lof, "Open cycle absorption cooling using packed bed absorbent reconcentration", *Proceedings of the 1980 Annual Meeting of the American Section of the International Solar Energy Society*, 205, 1980.

52. G. O. G. Lof, S. Rao and T. Lenz, "Open cycle lithium chloride (solar) cooling", DOE Report CS/3026-TI, Dec. 1981.

53. R. Rautenbach and R. Albrecht, Membrane Processes, Wiley, New York, 1989.

54. A. A. Al-Farayedhi, P. Gandhidasan and S. Younus Ahmed, "Regeneration of liquid desiccants using membrane technology", *Energy Conversion and Management*, **40**,1405-1411, 1999.

55. V. Martin and D. Y. Goswami, "Effectiveness of heat and mass transfer processes in a packed bed liquid desiccant dehumidifier/regenerator", *HVAC & R Research*, **6**,**1**,21-39, 2000.

56. W. P. Jones, Air Conditioning Engineering, Edward Arnold Publishers, 2ed Ed., London, 1973.

57. M. R. Ullah, C. F. Kettleborough, and P. Gandhidasan, "Effectiveness of moisture removal for an adiabatic counterflow packed tower absorber operating with $CaCl_2$-Air contact system", *Trans. of the ASME Journal of Solar Energy Engineering*, **110**, **2**, 98-101, 1988.

58. T. W. Chung and H. Wu, "Comparison between spray towers with and without fin coils for air dehumidification using triethylene glycol solutions and development of the mass-transfer correlations", *Ind. Eng. Chem. Res.*, **39**, **6**, 2076-2084, 2000.

59. A. A. Kinsara, M. M. Elsayed and O. M. Al-Rabghi, "Proposed energy-efficient air-conditioning system using liquid desiccant", *Applied Thermal Engineering*, **16**,**10**, 791-806, 1996.

60. Max Leva, "Tower Packings and Packed Tower Design", The United States Stoneware Company, Akron, U.S.A., 1953.

61. J. L. Bravo, J. A. Rocha and J. R. Fair, "Pressure drop in structured packings", *Hydrocarbon Processing*, **56**, **3**, 45-59, 1986.

62. J. Stichlmair, J. L. Bravo and J. R. Fair, "General Model for Prediction of Pressure Drop and Capacity of Countercurrent Gas/Liquid Packed Columns", *Gas Separation and Purif*ication, **3**, 19-28, 1989.

63. J. R. Fair and J. L. Bravo, "Distillation Columns Containing Structured Packings", *Chem. Eng. Prog.* **86**, 19-29, 1990.

VITA

- ★ Musaad A. Al-Mutairi
- ★ Born in 1393H (1973) at Hafar Al-Batin, Saudi Arabia.
- ★ Received the **DEGREE OF BACHELOR OF SCINCE IN MECHANICAL ENGINEERING** from King Fahd University of Petroleum & Minerals, Dhahran, Saudi Arabia in 1417H (1996).
- ★ Has been worked in ministry of education since 1417H (1996) as a teacher of manufacturing process and physics.
- ★ Received the **DEGREE OF MASTER OF SCINCE IN MECHANICAL ENGINEERING** with specialization in **THERMAL SCINCE** from King Fahd University of Petroleum & Minerals in 1421H (2000).
- ★ Permanent Address: Dhahran 31261, P. O. Box# 7170, Saudi Arabia.